論文 / 著書情報
Article / Book Information

題目(和文)	非一様宇宙の動力学
Title(English)	Dynamics in inhomogeneous cosmology
著者(和文)	井口修
Author(English)	Osamu Iguchi
出典(和文)	学位:博士(理学), 学位授与機関:東京工業大学, 報告番号:甲第3645号, 授与年月日:1998年3月26日, 学位の種別:課程博士, 審査員:
Citation(English)	Degree:Doctor (Science), Conferring organization: Tokyo Institute of Technology, Report number:甲第3645号, Conferred date:1998/3/26, Degree Type:Course doctor, Examiner:
学位種別(和文)	博士論文
Type(English)	Doctoral Thesis

Dynamics in Inhomogeneous Cosmology

Osamu Iguchi
Department of Physics, Tokyo Institute of Technology

February 1998

Abstract

Recently the development of the astronomical observation gives us a great deal of the contribution to the understanding of the structure of the universe. The observational results have shown that the large scale structure of the universe is isotropic to an extraordinary degree while the distribution of the galaxies and of the clusters of galaxies are very irregular. From the irregularity of the distribution, one might even speculate a self-similarity which is characterized by the fractal dimension $D \sim 2$.

In modern cosmology, it is important to study the origin and evolution of the universe in a consistent way with these observational results. A widely accepted cosmological scenario is the inflation scenario in the very early stage of the universe and the standard Big-Bang cosmology after the inflationary epoch. The inflationary scenario explains a homogeneous and isotropic universe with a small initial fluctuations which was previously assumed in the standard cosmology. In the standard cosmology, the small fluctuations grow via the gravitational instability and lead to cosmic structures.

There remain some important unsolved problems in the cosmological scenario. As for the inflation scenario, the dynamics of the universe has been investigated mainly in a homogeneous and flat universe. In order to investigate whether the inflation scenario is a realistic one, it is necessary to study the effect of the inhomogeneities in the universe on the inflation. As for the structure formation of the universe, the description of the standard Big-Bang cosmology is not acceptable in the present universe if the universe has a very irregular structure such as a fractal.

We apply the improved gradient expansion method and the renormalization group approach to the some problems in the cosmological scenario, especially from the viewpoint of the dynamics.

In the first part of this thesis, we apply the long wavelength approximation to study how the initial inhomogeneities of the spatial curvature affect the onset of inflation in the closed universe. In order to treat the inhomogeneities in the closed universe, we improve the long wavelength approximation such that the nonsmall spatial curvature is tractable in the lowest order. Using the improved scheme, we show the condition of the inhomogeneities for the universe to enter the inflationary phase.

In the second half of this thesis, we apply the renormalization group method, which has been adapted to the analysis of the long-time behavior of nonlinear partial differential equation, to the Einstein equations in the context of the dynamics and the scale invariance, motivated by the spatial distribution of galaxies, in the expanding universe. We carry out detailed analysis of renormalization group flow in the vicinity of the scale-invariant fixed point in the spherically symmetric and inhomogeneous dust filled universe model.

Contents

Chapter 1

Introduction

In the last twenty years the collection of a huge body of observational data has revealed the structure of the universe. The detection and the high degree of isotropy of the Cosmic Microwave Background Radiation (CMBR) which shows an almost perfect black body spectrum at temperature 2.7 K teaches us that the large scale structure of the universe ($\sim 3000h^{-1}$ Mpc [1]) is isotropic. Many redshifts surveys have shown that the three-dimension distribution of galaxies and clusters of galaxies turn out to be very irregular and unveiled a large structure such as the *Great Wall* and large voids up to $\sim 170h^{-1}$ Mpc or more and permits the characterization of their correlation properties. By the gravitational lensing effects which is a gravitational light deflection, we have been able to observe objects which are too distant or intrinsically too faint to be observed, so called dark matter. Through the statistics of the gravitational lensing events, the cosmological parameters can be significantly constrained (for example, the value of the dimensionless cosmological constant is larger than 0.3 and the value of the density parameter of the universe is larger than 0.65).

In modern cosmology it is important to study the origin and evolution of the universe which is consistent with these observational results. The cosmological scenario which is so widely accepted is as follows [1, 2]. In the early universe, once the universe emerged from the quantum gravity era, there was an epoch when the vacuum energy like as the cosmological constant was the dominant component of the energy density of the universe, so that inflation which is the phase of the exponential expansion has taken place. During the inflationary epoch, since a small, smooth, and causally coherent region of the universe can grow up, the universe becomes a homogeneous and isotropic on a large scale and has a small density fluctuation which is a seed of structure in the present universe. By the decay of the vacuum energy, the universe was reheated, so that the energy of radiation which consists of relativistic particles such as photons dominated the universe. After this era, the universe can be described by the Friedmann-Robertson-Walker model (FRW) with a small perturbation. By the expansion of the universe, the energy density of non-relativistic matter, such as the dust, becomes the dominant component of the energy density of the universe. By the gravitational instability, the small perturbation grows and builds up a various structure such as galaxies and clusters of galaxies and voids.

There remain some important unsolved problems in the cosmological scenario. As for

[1] $H_0 = 100h\text{km s}^{-1}\text{Mpc}^{-1}$ where H_0 is the Hubble constant at the present time and $0.5 \leq h \leq 1$.

the inflation model, the dynamics of the universe has been investigated mainly in a flat FRW. In this case, inflation is generic. However, since the advantage of inflation model is to free cosmology from the need of having initially very homogeneous and flat conditions, it is necessary to study the effect of the initial inhomogeneities in the universe on the onset of inflation. As for the structure formation, the description of the FRW with a small perturbation is not acceptable in the present universe at least up to $\sim 10h^{-1}$ Mpc where the order of the density contrast nearly equals to 1. The two-point correlation functions of the galaxies and of the clusters of galaxies which characterize the distribution of the matter in the universe is roughly written by the single power law (its exponent ~ -1.8 and in fractal dimension $D \sim 1.2$ [2] , see the Appendix A). Recently the temperature fluctuations of about 13μK have been detected by the COBE in the 2.7 K CMBR over angular scales larger than 7°[3] and are shown a fractal structure with fractal dimension $\sim 1.43 \pm 0.07$ [4]. These suggest the possibility that the present universe has a scale invariance up to a very large scale $\sim 1000h^{-1}$ Mpc and might be described by a fractal universe rather than the FRW model. If it is really the case, it is necessary to explain such a fractal universe, from the viewpoint of the dynamics of the universe. There are several methods to investigate the dynamics in the inhomogeneous universe.

For a non-perturbative one, there is a junction method [5] and a numerical simulation [6]. Using the junction method, it is possible to build up an inhomogeneous universe model, so called " Swiss cheese "-type model. For example, it can be described by an inhomogeneous universe model with the interior solution consisting of the Schwarzschild solution and the exterior one of the FRW filled with dust [7, 8] and with the interior solution consisting of the Tolman-Bondi solution, which is a general solution of the spherically symmetric dust filled universe, and the exterior one of the FRW filled with dust [9, 10, 11]. As for the numerical simulation, the nonlinear clustering and the n-point correlation function has been studied by N-body simulations and the effect of initial conditions on inflation models and cosmological models is investigated by assuming a special symmetry of spacetime.

As for a perturbative method, there are two schemes: the Amplitude Expansion (AE) and the Gradient Expansion (GE). Both methods are complementary to each other. In the AE which is one of the most used in cosmology, the metric is expanded in power of the amplitude of fluctuations. By using the linear approximation in the AE [12, 13, 14, 15], the gravitational instability in the expansing universe has been demonstrated. In order to investigate the nonlinearity of perturbation, the second order solution is analyzed in [16, 17, 18]. The obvious drawback of this perturbation scheme is its technical difficulty to treat the nonlinearity of fluctuations to higher orders. On the other hand, quantities can be expanded according to the order of its spatial derivatives in the GE. It is assumed that the spatial derivatives are much smaller than the time derivatives. Since the time derivatives of the metric dominates over the spatial derivatives near the initial singularity of the universe, the lowest order solution is useful to study the general behaviors of the early universe [19, 20]. In order to study the evolution of the nonlinear inhomogeneities, an iteration scheme of the GE has been developed [21, 22].

In this thesis, we investigate the dynamics in inhomogeneous universe by use of the

[2] In Ref. [3], $D \sim 2$.

[3] For example, an angle $\theta = 10^{\circ}$ corresponds to $\sim 1000h^{-1}$ Mpc.

improved GE and the renormalization group approach (RG).

To begin with, we tackle the problem of onset of inflation in inhomogeneous cosmology by use of the improved GE. This problem has been studied by various approaches, the numerical simulation with special symmetries [23, 24], the linear approximation in the AE [25] and the GE [26, 27]. The advantage of using the GE is to treat the nonlinear inhomogeneities without assuming any symmetries. However, though the effect of the positive spatial curvature is essential as shown by the analysis of a homogeneous universe [28], the spatial curvature is to be treated as a small quantity in the usual GE scheme. In order to overcome this drawback, we improve the usual GE so that the nonsmall spatial curvature can be tractable in the lowest order. By using the first order solution in the improved GE, we will show the condition of the inhomogeneities of the spatial curvature for the universe to enter the inflationary phase.

Next, we shall consider the distribution of the matter in the present universe which has a scale invariance in the framework of the RG approach. There have been many works on the scale-invariant or fractal structure in the universe [3, 29, 30]. The fractal dimension of the distribution of the matter in the present universe is analyzed by using an effective model which is used to study the pattern formation [31, 32] and the RG which is used to analyze the critical phenomena [33, 34]. In the context of the observations in the fractal universe, the fractal universe is modeled by the power-law distribution of the energy density of the matter in the universe [35, 36, 37, 38] and the self-similar solution in which the metric is expressed by a single variable [39, 40]. However, these approaches are not adequate to investigate the origin and evolution of the fractal structure. From the viewpoint of both the dynamics and the scale invariance, we apply the RG [41], which has been adapted from the analysis of the long-time behavior of nonlinear partial differential equation, to the Einstein equations in a cosmological situation.

Chapter 2

Gradient expansion method

By the use of the long wavelength approximation method we can construct approximate solutions of Einstein equations which describe an inhomogeneous universe on scales larger than the local Hubble radius. Belinski, Khalatnikov, and Lifshitz [19] studied the general behaviors of the universe in the neighborhood of initial singularity by this approximation, and Tomita [20] focused attention on the evolutions of inhomogeneities of the early universe in this framework.

The long wavelength approximation assumes that the spatial derivative of a metric is smaller than the time derivative. The spatial curvature which consists of the spatial derivative of second order is neglected in the lowest order of this approximation and it is taken into account perturbatively by the series expansion in the higher order. This approximation is called the gradient expansion method for the Einstein equations. For the higher order solutions, Comer *et al.* [21] developed an iteration scheme of Einstein equations, Deruelle and Langlois [42] generalized it, and Salopek *et al.* [22] developed one of the Hamilton-Jacobi equations for general relativity.

In the long wavelength approximation we take a synchronous reference frame where the line element is of the form

$$ds^2 = g_{\mu\nu}dx^\mu dx^\nu = -dt^2 + \gamma_{ij}(t,x)dx^i dx^j. \tag{2.1}$$

Throughout this thesis Latin letters will denote spatial indices and Greek letters spacetime indices. In the usual method, we neglect all spatial gradients of $\gamma_{ij}(t,x)$ in the Einstein equations and construct an approximate solution with the characteristic physical scale of inhomogeneities larger than the Hubble radius [19, 20, 21, 22, 42]. Furthermore, we consider the quasi-isotropic universe as a special case in the form

$$ds^2 = -dt^2 + a^2(t)h_{ij}(x)dx^i dx^j, \tag{2.2}$$

where $h_{ij}(x)$ is an arbitrary function called " seed metric ". The universe is assumed to be filled with a perfect fluid characterized by energy density ρ and pressure $p = (\Gamma - 1)\rho$. In this case the Einstein equations reduce to

$$\frac{\ddot{a}}{a} - \frac{2-3\Gamma}{2}\left(\frac{\dot{a}}{a}\right)^2 = 0, \tag{2.3}$$

$$\left(\frac{\dot{a}}{a}\right)^2 = \frac{1}{3}\kappa\rho, \tag{2.4}$$

where an overdot denotes the derivative with respect to t and $\kappa \equiv 8\pi G$. These are nothing but the equations which the scale factor $a(t)$ of the flat Friedmann universe should satisfy. We call the approximate inhomogeneous solution given by Eq. (2.2) satisfying Eqs. (2.3) and (2.4) the locally flat Friedmann solution and it is used as a starting point to solve the Einstein equations iteratively [21, 22]. In the iteration scheme, the spatial metric can be expanded as a sum of spatial tensors of increasing order in spatial gradients of $h_{ij}(x)$. Thus the approximation is called the gradient expansion method.

In this chapter, we improve the gradient expansion scheme so that the nonsmall spatial curvature associated with a three space, which is conformal to the constant curvature space, can be tractable in the lowest order. By this improved gradient expansion scheme, we study how the inhomogeneities of the spatial curvature affect the occurrence of inflation in the closed [1] universe. We investigate the time evolution of the spatial region with nonsmall positive spatial curvature.

2.1 Brief review

In this section, we review the usual gradient expansion method briefly and show the relation between the GE method and the AE method. By the correspondence of the approximate solution in the GE and the solution of the linear approximation in the AE, we investigate the gauge used in the GE.

2.1.1 Expansion scheme

We explain the iteration scheme of the Einstein equations by the usual GE method [21].

We take a synchronous reference frame where the line element is

$$ds^2 = -dt^2 + \gamma_{ij}(t, x^k)dx^i dx^j.$$

The matter is taken to be a perfect fluid characterized by the energy-momentum tensor

$$T_{\mu\nu} = (\rho + p)u_\mu u_\nu + p g_{\mu\nu}, \tag{2.5}$$

where p, ρ, and u_μ are pressure, energy density, and four velocity, respectively. We assume the equation of state of the fluid is $p/\rho = \Gamma - 1$, where Γ is a constant. The Einstein equations with a cosmological constant Λ are

$${}^3R_i^j + \frac{1}{2\sqrt{\gamma}}\frac{\partial}{\partial t}(\sqrt{\gamma}K_i^j) = \frac{2\dot{K} + K_l^m K_m^l - 4\Lambda}{4(2 - 3\Gamma - 2\Gamma u_l u^l)}[2\Gamma u_i u^j + \delta_i^j(2 - \Gamma)] + \Lambda\delta_i^j, \tag{2.6}$$

$$\kappa\rho = \frac{2\dot{K} + K_l^m K_m^l - 4\Lambda}{2(2 - 3\Gamma - 2\Gamma u_l u^l)}, \tag{2.7}$$

$$\kappa\Gamma\rho u_i = -\frac{1}{2\sqrt{1 + u_l u^l}}(K_{i;j}^j - K_{,i}), \tag{2.8}$$

[1] The word " closed universe " does not mean the universe with spatial surface of closed topology in this thesis.

where ${}^3R^j_i$ is the Ricci tensor associated with γ_{ij}, $K_{ij} \equiv \dot{\gamma}_{ij}$ is the extrinsic curvature, $\gamma \equiv \det \gamma_{ij}$, an overdot denotes the derivative with respect to t, a semicolon denotes the covariant derivative with respect to γ_{ij}, and $\kappa \equiv 8\pi G$.

We consider the situation in which all spatial gradients are much smaller than time derivatives and assume that the spatial metric is expanded as

$$\gamma_{ij}(t,x) = \overset{(0)}{\gamma}_{ij}(t,x) + \overset{(1)}{\gamma}_{ij}(t,x) + \cdots = \sum_p \overset{(p)}{\gamma}_{ij}(t,x). \tag{2.9}$$

Here the lowest term $\overset{(0)}{\gamma}_{ij}$ in Eq. (2.9) is assumed in the quasi isotropic form

$$\overset{(0)}{\gamma}_{ij}(t,x) = a^2(t) h_{ij}(x), \tag{2.10}$$

where $a(t)$ is the scale factor in the lowest order which depends on only t and $h_{ij}(x)$ is an arbitrary function of only spatial variables. The next-order term $\overset{(1)}{\gamma}_{ij}$ is constructed by the symmetric tensors of the second order in the spatial gradients of h_{ij} in the form

$$\overset{(1)}{\gamma}_{ij}(t,x) = a^2(t)\left[f_1(t) R_{ij}(h) + g_1(t) R(h) h_{ij}\right], \tag{2.11}$$

where $R_{ij}(h)$ is the Ricci tensor associated with $h_{kl}(x)$, $R(h) \equiv h^{ij} R_{ij}(h)$, and $f_1(t)$ and $g_1(t)$ are functions of time. The subsequent general terms $\overset{(p)}{\gamma}_{ij}$ in Eq. (2.9) are spatial tensors which are of order $2p$ in the spatial gradients of $h_{ij}(x)$ with time dependent coefficients. Since the spatial inhomogeneities of the spacetime is generated by $h_{ij}(x)$, then we call it " seed metric ".

Substituting Eq. (2.10) into Eqs. (2.6)–(2.8) and neglecting the spatial derivatives we get the lowest (zeroth) order solution

$$a(t) = \left[\sinh\left(\frac{3\Gamma}{2} H_0 t\right)\right]^{2/(3\Gamma)}, \tag{2.12}$$

$$\overset{(0)}{\rho} = \frac{3H_0^2}{\kappa \sinh^2(\frac{3\Gamma}{2} H_0 t)}, \tag{2.13}$$

$$\overset{(0)}{u}_i = 0, \tag{2.14}$$

where $H_0 \equiv \sqrt{\Lambda/3}$. The evolution of scale factor at zeroth order is the same as the one of flat FRW universe. So, we call the solution described by Eqs. (2.12)–(2.14) "locally flat Friedmann solution".

At next (first) order, substituting the spatial metric $\gamma_{ij} = \overset{(0)}{\gamma}_{ij} + \overset{(1)}{\gamma}_{ij}$ given by Eqs. (2.10) and (2.11) into Eq. (2.6) and taking the spatial derivative terms of the seed metric, we get ordinary differential equations for the functions of time $f_1(t)$ and $g_1(t)$ (see [21]).

At higher order, we consider the corrections which are constructed by the spatial derivatives of $h(x)_{ij}$ and solve the Einstein equations order by order in the gradient expansion. The spatial metric can be expanded as

$$\gamma_{ij}(t,x) = a^2(t)\Bigg[h_{ij} + \sum_A F^A_{(2)}(t)(R^{(2)}(h))^A_{ij} + \sum_A F^A_{(4)}(t)(R^{(4)}(h))^A_{ij} + \cdots + \sum_A F^A_{(2p)}(t)(R^{(2p)}(h))^A_{ij} + \cdots\Bigg], \tag{2.15}$$

where the notation $(R^{(2p)}(h))^A_{ij}$ denotes symbolically symmetric spatial tensors which contain p spatial gradients of $R(h)_{ij}$, the suffix A distinguishes the tensors belonging to the same class, and $a(t)$ and $F^A_{(2p)}(t)$ are functions of t which is determined by the Einstein equations. Similarly, we can calculate the higher order solutions iteratively. The locally flat Friedmann universe, Eqs. (2.12)–(2.14), is used as a starting point to solve Eq. (2.6) in the expansion scheme, thus we call this scheme the gradient expansion from the flat Friedmann universe (GEFF). In the GEFF, the spatial curvature is treated perturbatively as a small quantity in the series expansion.

2.1.2 Correspondence of the GE to the AE

We show the correspondence of the GE to the AE and consider the gauge condition of the solution in the GE.

To see the relation between the GE and the AE around the flat Friedmann universe, we take $h_{ij}(x) = \delta_{ij} + \delta h_{ij}(x)(\delta h_{ij} \ll \delta_{ij})$ as a seed metric. The inverse metric tensor h^{ij} contains all order in δh_{ij} as follows:

$$\begin{aligned} h^{ij} &= \delta^{ij} - \delta h_{lm}\delta^{il}\delta^{jm} + \delta h_{lm}\delta h_{nk}\delta^{nl}\delta^{ik}\delta^{jm} + \cdots \\ &\sim O\left[(\delta h)^0\right] + O\left[(\delta h)^1\right] + O\left[(\delta h)^2\right] + \cdots . \end{aligned}$$

In the GE method, the metric is symbolically expanded in the form

$$\gamma_{ij} = A(t)h_{ij} + B(t)R_{ij}(h) + C(t)R^2_{ij}(h) + \cdots \tag{2.16}$$

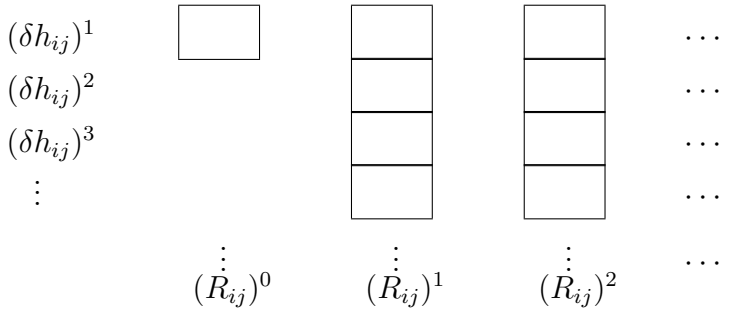

Fig. 2.1

Noting $R_{ij}(h)$ has the form

$$R_{ij}(h) \sim \partial_j \left(h^{lm}\partial_m h_{il}\right) + h^{ln}\left(\partial_n h_{im}\right) h^{mk}\left(\partial_k h_{jl}\right) + \cdots , \tag{2.17}$$

it also contains all order in h^{ij}. Then each curvature term in the GE (2.16) contains all order in δh_{ij}. Taking this fact into account, the expansion schemes are schematically represented in Fig. 2.1.

Gathering all linear terms in δh_{ij} (*e.g.* δh, $\partial\delta h$, $\partial^2\delta h$, $\cdots$) which contained in the curvature terms in Eq. (2.16), we should get the solution of the linear approximation in the AE. Moreover, gathering all bilinear terms in δh_{ij} (*e.g.* δh^2, $(\partial\delta h)^2$, $\delta h\partial^2\delta h$, $\cdots$) which contained in the curvature terms in Eq. (2.16), we should get the solution of the second order approximation in the AE. Like as this, we can relate the GE and the AE.

In oder to see the gauge condition of solutions in the GE, we examine the relation of the solutions in the GE to the one of the linear approximation in the AE around a flat Friedmann universe filled with a perfect fluid (see the Appendix B). It is impossible to sum all terms in Eq. (2.16). In this paper, we calculate the solution up to the second order (see the Appendix C), which includes the fourth order in spatial derivative, and sum the linear terms in δh_{ij}. We compare it to the solution of the linear approximation in the AE.

In the GE method, the synchronous gauge is adopted. Furthermore we assume that the spatial metric at lowest order can be expressed in the quasi isotropic from, Eq. (2.10), in order to calculate the higher order terms. However, in the linear approximation of the AE, the synchronous gauge admits residual gauge freedom. Therefore, we impose a coordinate condition, $h_{0i} = 0$ and $\delta u^i = 0$, in the linear approximation of the AE. This condition fixes the gauge completely. If there are one-to-one correspondence between the solutions in the linear approximation of the AE in this gauge and the solutions in the GE via a gauge transformation, the unphysical solution is not contained in the latter solution.

In the linear approximation of the AE, the perturbation is decomposed in tensor, vector, and scalar modes. As far as we consider the linear approximation of the AE around the flat Friedmann universe, we assume that spatial dependence of δh_{ij} is $\exp(ik_l x^l)$ without loss of generality. In this case, we replace the spatial derivative by ik_l.

The tensor mode contains no gauge solution, thus solutions for two formalisms coincide. In the GE method, the spatial dependence of the solution comes through $R_{ij}(h)$. For the seed metric of vector mode, $R_{ij}(h)$ is vanishing. Thus, there is no solution corresponding to the vector mode solution in the linear approximation of the AE.

The growing solution of the density contrast in the GE up to the second order is

$$\frac{\overset{(1)}{\rho} + \overset{(2)}{\rho}}{\overset{(0)}{\rho}} = \left[\frac{\Gamma(3\Gamma-2)^2}{12(9\Gamma-4)}(k\eta)^2 - \frac{\Gamma(\Gamma-1)(3\Gamma-2)^3}{24(3\Gamma+2)(15\Gamma-8)}(k\eta)^4\right]\exp(ikx), \tag{2.18}$$

where $\eta = \frac{3\Gamma}{3\Gamma-2}t^{(3\Gamma-2)/(3\Gamma)}$. On the other hand, the growing solution in the linear approximation of the AE is

$$\frac{\delta\rho}{\overset{(0)}{\rho}} = \left[\frac{\Gamma(3\Gamma-2)^2}{12(3\Gamma+2)}(k\eta)^2 - \frac{\Gamma(\Gamma-1)(3\Gamma-2)^3}{24(3\Gamma+2)(9\Gamma-2)}(k\eta)^4\right]\exp(ikx). \tag{2.19}$$

We can find a unique gauge transformation which connects these two solutions. The gauge transformation is in the following form:

$$\eta \longrightarrow \eta + \delta\eta(\eta)\exp(ikx) \tag{2.20}$$

$$x^i \longrightarrow x^i + \delta r(\eta)\frac{ik^i}{k^2}\exp(ikx) \tag{2.21}$$

where $\delta\eta$ and δr are

$$\delta\eta = \frac{1}{k^2}\delta\partial_\eta r, \tag{2.22}$$

$$\delta r = \frac{(1-\Gamma)(3\Gamma-2)^3}{48(3\Gamma+2)(9\Gamma-4)}(k\eta)^4 - \frac{(1-\Gamma)^2(3\Gamma-2)^2}{144(3\Gamma+2)(9\Gamma-2)(15\Gamma-8)}(k\eta)^6. \tag{2.23}$$

The one-to-one correspondence between Eq. (2.18) and Eq. (2.19) guarantees that the solution Eq. (2.18) is physical.

2.2 Improved method

In this section, we improve the GEFF such that we can treat non-vanishing three curvature which is discarded at lowest order [43]. We show that when the seed metric has maximally symmetry [2] , the closed or open Friedmann solution is derived by summing up all terms in the GEFF. After that we extend the method such that the inhomogeneities around the closed or open Friedmann universe are tractable.

First, we consider a seed metric in the maxmally symmetric form with non-vanishing curvature:

$$h_{ij}(x) = h^{\pm}_{ij}(x),$$

where the Ricci curvature associated with the metric is

$$R_{ij}(h^{\pm}) = \pm 2h^{\pm}_{ij}.$$

Since all spatial tensors of rank two derived from $h^{\pm}_{ij}$ are proportional to $h^{\pm}_{ij}$ itself, then time dependent part in Eq. (2.9) is factorized in the form

$$\begin{aligned}\gamma_{ij}(t,x) &= a^2(t)\left[h^{\pm}_{ij} + f_1(t)R_{ij}(h^{\pm}) + g_1(t)R(h^{\pm})h^{\pm}_{ij} + f_2(t)R(h^{\pm})R_{ij}(h^{\pm}) + \cdots\right] \\ &= a^2_{\pm}(t)h^{\pm}_{ij}(x),\end{aligned} \tag{2.24}$$

where

$$a^2_{\pm}(t) \equiv a^2(t)\Big[1 \pm \{2f_1(t) + 6g_1(t)\} + \{12f_2(t) + \cdots\} + \cdots\Big]. \tag{2.25}$$

Substituting Eq. (2.24) into Eqs. (2.6)–(2.7), we obtain the equation which $a_\pm$ must satisfy

$$\frac{\ddot{a}_\pm}{a_\pm} - \frac{2-3\Gamma}{2}\left(\frac{\dot{a}_\pm}{a_\pm}\right)^2 \mp \frac{2-3\Gamma}{2a^2_\pm} = \frac{\Gamma}{2}\Lambda, \tag{2.26}$$

$$\left(\frac{\dot{a}_\pm}{a_\pm}\right)^2 \pm \frac{1}{a^2_\pm} = \frac{1}{3}(\kappa\rho + \Lambda). \tag{2.27}$$

These are nothing but the equations for the closed or open Friedmann universe. Of course, the universe described by the solution satisfying these equations is far from the flat Friedmann universe but no more than the homogeneous universe.

[2] In the Appendix of [21], the solution for the maximally symmetric seed metric is discussed.

Next, we consider the inhomogeneities of the spatial curvature. Here we think of a simple case where the inhomogeneities are expressed by a single spatial function. We take the seed metric to be conformal to the metric of constant curvature:

$$h_{ij}(x) = \Omega^2(x) h^{\pm}_{ij}(x), \tag{2.28}$$

where $\Omega(x)$ is an arbitrary spatial function.

In this case, the Ricci and scalar curvatures are given by

$$R_{ij}(h(x)) = \pm 2 h^{\pm}_{ij}(x) - \frac{\nabla_i \nabla_j \Omega}{\Omega} + 2\frac{\nabla_i \Omega \nabla_j \Omega}{\Omega^2} - \frac{\nabla_l \nabla^l \Omega}{\Omega} h^{\pm}_{ij}, \tag{2.29}$$

$$R(h(x)) = \frac{1}{\Omega^2}\left[\pm 6 - 4\frac{\nabla_l \nabla^l \Omega}{\Omega} + 2\frac{\nabla_l \Omega \nabla^l \Omega}{\Omega^2}\right], \tag{2.30}$$

where ∇_i is the covariant derivative with respect to $h^{\pm}_{ij}$. The spatial metric, therefore, in the expansion form Eq. (2.9) becomes

$$\gamma_{ij}(t,x) = a^2(t)\left[h_{ij} + f_1(t) R_{ij}(h) + g_1(t) R(h) h_{ij} + f_2(t) R(h) R_{ij}(h) + \cdots\right] \tag{2.31}$$

$$\begin{aligned} &= a^2(t)\Bigg[\left\{\Omega^2 \pm (2f_1(t) + 6g_1(t)) + \Omega^{-2}\left[12 f_2(t) + \cdots\right] + \cdots\right\} h^{\pm}_{ij} \\ &\quad - \left\{(f_1(t) + 4g_1(t)) + \Omega^{-2}\left[\pm 14 f_2(t) + \cdots\right] + \cdots\right\} \frac{\nabla_l \nabla^l \Omega}{\Omega} h^{\pm}_{ij} \\ &\quad + \{2g_1(t) + \Omega^{-2}\left[\pm 4 f_2(t) + \cdots\right] + \cdots\} \frac{\nabla_l \Omega \nabla^l \Omega}{\Omega^2} h^{\pm}_{ij} \\ &\quad - \{f_1(t) + \Omega^{-2}\left[\pm 6 f_2(t) + \cdots\right] + \cdots\} \frac{\nabla_i \nabla_j \Omega}{\Omega} \\ &\quad + \{2f_1(t) + \Omega^{-2}\left[\pm 12 f_2(t) + \cdots\right] + \cdots\} \frac{\nabla_i \Omega \nabla_j \Omega}{\Omega^2} \\ &\quad + \left\{\Omega^{-2}\left[4 f_2(t) + \cdots\right] + \cdots\right\} \left(\frac{\nabla_l \nabla^l \Omega}{\Omega}\right)^2 h^{\pm}_{ij} + \cdots\Bigg]. \end{aligned} \tag{2.32}$$

Here we consider the situation that the spatial derivative of Ω is small. From Eq. (2.30), it means that the derivative of spatial curvature is smaller than the value of curvature itself.

Introducing

$$a^2_{\pm}(t,x) \equiv a^2(t)\left[\Omega^2(x) \pm \{2f_1(t) + 6g_1(t)\} + \Omega^{-2}(x)\{12 f_2(t) + \cdots\} + \cdots\right], \tag{2.33}$$

we rewrite Eq. (2.32) as

$$\begin{aligned} \gamma_{ij}(t,x) = a^2_{\pm}(t,\Omega)\Bigg[&h^{\pm}_{ij} + \sum_A F^A_{(2)}(t,\Omega)(\nabla^{(2)}\Omega)^A_{ij} + \sum_A F^A_{(4)}(t,\Omega)(\nabla^{(4)}\Omega)^A_{ij} + \cdots \\ &+ \sum_A F^A_{(2p)}(t,\Omega)(\nabla^{(2p)}\Omega)^A_{ij} + \cdots\Bigg]. \end{aligned} \tag{2.34}$$

Here the notation $(\nabla^{(2p)}\Omega)^A_{ij}$ denotes symbolically symmetric spatial tensors which contain $2p$ spatial gradients of $\Omega(t,x)$, where the suffix A distinguishes the tensor belonging to

the same class, and $F^A_{(2p)}(t,\Omega)$ is a function of t and $\Omega(x)$ which is determined by the Einstein equations later. This is nothing but a resummation of the usual GE. We restrict our consideration to the situation in which the series expansion Eq. (2.34), converges.

Substituting Eq. (2.34) into Eqs. (2.6) and (2.7) and neglecting the spatial gradients of Ω we obtain Eqs. (2.26) and (2.27) again for $a_\pm(t,x)$ for the zeroth order solution

$$\overset{(0)}{\gamma}{}^{\pm}_{ij}(t,x) = a^2_\pm(t,\Omega(x))h^\pm_{ij}(x). \tag{2.35}$$

In contrast to Eq. (2.25), the behavior of $a_\pm(t,x)$, defined by Eq. (2.33), depends on $\Omega(x)$. The solution of Eqs. (2.26) and (2.27) is the same form as the one for the closed (open) Friedmann universe. The new expansion scheme, Eq. (2.34), is based on the local closed (open) Friedmann universe, so we call it "the gradient expansion from a locally closed (open) Friedmann universe" (GECF (GEOF)).

Next, we consider the parts of the second order in spatial gradients of $\Omega(x)$ in Eq. (2.34). The tensors $(\nabla^{(2)}\Omega)^A_{ij}$ consist of the following four types and $\overset{(1)}{\gamma}{}^{\pm}_{ij}(t,x)$ is in the form

$$\begin{aligned}\overset{(1)}{\gamma}{}^{\pm}_{ij}(t,x) = a^2_\pm(t,x)\Bigg[&\frac{1}{3}F(t,\Omega)\frac{\nabla_l\nabla^l\Omega}{\Omega}h^\pm_{ij} + \overline{F}(t,\Omega)\frac{\overline{\nabla_i\nabla_j\Omega}}{\Omega}\\ &+\frac{1}{3}G(t,\Omega)\frac{\nabla_l\Omega\nabla^l\Omega}{\Omega^2}h^\pm_{ij} + \overline{G}(t,\Omega)\frac{\overline{\nabla_i\Omega\nabla_j\Omega}}{\Omega^2}\Bigg],\end{aligned} \tag{2.36}$$

where $\overline{\nabla_i\nabla_j\Omega/\Omega}$ and $\overline{\nabla_i\Omega\nabla_j\Omega/\Omega^2}$ are defined by

$$\frac{\overline{\nabla_i\nabla_j\Omega}}{\Omega} \equiv \frac{\nabla_i\nabla_j\Omega}{\Omega} - \frac{1}{3}\frac{\nabla_l\nabla^l\Omega}{\Omega}h^\pm_{ij}, \qquad \frac{\overline{\nabla_i\Omega\nabla_j\Omega}}{\Omega^2} \equiv \frac{\nabla_i\Omega\nabla_j\Omega}{\Omega^2} - \frac{1}{3}\frac{\nabla_l\Omega\nabla^l\Omega}{\Omega^2}h^\pm_{ij}.$$

From Eqs. (2.32) and (2.36), we see that functions F, $\overline{F}$, G, and $\overline{G}$ are expressed as

$$\begin{aligned}F(t,\Omega) &= -\frac{a}{a_\pm}{}^2\left\{[4f_1(t)+12g_1(t)] + \Omega^{-2}\left[\pm 48 f_2(t)+\cdots\right]+\cdots\right\},\\ \overline{F}(t,\Omega) &= -\frac{a}{a_\pm}{}^2\left\{f_1(t) + \Omega^{-2}\left[\pm 6 f_2(t)+\cdots\right]+\cdots\right\},\\ G(t,\Omega) &= \frac{a}{a_\pm}{}^2\left\{[2f_1(t)+6g_1(t)] + \Omega^{-2}\left[\pm 24 f_2(t)+\cdots\right]+\cdots\right\},\\ \overline{G}(t,\Omega) &= \frac{a}{a_\pm}{}^2\left\{2f_1(t) + \Omega^{-2}\left[\pm 12 f_2(t)+\cdots\right]+\cdots\right\}.\end{aligned}$$

These functions contain all orders of coefficients of the usual GE f_1, g_1, f_2, $\cdots$ which appear in Eq. (2.31). When Ω is large so that ${}^3R$ is small, the GECF (GEOF) reduces to the GEFF.

From Eq. (2.8), we obtain

$$u_i = \frac{(2-3\Gamma)\left[2\left(\dot{a}'_\pm/a_\pm - \dot{a}_\pm a'_\pm/a^2_\pm\right)\Omega - \dot{\overline{F}}\right]}{2\Gamma\left[3\ddot{a}_\pm/a_\pm - \Lambda\right]}\frac{\nabla_i\Omega}{\Omega}, \tag{2.37}$$

where the prime denotes the differentiation with respect to Ω.

Substituting $\gamma_{ij} = \overset{(0)}{\gamma}{}^{\pm}_{ij} + \overset{(1)}{\gamma}{}^{\pm}_{ij}$ and u_i given by Eqs. (2.35), (2.36), and (2.37) into Eq. (2.6), and comparing the coefficients of the second order derivative terms of Ω, we obtain evolution equations

$$\ddot{F} + 3\Gamma\frac{\dot{a}_\pm}{a_\pm}\dot{F} = -\frac{(2-3\Gamma)}{a_\pm^2}\left[\pm F - \overline{F} + 2\frac{a'_\pm\Omega}{a_\pm}\right], \tag{2.38}$$

$$\dot{\overline{F}} + 3\frac{\dot{a}_\pm}{a_\pm}\dot{\overline{F}} = \frac{2}{a_\pm^2}\left[\frac{a'_\pm\Omega}{a_\pm} + 2(\pm\overline{F} - \overline{F})\right], \tag{2.39}$$

$$\begin{aligned}\ddot{\widetilde{G}} + 3\Gamma\frac{\dot{a}_\pm}{a_\pm}\dot{\widetilde{G}} = &-\frac{(4-3\Gamma)(2-3\Gamma)}{2\Gamma a_\pm\left(3\ddot{a}_\pm - \Lambda a_\pm\right)}\left[\dot{\overline{F}} - 2\left(\frac{\dot{a}'_\pm}{a_\pm} - \frac{\dot{a}_\pm a'_\pm}{a_\pm^2}\right)\Omega\right]^2 \\ &-\frac{(2-3\Gamma)}{a_\pm^2}\left[\pm G + \overline{F} - \overline{F}'\Omega \pm 2\overline{F}^2 - \overline{F}^2 + \Omega^2\left(2\frac{a''_\pm}{a_\pm} - \frac{a'^2_\pm}{a_\pm^2}\right)\right],\end{aligned} \tag{2.40}$$

$$\begin{aligned}\ddot{\widehat{G}} + 3\frac{\dot{a}_\pm}{a_\pm}\dot{\widehat{G}} = &\frac{(2-3\Gamma)}{\Gamma a_\pm\left(3\ddot{a}_\pm - \Lambda a_\pm\right)}\left[\dot{\overline{F}} - 2\left(\frac{\dot{a}'_\pm}{a_\pm} - \frac{\dot{a}_\pm a'_\pm}{a_\pm^2}\right)\Omega\right]^2 \\ &+\frac{2}{a_\pm^2}\left[\pm 2\overline{G} + 2\overline{F} - 2\overline{F}'\Omega - (\pm 2 + \frac{1}{2})\overline{F}^2 - 2\left(\frac{a'_\pm\Omega}{a_\pm}\right)^2 + \frac{a''_\pm\Omega^2}{a_\pm}\right],\end{aligned} \tag{2.41}$$

where we put $\widetilde{G} \equiv G + \overline{F}^2$ and $\widehat{G} \equiv \overline{G} - \frac{1}{2}\overline{F}^2$ for the simplicity of the equation form. Readers should pay attention to the commutation relation of the covariant derivative which is not vanishing because the spatial curvature in the lowest order solution has a non zero constant curvature. To solve Eqs. (2.38)–(2.41), we need to know the time evolution of $\overline{F}'$. Differentiating Eq. (2.39) we find that $\overline{F}'$ must satisfy the equation

$$\begin{aligned}\dot{\overline{F}}' + 3\frac{\dot{a}_\pm}{a_\pm}\dot{\overline{F}}' = &\frac{2}{a_\pm^2}\left[\frac{a'_\pm}{a_\pm} + \frac{a''_\pm\Omega}{a_\pm} - 3\frac{{a'_\pm}^2\Omega}{a_\pm^2} - 4\frac{a'_\pm}{a_\pm}(\pm\overline{F} - \overline{F}) + 2(\pm\overline{F}' - \overline{F}')\right] \\ &-3\dot{\overline{F}}\left[\frac{\dot{a}'_\pm a_\pm - \dot{a}_\pm a'_\pm}{a_\pm^2}\right].\end{aligned} \tag{2.42}$$

Similarly we can calculate the higher order solutions in the form (2.34) iteratively. In the case of $p = 1, 2$, the explicit form of $(\nabla^{(2p)}\Omega)^A_{ij}$ appears in the Appendix D.

This expansion scheme is valid when the characteristic physical scale of inhomogeneities of the spatial curvature is larger than the Hubble radius $(\dot{a}/a)^{-1}$ or the spatial curvature radius $(\overset{(0)}{{}^3R})^{-1/2}$. If the Hubble radius is smaller than the spatial curvature radius, this expansion scheme reduces to a special case of the usual GE.

2.3 Application of onset of inflation in inhomogeneous cosmology

The main objective of inflationary scenario [44] is to explain why the present universe is homogeneous and isotropic on large scales without a fine-tuning of initial conditions. It is important to study the generality of initial conditions for the onset of inflation.

Many works on inflation assume homogeneous and flat universe at the pre-inflationary phase [45]. In this case, inflation is generic. The spatial curvature effect on the occurrence of inflation is investigated in the Friedmann-Robertoson-Walker model with a massive scalar field by Belinsky *et al.* [46], and in the Bianchi IX model with a cosmological constant by Wald [28]. They concluded that inflation is not a general property and only the positive spatial curvature can prevent the universe from inflating.

On the other hand, the role of initial inhomogeneities on the occurrence of inflation was studied by a linear approximation in the AE [25] and by a numerical simulation with special symmetries [23, 24]. In [23], Goldwirth and Piran concluded that the crucial feature necessary for inflation is a sufficient high average value of the scalar field which drives inflation over a region of several Hubble radius.

We study how the initial inhomogeneities of the universe affect the onset of inflation by use of an alternative approach. In order to treat the inhomogeneities of the universe, we use the long wavelength approximation.

Recently, the influence of initial inhomogeneities on the occurrence of inflation is studied by using the GE method [26, 27, 43]. From investigations in the homogeneous universe model, as noted above, the effect of positive curvature is important because it can prevent inflation. So, we should investigate the inhomogeneities of universe with a nonsmall positive spatial curvature to clarify the generality of inflation. However, the lowest order solution in the GE method is a locally flat Friedmann universe and the spatial curvature is treated as a small quantity in the expansion scheme.

In this section, by using the improved GE so that the nonsmall spatial curvature associated with a three-space is conformal to the constant curvature is tractable in the lowest order, we study how the inhomogeneities of the spatial curvature affect the occurrence of inflation in the closed universe.

We shall consider the two cases as an inflation model. One is a model in which the cosmological constant gives rise to inflation instead of the scalar field and a radiation fluid fills the universe. The other is a chaotic inflation model which is driven by a massive scalar field in the inhomogeneous universe. The inhomogeneous universe can be constructed by use of the first order approximation of the GECF. We will show the condition of the inhomogeneities of the spatial curvature for the universe to enter the inflationary phase.

2.3.1 Radiation fluid and cosmological constant case

In this subsection, we consider a simple model, in which the inflation is driven by a cosmological constant Λ. We construct the inhomogeneous universe by the GECF which is introduced in the previous section. The matter is taken to be a radiation fluid with $\Gamma = 4/3$ for simplicity.

Basic equations in GECF

We get the lowest order solution of Eqs. (2.26) and (2.27) for the system in the form

$$a_+^2(t, \Omega(x)) \equiv \frac{1}{2H_0^2}\left[2H_0^2\Omega^2 \sinh(2H_0 t) + 1 - \cosh(2H_0 t)\right], \tag{2.43}$$

$$\overset{(0)}{\rho} = \frac{3H_0^2\Omega^4}{\kappa a_+^4}. \tag{2.44}$$

Here we see the behavior of the locally closed Friedmann solution Eq. (2.43). The solution has an early phase during which the local scale factor behaves as $a_+ \propto t^{1/2}$. After the period, the behavior of local scale factor depends on the local value of $\Omega(x)$. The local scale factor $a_+(t,x)$ with $\Omega(x) > \Omega_{cr}$ approaches the de Sitter solution [3] and $a_+(t,x)$ with $\Omega(x) < \Omega_{cr}$ recollapses to the singularity, where $\Omega_{cr} \equiv \sqrt{1/(2H_0^2)}$. The local scale factor $a_+(t,x)$ with the critical value of $\Omega = \Omega_{cr}$ approaches a static solution:

$$a_+^2 = \frac{3}{2\Lambda}, \quad \overset{(0)}{\rho} = \frac{\Lambda}{\kappa}. \tag{2.45}$$

In the early stage $t \ll H_0^{-1}$, the local scale factor is proportional to $\Omega(x)t^{1/2}$ then the spatial curvature ${}^3R$ is proportional to $1/(\Omega^2 t)$. The fate of the local scale factor is determined by the value of ${}^3R(t,x)t$ in the lowest order. The condition for the occurrence of inflation is

$$\frac{1}{\Omega^2} < \frac{1}{\Omega_{cr}^2}. \tag{2.46}$$

In other words, it is

$${}^3R_{init} < {}^3R_{cr}(t) \equiv \frac{3}{\Omega_{cr}^2}\frac{1}{H_0 t}, \tag{2.47}$$

where ${}^3R_{init}$ is the spatial curvature in the early phase $t \ll H_0^{-1}$.

Next, we consider the first order corrections which are proportional to the second order of spatial gradients of $\Omega(x)$ in the form

$$\begin{aligned}\overset{(1)}{\gamma}{}_{ij}^{+}(t,x) = a_+^2(t,\Omega(x))\Bigg[&\frac{1}{3}F(t,\Omega)\frac{\nabla_l\nabla^l\Omega}{\Omega}h_{ij}^+ + \overline{F}(t,\Omega)\frac{\overline{\nabla_i\nabla_j\Omega}}{\Omega} \\ &+\frac{1}{3}G(t,\Omega)\frac{\nabla_l\Omega\nabla^l\Omega}{\Omega^2}h_{ij}^+ + \overline{G}(t,\Omega)\frac{\overline{\nabla_i\Omega\nabla_j\Omega}}{\Omega^2}\Bigg].\end{aligned} \tag{2.48}$$

From Eqs. (2.38)–(2.42), the equations for F, $\overline{F}$, G, and $\overline{G}$ reduce to

$$\ddot{F} + 4\left(\frac{\dot{a}_+}{a_+}\right)\dot{F} = \frac{2}{a_+^2}\left[F - \overline{F} + \frac{2\Omega^2\sinh(2H_0t)}{a_+^2}\right], \tag{2.49}$$

$$\ddot{\widetilde{G}} + 4\left(\frac{\dot{a}_+}{a_+}\right)\dot{\widetilde{G}} = \frac{2}{a_+^2}\left[\widetilde{G} + \overline{F} - \overline{F}'\Omega + \frac{\Omega^2\sinh(2H_0t)}{a_+^2}\left(2 - \frac{3\Omega^2\sinh(2H_0t)}{a_+^2}\right)\right], \tag{2.50}$$

$$\ddot{\overline{F}} + 3\left(\frac{\dot{a}_+}{a_+}\right)\dot{\overline{F}} = \frac{2}{a_+^2}\left[\frac{\Omega^2\sinh(2H_0t)}{a_+^2}\right], \tag{2.51}$$

$$\begin{aligned}\ddot{\widehat{G}} + 3\left(\frac{\dot{a}_+}{a_+}\right)\dot{\widehat{G}} = \frac{2}{a_+^2}&\left[2\widehat{G} + 2\overline{F} - 2\overline{F}'\Omega - \frac{3\overline{F}^2}{2} + \frac{\Omega^2\sinh(2H_0t)}{a_+^2}\left(1 - \frac{3\Omega^2\sinh(2H_0t)}{a_+^2}\right)\right] \\ &+\frac{1}{2H_0^4\Omega^4a_+^6}\left[2\Omega^2(\cosh(2H_0t) - 1) - H_0a_+^4\dot{\overline{F}}\right]^2.\end{aligned} \tag{2.52}$$

[3] In the de Sitter solution, the local scale factor behaves as $a_+ \propto \exp(2H_0t)$.

For $\overline{F}'$ we get

$$\ddot{\overline{F}}' + 3\frac{\dot{a}_+}{a_+}\dot{\overline{F}}' = \frac{4\Omega\sinh(2H_0t)}{a_+^4}\left[1 - \frac{2\Omega^2\sinh(2H_0t)}{a_+^2}\right] - 3\dot{\overline{F}}\frac{\Omega}{H_0 a_+^4}(\cosh(2H_0t) - 1). \tag{2.53}$$

Numerical results

We solve Eqs. (2.49)–(2.53) by numerical integration. These coupled ordinary differential equations have growing and decaying solutions. In the course of time, since the growing mode dominates the solution, we concentrate on the growing solution. Then we choose initial conditions for F, $\overline{F}$, $\overline{F}'$, $\widetilde{G}$, and $\widehat{G}$ in the form

$$F = \overline{F} = \overline{F}' = \widetilde{G} = \widehat{G} = 0. \tag{2.54}$$

The growing mode is generated by the source terms in the right hand side of Eqs. (2.49)–(2.53). In order to take a growing mode solution, asymptotic behaviors of these variables at the early time should be

$$F = \frac{1}{\Omega^2 H_0}t, \quad \overline{F} = \frac{2}{3\Omega^2 H_0}t, \quad \overline{F}' = -\frac{4}{3\Omega^3 H_0}t, \quad \widetilde{G} = -\frac{1}{2\Omega^2 H_0}t, \quad \widehat{G} = -\frac{4}{3\Omega^2 H_0}t. \tag{2.55}$$

The time evolution of F and $\widetilde{G}$ is shown in Figs. 2.2 and 2.3. In the case of $\Omega > \Omega_{cr}$, F and $\widetilde{G}$ grow for a while and become constant as the universe expands exponentially. And in the case of $\Omega < \Omega_{cr}$, they grow and diverge and the approximation breaks down [47].

We demonstrate a time evolution of the spatial scalar curvature given by Eq. (E.3) (see Fig. 2.4). When we fix initial time, there are infinite number of combinations of parameters $(\Omega, \nabla_l\nabla^l\Omega/\Omega, \nabla_l\Omega\nabla_l\Omega/\Omega^2)$ which give the same value of ${}^3R$. Time evolution of ${}^3R$ depends on the parameters. Fixing Ω, we vary $\nabla_l\Omega\nabla_l\Omega/\Omega^2$ and $\nabla_l\nabla^l\Omega/\Omega$ keeping ${}^3R$ constant. When Ω is fixed, since the evolution of ${}^{3\overset{(0)}{}}R$ depends only on Ω, the time evolution of ${}^3R$ depends on $\nabla_l\Omega\nabla_l\Omega/\Omega^2$. We see from Fig. 2.4 that when $\nabla_l\Omega\nabla_l\Omega/\Omega^2$ is large ${}^3R$ grows rapidly.

By the use of the trace part of the corrections, we define an effective local scale factor which includes up to first order by

$$\begin{aligned} a_{\mathit{eff}}(t,x) &\equiv \left[\det\left[\overset{(0)}{\gamma}_{ij}^{+} + \overset{(1)}{\gamma}_{ij}^{+}\right]\right]^{1/6} \\ &= a_+(t,\Omega)\left[1 + \frac{1}{6}F(t,\Omega)\frac{\nabla_l\nabla^l\Omega}{\Omega} + \frac{1}{6}\widetilde{G}(t,\Omega)\frac{\nabla_l\Omega\nabla^l\Omega}{\Omega^2}\right]. \end{aligned} \tag{2.56}$$

The effective local scale factor $a_{\mathit{eff}}(t,x)$ describes how the universe expands at the point x.

We can follow the evolution of the effective local scale factor $a_{\mathit{eff}}(t,x)$ by the evolution of $F(t,\Omega)$ and $G(t,\Omega)$. As is already seen, at lowest order the behavior of the local

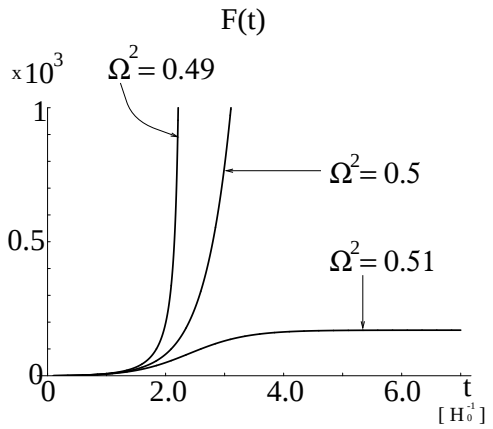

Fig. 2.2 A typical example of the time evolution of $F(t)$.

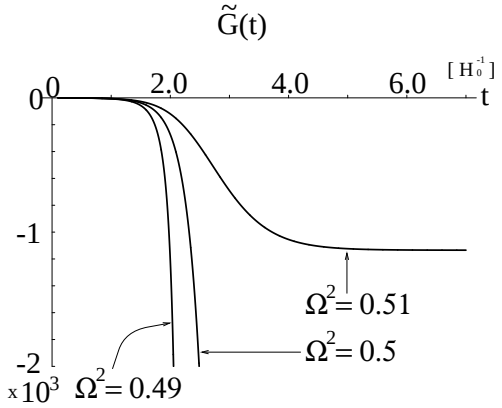

Fig. 2.3 A typical example of the time evolution of $\widetilde{G}(t)$.

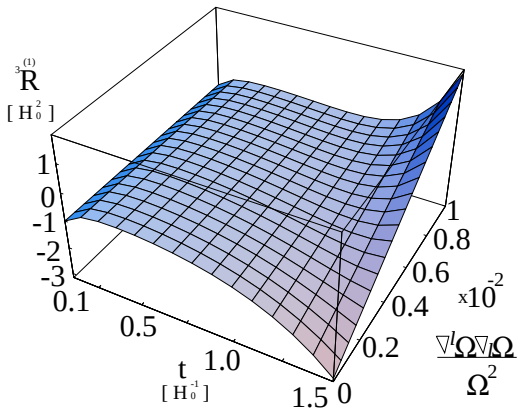

Fig. 2.4 Evolution of the spatial curvature which has the same initial value but different $\nabla_l\Omega\nabla^l\Omega/\Omega^2$.

scale factor $a_+(t,\Omega)$ is determined by the value of $\Omega(x)$. On the other hand, the spatial derivatives of Ω affect the time evolution of $a_{\mathit{eff}}(t,x)$ at first order. This means that the effective local scale factor evolves under the influence of the local value of Ω and the value of it in the neighborhood. If a point in the three-dimensional parameter space $(\Omega, \nabla_l\nabla^l\Omega/\Omega, \nabla_l\Omega\nabla_l\Omega/\Omega^2)$ is specified we know the time evolution of the effective local scale factor $a_{\mathit{eff}}(t,x)$.

The effective local expansion rate and acceleration rate are given by

$$\frac{\dot{a}_{\mathit{eff}}}{a_{\mathit{eff}}} = \frac{\dot{a}_+}{a_+} + \frac{1}{6}\left[\dot{F}(t,\Omega)\frac{\nabla_l\nabla^l\Omega}{\Omega} + \dot{\tilde{G}}(t,\Omega)\frac{\nabla_l\Omega\nabla^l\Omega}{\Omega^2}\right], \tag{2.57}$$

$$\frac{\ddot{a}_{\mathit{eff}}}{a_{\mathit{eff}}} = \frac{\ddot{a}_+}{a_+} + \frac{1}{6}\left[\ddot{F}(t,\Omega) + 2\frac{\dot{a}_+}{a_+}\dot{F}(t,\Omega)\right]\frac{\nabla_l\nabla^l\Omega}{\Omega} + \frac{1}{6}\left[\ddot{\tilde{G}}(t,\Omega) + 2\frac{\dot{a}_+}{a_+}\dot{\tilde{G}}(t,\Omega)\right]\frac{\nabla_l\Omega\nabla^l\Omega}{\Omega^2}. \tag{2.58}$$

When the correction terms which contain the second order derivatives grow to be as large as the lowest order term, the expansion scheme breaks down. Since the first order terms in Eq. (2.34) contain all of the second order spatial derivatives, then when $(\dot{a}_+/a_+)^2 > {}^3\overset{(0)}{R}$, the GECF reduces to the GEFF. We, thus, assume the approximation is valid if

$$\left|\frac{\det(\overset{(0)}{\gamma}{}^+_{ij} + \overset{(1)}{\gamma}{}^+_{ij}) - \det\overset{(0)}{\gamma}{}^+_{ij}}{\det\overset{(0)}{\gamma}{}^+_{ij}}\right| < 0.5, \tag{2.59}$$

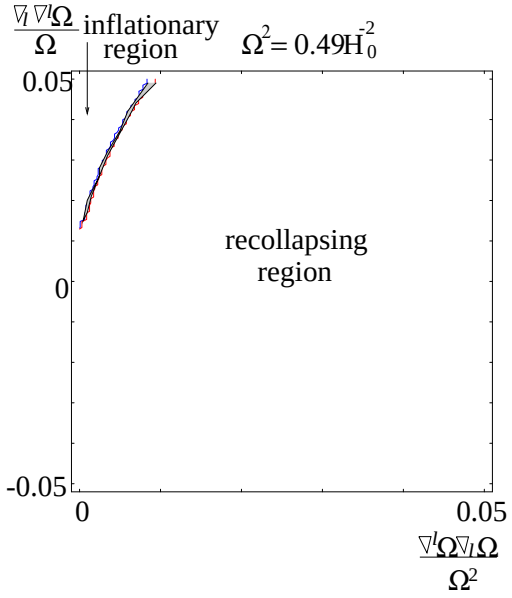

Fig. 2.5 An inflationary region and a recollapsing region are shown in the three dimensional parameter space $(\Omega, \nabla_l \nabla^l \Omega/\Omega, \nabla_l \Omega \nabla^l \Omega/\Omega^2)$. A meshed region is a region where the approximation breaks down. At lowest order, universe will recollapse.

$$\left| \frac{{}^3\overset{(1)}{R}}{\max\{(\dot{a}_+/a_+)^2, {}^3\overset{(0)}{R}\}} \right| < 0.5. \tag{2.60}$$

We divide the three-dimensional parameter space $(\Omega, \nabla_l \nabla^l \Omega/\Omega, \nabla_l \Omega \nabla_l \Omega/\Omega^2)$ into two regions: inflationary region and recollapsing region (see Figs. 2.5–2.7). The effective local scale factor with the parameters in the inflationary region enters the accelerating expansion phase: $\dot{a}_{\mathit{eff}}/a_{\mathit{eff}} > 0$ and $\ddot{a}_{\mathit{eff}}/a_{\mathit{eff}} > 0$. On the other hand, the effective local scale factor with the parameters in the recollapsing region enters recollapsing phase: $\dot{a}_{\mathit{eff}}/a_{\mathit{eff}} < 0$ and $\ddot{a}_{\mathit{eff}}/a_{\mathit{eff}} < 0$. Between these two regions, there emerges a fuzzy region where error becomes large and either Eq. (2.59) or Eq. (2.60) does not hold before the effective local scale factor enters the inflationary or recollapsing phase.

From Figs. 2.5–2.7, we get the criterion for the occurrence of inflation in the vicinity of $\Omega/\Omega_{cr} - 1 = \nabla_l \nabla^l \Omega/\Omega = \nabla_l \Omega \nabla^l \Omega/\Omega^2 = 0$ in a simple time independent form:

$$\frac{1}{\Omega^2}\left[1 + \alpha\left(-\frac{\nabla_l \nabla^l \Omega}{\Omega} + \beta \frac{\nabla_l \Omega \nabla^l \Omega}{\Omega^2}\right)\right] < \frac{1}{\Omega_{cr}^2}, \tag{2.61}$$

where $\alpha \sim 5/4$ and $\beta \sim 6$. If the condition Eq. (2.61) holds, the effective local scale factor enters the inflationary phase. By the use of Eq. (E.3) in the limit $t \to 0$, the criterion (2.61) is translated into

$${}^3R_{init} + \widetilde{\alpha}\left[\frac{({}^3R_{init})_{;l}^{\ ;l}}{{}^3R_{init}} + \widetilde{\beta}\frac{({}^3R_{init})_{;l}({}^3R_{init})^{;l}}{{}^3R_{init}^2}\right] < {}^3R_{cr}(t), \tag{2.62}$$

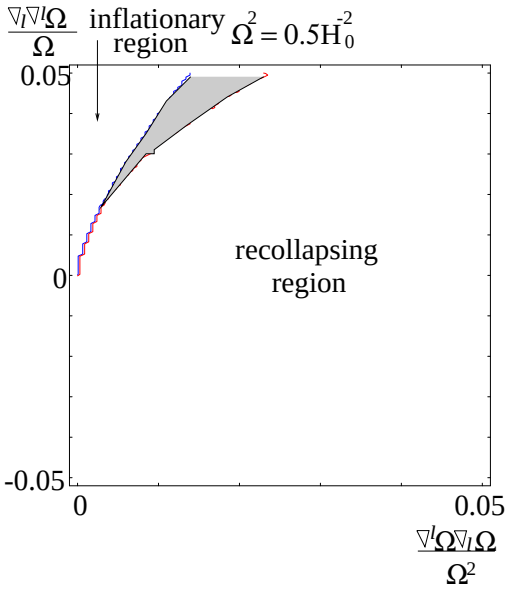

Fig. 2.6 An inflationary region and a recollapsing region are shown in the three dimensional parameter space $(\Omega, \nabla_l\nabla^l\Omega/\Omega, \nabla_l\Omega\nabla^l\Omega/\Omega^2)$. A meshed region is a region where the approximation breaks down. At lowest order, universe will approach a static solution.

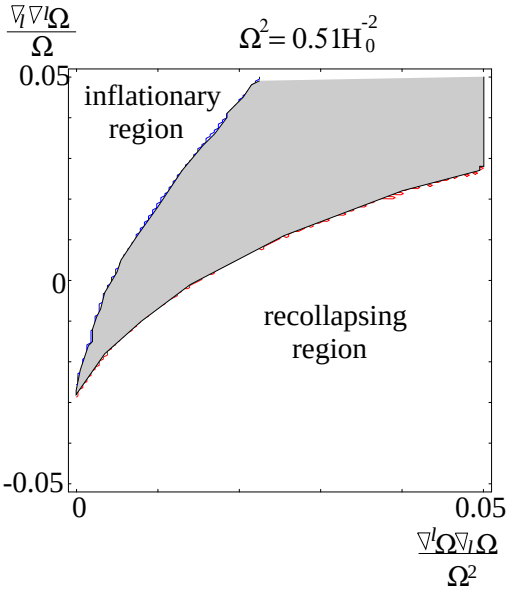

Fig. 2.7 An inflationary region and a recollapsing region are shown in the three dimensional parameter space $(\Omega, \nabla_l\nabla^l\Omega/\Omega, \nabla_l\Omega\nabla^l\Omega/\Omega^2)$. A meshed region is a region where the approximation breaks down. At lowest order, universe will inflate.

where $\widetilde{\alpha} \sim 9/5$ and $\widetilde{\beta} \sim 4$ and ${}^3R_{cr}(t)$ is given in Eq. (2.47). Equations (2.61) and (2.62) correspond to Eqs. (2.46) and (2.47). Equation (2.62) means that the occurrence of inflation at a spatial point is determined by ${}^3R_{init}$ and its gradients. The spatial curvature at an early time t should be less than the critical curvature value ${}^3R_{cr}(t)$ over a region which has several times size of the local curvature radius $[{}^3R_{init}(t)]^{-1/2}$ for the onset of inflation in the future, where ${}^3R_{cr}(t)$ is the marginal value for inflation of the closed Friedmann universe.

2.3.2 Scalar field case

In this subsection, we consider a chaotic inflation model with a massive scalar field, i.e., $V(\phi) = \frac{1}{2}m^2\phi^2$ as an inflaton field. By the GECF method, we construct the inhomogeneous universe with a scalar field minimaly coupled to gravity and apply to the ploblm of the onset of inflation.

Basic equations in GECF

We explain the GECF with a scalar field minimally coupled to gravity [48].

The energy-momentum tensor of a scalar field is given by

$$T_{\mu\nu} = \phi_{,\mu}\phi_{,\nu} - g_{\mu\nu}\left[\frac{1}{2}\phi_{,\lambda}\phi^{,\lambda} + V(\phi)\right], \tag{2.63}$$

where $V(\phi)$ is the potential of the scalar field. In the synchronous reference frame Eq. (2.1), the Einstein equations for the gravitational field coupled to the scalar field read

$$\frac{1}{2}\dot{K} + \frac{1}{4}K^l_m K^m_l = \kappa\left[-\dot{\phi}^2 + V(\phi)\right], \tag{2.64}$$

$${}^3R^j_i + \frac{1}{2\sqrt{\gamma}}\frac{\partial}{\partial t}(\sqrt{\gamma}K^j_i) = \kappa\left[\partial_i\phi\partial^j\phi + V(\phi)\delta^j_i\right], \tag{2.65}$$

$$\frac{1}{2}(K^j_{i;j} - K_{,i}) = \kappa\dot{\phi}\partial_i\phi, \tag{2.66}$$

where ${}^3R^j_i$ is the Ricci tensor associated with γ_{ij}, $K_{ij} \equiv \dot{\gamma}_{ij}$, $K \equiv \gamma^{ij}K_{ij}$, $\gamma \equiv \det\gamma_{ij}$, and a semicolon denotes the covariant derivative with respect to γ_{ij}. The equation of motion for the scalar field is

$$\ddot{\phi} + \frac{1}{2}K\dot{\phi} - \phi^{;l}_{;l} + \frac{dV(\phi)}{d\phi} = 0. \tag{2.67}$$

In this case, since we don't have the explicit form of the lowest order solution, we don't know how the function $\Omega(x)$ which is introduced in the previous section, depends on the metric and the scalar filed at lowest order. Here we show the GECF method in such a situation.

Now, we assume the metric in the form (2.35)

$$\overset{(0)}{\gamma}_{ij}(t,x) = a^2(t,\Omega(x))h_{ij}(x), \tag{2.68}$$

where $h_{ij}(x)$ is the metric of a three-dimensional sphere whose Ricci curvature is $R_{ij}(h_{kl}) = 2h_{ij}$ [4] . The scale factor $a(t, \Omega(x))$ in the spatial metric, Eq. (2.68), has the spacedependence by an arbitrary function $\Omega(x)$.

In the usual GE method, all spatial gradients of $\overset{(0)}{\gamma}_{ij}(t, x)$ are assumed to be much smaller than time derivatives. Roughly speaking, the spatial curvature ${}^3R$ is assumed to be smaller than K^2 and is neglected in the lowest approximation. Here, we consider slightly different approximation. The spatial scalar curvature for the metric in the form of Eq. (2.68) is

$$ {}^3R(\overset{(0)}{\gamma}_{ij}) = \frac{6}{a^2(t,\Omega)} + \frac{1}{a^2(t,\Omega)}\left[-4\frac{a'}{a}\Omega\frac{\nabla_l\nabla^l\Omega}{\Omega} + 2\left(\frac{a'^2}{a^2} - 2\frac{a''}{a}\right)\Omega^2\frac{\nabla_l\Omega\nabla^l\Omega}{\Omega^2}\right], \tag{2.69} $$

where a prime denotes the derivative with respect to Ω and ∇_l denotes the covariant derivative with respect to h_{ij}. We assume that the second term in the right-hand side of Eq. (2.69) which contains spatial gradients of Ω is smaller than the first term. If we set ${}^3\overset{(0)}{R}(\overset{(0)}{\gamma}_{ij}) \equiv 6a^{-2}(t, \Omega)$, Eq. (2.69) is rewritten in the form

$$ {}^3R(\overset{(0)}{\gamma}_{ij}) = {}^3\overset{(0)}{R}(\overset{(0)}{\gamma}_{ij}) + \left[2\frac{{}^3\overset{(0)}{R}{}_{;l}^{;l}}{{}^3\overset{(0)}{R}} - \frac{3}{2}\frac{{}^3\overset{(0)}{R}{}_{;l}\,{}^3\overset{(0)}{R}{}^{;l}}{{}^3\overset{(0)}{R}{}^2}\right]. \tag{2.70} $$

Thus the case we consider here is that the spatial variation of the spatial curvature is smaller than the value of itself. All spatial gradients of $\Omega(x)$ are neglected in the first step of our approach. It should be noted that even if the second term in Eq. (2.69) or (2.70) exceeds the first term, the approximation reduces to a special case of the usual GE so far as these are smaller than K^2.

Though the metric in the form of Eq. (2.68) dose not have adequate degree of gravitational freedom, the simple form on which we concentrate is useful to investigate the inhomogeneities of the spatial curvature. It might be very complicate to treat the general form of inhomogeneities of curvature [42].

From now on, we consider that the spatial metric in the lowest order is described by Eq. (2.68). Substituting Eq. (2.68) into Eq. (2.64), and neglecting all spatial derivatives of $\Omega(x)$, we obtain the equation which a and ϕ must satisfy

$$ \frac{\ddot{a}(t,\Omega(x))}{a(t,\Omega(x))} = \frac{\kappa}{3}\left[-\dot{\phi}^2(t,x) + V(\phi(t,x))\right]. \tag{2.71} $$

From Eq. (2.71), it is natural that the scalar field has the spacedependence through $\Omega(x)$. We assume that the form of the scalar field in the lowest order is

$$ \overset{(0)}{\phi}(t,x) = \phi_0(t,\Omega(x)). \tag{2.72} $$

Substituting Eqs. (2.68) and (2.72) into Eqs. (2.65) and (2.67), and neglecting all spatial derivatives of $\Omega(x)$, we have

$$ \frac{\ddot{a}(t,\Omega)}{a(t,\Omega)} + 2\left(\frac{\dot{a}(t,\Omega)}{a(t,\Omega)}\right)^2 + \frac{2}{a^2(t,\Omega)} = \kappa V(\phi_0(t,\Omega)), \tag{2.73} $$

[4] Hereafter $a(t, \Omega(x))$ is used in place of $a_+(t, \Omega(x))$.

$$\ddot{\phi}_0(t,\Omega) + 3\frac{\dot{a}(t,\Omega)}{a(t,\Omega)}\dot{\phi}_0(t,\Omega) + \frac{dV(\phi_0(t,\Omega))}{d\phi_0(t,\Omega)} = 0. \tag{2.74}$$

Equation (2.66) is trivial in the lowest order. Equations (2.71), (2.73), and (2.74) have the same form of the equations for the closed Friedmann universe with a homogeneous scalar field.

At next order, we consider the second order in spatial gradients of $\Omega(x)$. We will take corrections to the metric and the scalar field of the form

$$\overset{(1)}{\gamma}_{ij}(t,x) = a^2(t,\Omega)\left[\frac{1}{3}F(t,\Omega)\frac{\nabla_l\nabla^l\Omega}{\Omega}h_{ij} + \overline{F}(t,\Omega)\frac{\overline{\nabla_i\nabla_j\Omega}}{\Omega} + \frac{1}{3}G(t,\Omega)\frac{\nabla_l\Omega\nabla^l\Omega}{\Omega^2}h_{ij} + \overline{G}(t,\Omega)\frac{\overline{\nabla_i\Omega\nabla_j\Omega}}{\Omega^2}\right], \tag{2.75}$$

$$\overset{(1)}{\phi}(t,x) = P(t,\Omega)\frac{\nabla_l\nabla^l\Omega}{\Omega} + Q(t,\Omega)\frac{\nabla_l\Omega\nabla^l\Omega}{\Omega^2}. \tag{2.76}$$

Substituting $\gamma_{ij} = \overset{(0)}{\gamma}_{ij} + \overset{(1)}{\gamma}_{ij}$ and $\phi = \overset{(0)}{\phi} + \overset{(1)}{\phi}$ given by Eqs. (2.68), (2.75), (2.72), and (2.76) into the Einstein equations and the equation of motion for the scalar field, Eqs. (2.64)–(2.67), and comparing the coefficients of the derivative of Ω, we get the first order equations which govern the evolution of variables F, $\overline{F}$, G, $\overline{G}$, P, and Q. We should perform tedious calculation to get ${}^3R^i_j$ associated with $\gamma_{ij} = \overset{(0)}{\gamma}_{ij} + \overset{(1)}{\gamma}_{ij}$. The expression of it in the first order approximation appears in the Appendix E.

From Eq. (2.65), we obtain

$$\ddot{F} + 6H\dot{F} = 6\kappa\frac{dV}{d\phi}\Big|_0 P + \frac{4}{a^2}\left[F - \overline{F} + 2\frac{a'}{a}\Omega\right], \tag{2.77}$$

$$\ddot{\overline{F}} + 3H\dot{\overline{F}} = \frac{2a'}{a^3}\Omega, \tag{2.78}$$

$$\ddot{\widetilde{G}} + 6H\dot{\widetilde{G}} = 6\kappa\frac{dV}{d\phi}\Big|_0 Q + \frac{2\kappa}{a^2}\phi_0'^2\Omega^2 + \frac{4}{a^2}\left[\widetilde{G} + \overline{F} - \overline{F}'\Omega + \left(2\frac{a''}{a} - \frac{a'^2}{a^2}\right)\Omega^2\right], \tag{2.79}$$

$$\ddot{\widehat{G}} + 3H\dot{\widehat{G}} = \frac{2\kappa}{a^2}\phi_0'^2\Omega^2 + \frac{2}{a^2}\left[2\widehat{G} + 2\overline{F} - 2\overline{F}'\Omega - \frac{3}{2}\overline{F}^2 + \left(\frac{a''}{a} - \frac{2a'^2}{a^2}\right)\Omega^2\right], \tag{2.80}$$

where $\dfrac{dV}{d\phi}\Big|_0$ is the lowest order value of $\dfrac{dV}{d\phi}$, $H \equiv \dot{a}/a$, $\widetilde{G} \equiv G + \overline{F}^2$, and $\widehat{G} \equiv \overline{G} - \frac{1}{2}\overline{F}^2$. From Eq. (2.67), we have

$$\ddot{P} + 3H\dot{P} + \frac{d^2V}{d\phi^2}\Big|_0 P = -\frac{1}{2}\dot{\phi}_0\dot{F} + \frac{1}{a^2}\phi_0'\Omega, \tag{2.81}$$

$$\ddot{Q} + 3H\dot{Q} + \frac{d^2V}{d\phi^2}\Big|_0 Q = -\frac{1}{2}\dot{\phi}_0\dot{\widetilde{G}} + \frac{1}{a^2}\left[\phi_0'' + \frac{a'}{a}\phi_0'\right]\Omega^2. \tag{2.82}$$

From Eqs. (2.64) and (2.66), we obtain

$$\dot{\overline{F}} = 2\left[\frac{\dot{a}'}{a} - \frac{\dot{a}a'}{a^2}\right]\Omega + \kappa\dot{\phi}_0\phi_0'\Omega, \tag{2.83}$$

$$\ddot{\overline{F}} + 2H\dot{\overline{F}} = 2\kappa\left[-2\dot{\phi}_0\dot{P} + \frac{dV}{d\phi}\Big|_0 P\right], \tag{2.84}$$

$$\ddot{\widetilde{G}} + 2H\dot{\widetilde{G}} = 2\kappa\left[-2\dot{\phi}_0\dot{Q} + \frac{dV}{d\phi}\Big|_0 Q\right] + \dot{\overline{F}}^2. \tag{2.85}$$

There are nine equations (2.77)–(2.85) for the six variables F, $\overline{F}$, $\widetilde{G}$, $\widehat{G}$, P, and Q. All of these equations are not independent. Six equations govern the evolution and three are constraint conditions. So we find a solution of Eqs. (2.77)–(2.82) with an initial condition which satisfies the constraints. In order to solve these equations, we need to know the time evolution of a', a'', ϕ_0', ϕ_0'', and $\overline{F}'$. Differentiating Eqs. (2.71), (2.73), (2.74), and (2.83), we obtain the equations for them, Eqs. (F.2)–(F.6), which appear in the Appendix F.

At higher order, we consider the corrections which are constructed by the spatial derivatives of $\Omega(x)$ and solve the Einstein equations order by order in the GE. The spatial metric and the scalar field can be expanded as

$$\gamma_{ij}(t,x) = a^2(t,\Omega)\Bigg[h_{ij} + \sum_A F^A_{(2)}(t,\Omega)(\nabla^{(2)}\Omega)^A_{ij} + \sum_A F^A_{(4)}(t,\Omega)(\nabla^{(4)}\Omega)^A_{ij} + \cdots + \sum_A F^A_{(2p)}(t,\Omega)(\nabla^{(2p)}\Omega)^A_{ij} + \cdots\Bigg], \tag{2.86}$$

$$\phi(t,x) = \phi_0(t,\Omega) + \sum_A P^A_{(2)}(t,\Omega)(\nabla^{(2)}\Omega)^A_{ij} + \sum_A P^A_{(4)}(t,\Omega)(\nabla^{(4)}\Omega)^A_{ij} + \cdots + \sum_A P^A_{(2p)}(t,\Omega)(\nabla^{(2p)}\Omega)^A_{ij} + \cdots, \tag{2.87}$$

where the notation $(\nabla^{(2p)}\Omega)^A_{ij}$ denotes symbolically symmetric spatial tensors which contain $2p$ spatial gradients of $\Omega(x)$, the suffix A distinguishes the tensors belonging to the same class, and $a(t,\Omega)$, $\phi_0(t,\Omega)$, $F^A_{(2p)}(t,\Omega)$ and $P^A_{(2p)}(t,\Omega)$ are functions of t and $\Omega(x)$ which is determined by the Einstein equations. In the case of $p = 1, 2$, the explicit form of $(\nabla^{(2p)}\Omega)^A_{ij}$ appears in the Appendix D.

Numerical results

We consider a chaotic inflation model with a massive scalar field, i.e., $V(\phi) = \frac{1}{2}m^2\phi^2$ as an inflaton field.

When the energy of the scalar field is dominated by the kinetic term at the early stage, the initial behavior of solution without inhomogeneities for Eqs. (2.71), (2.73), and (2.74) is expressed by series expansions in the form

$$a^2(t) = m^{-2}t^{2/3}\left[1 - \frac{9}{7}t^{4/3} + O(t^{8/3})\right], \tag{2.88}$$

$$\phi_0(t) = \sqrt{\frac{2}{3\kappa}}\left[\ln t + \frac{81}{56}t^{4/3} + O(t^{8/3})\right] + \widetilde{\phi}_0, \tag{2.89}$$

where $\widetilde{\phi}_0$ is the constant which corresponds to the freedom of initial value of the scalar field. The time variable t is made dimensionless by the use of m.

On assumption that we neglect all spatial derivatives of Ω, we can generalize the solution, Eqs. (2.88) and (2.89). We assume the spatial dependence of the scale factor at $t \to 0$ in the form

$$a(t, \Omega(x)) = \Omega(x) t^{1/3}. \tag{2.90}$$

When the potential energy of the scalar field is negligible, from Eqs. (2.71) and (2.90), we obtain the initial behavior of ϕ_0 at $t \to 0$ in the form

$$\phi_0(t, \Omega(x)) = \sqrt{\frac{2}{3\kappa}} \ln t + \widetilde{\phi}_0(\Omega(x)), \tag{2.91}$$

where $\widetilde{\phi}_0$ is an arbitrary function of $\Omega(x)$. Solving Eqs. (2.71), (2.73), and (2.74) iteratively, we obtain the generalized solution

$$a^2(t, \Omega(x)) = \Omega^2(x) t^{2/3} \left[1 - \frac{9m^{-2}}{7\Omega^2(x)} t^{4/3} + O(\frac{m^{-4}}{\Omega^4} t^{8/3}) \right], \tag{2.92}$$

$$\phi_0(t, \Omega(x)) = \sqrt{\frac{2}{3\kappa}} \left[\ln t + \frac{81m^{-2}}{56\Omega^2(x)} t^{4/3} + O(\frac{m^{-4}}{\Omega^4} t^{8/3}) \right] + \widetilde{\phi}_0. \tag{2.93}$$

The local scale factor and the scalar field are expressed by series expansions of $(m^{-2}/\Omega^2)t^{4/3}$ in the initial stage. At the beginning of the universe, the local scale factor behaves as $a(t, \Omega) \propto t^{1/3}$ and after that the time evolution depends on the local value of $\Omega(x)$. In the initial stage where the kinetic energy of scalar field dominates the potential energy, the behavior of $a(t, \Omega)$ does not depend on $\widetilde{\phi}_0$ but in the late stage where the potential energy becomes effective, it depends on $\widetilde{\phi}_0$.

We can see the time evolutions of these variables, which is characterized by the value of $\Omega(x)$ and $\widetilde{\phi}_0$, by solving Eqs. (2.71), (2.73), and (2.74) numerically. Figure 2.8 shows the inflationary region and the recollapsing one in the $(\Omega^2, \widetilde{\phi}_0)$ plane. The local scale factor with parameters in the inflationary region enters the accelerating expansion phase: $\dot{a}/a > 0$ and $\ddot{a}/a > 0$. On the other hand, the local scale factor with parameters in the recollapsing region enters the recollapsing phase: $\dot{a}/a < 0$ and $\ddot{a}/a < 0$. From Fig. 2.8, we see that inflation favors large Ω and large $|\widetilde{\phi}_0|$ as is expected by the investigation of the homogeneous model [46]. For fixed $\widetilde{\phi}_0$ there is a critical value of Ω, Ω_{cr}, if $\Omega > \Omega_{cr}$ inflation occurs. Since the critical value Ω_{cr} depends on $\widetilde{\phi}_0$ then the condition for the onset of inflation in the lowest order solution is written in the form

$$\frac{1}{\Omega^2} < \frac{1}{\Omega_{cr}^2(\widetilde{\phi}_0)}. \tag{2.94}$$

In Fig. 2.8, $\Omega_{cr}(\widetilde{\phi}_0)$ is drawn as the boundaries between the inflationary region and the recollapsing region.

In the initial stage where the local scale factor $a(t, \Omega(x))$ is proportional to $\Omega(x)t^{1/3}$, the spatial scalar curvature behaves as $\Omega^{-2}t^{-2/3}$. The condition (2.94) is, then, translated to the condition on the initial curvature as

$${}^3R_{init}(t, \Omega) < {}^3R_{cr}(t, \widetilde{\phi}_0), \tag{2.95}$$

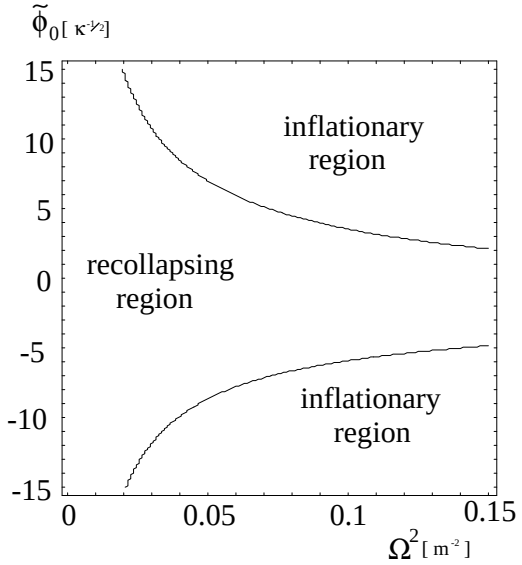

Fig. 2.8 In the lowest order approximation, an inflationary region and recollapsing region are shown in $(\Omega^2, \widetilde{\phi}_0)$ plane.

where ${}^3R_{cr} \equiv 6t^{-2/3}\Omega_{cr}^{-2}(\widetilde{\phi}_0)$. This condition for the onset of inflation is a restriction on only the local value of ${}^3R$.

Next, we take the first order correction terms into account. We integrate Eqs. (2.77)–(2.82) and Eqs. (F.2)–(F.6) numerically. We restrict ourselves to consider a growing solution whose initial asymptotic behavior is

$$F = \frac{18m^{-2}}{7\Omega^2}t^{4/3}, \overline{F} = \frac{9m^{-2}}{8\Omega^2}t^{4/3}, \widetilde{G} = -\frac{9m^{-2}}{7\Omega^2}t^{4/3}, \widehat{G} = -\frac{9m^{-2}}{4\Omega^2}t^{4/3},$$
$$P = -\sqrt{\frac{3}{2\kappa}}\frac{9m^{-2}}{14\Omega^2}t^{4/3}, Q = \sqrt{\frac{3}{2\kappa}}\frac{9m^{-2}}{28\Omega^2}t^{4/3}.$$

The time evolution of F, $\widetilde{G}$, P, and Q is shown in Figs. 2.9–2.12.

In the case that the local scale factor in the lowest order will enter the inflationary phase ($\Omega^2 > \Omega_{cr}^2$), F and $\widetilde{G}$ grow in proportion to time, and P and Q approach constant values. On the other hand, in the case that the local scale factor in the lowest order will enter the recollapsing phase ($\Omega^2 < \Omega_{cr}^2$), F, $\widetilde{G}$, P, and Q diverge and the approximation breaks down in the course of time. These behavior are consistent with the results by the linear approximation in the AE [25]. The trajectory of scalar field in $(\phi, \dot{\phi})$ space is shown in Figs. 2.13–2.14.

At each spatial point, we define an effective local scale factor $a_{\mathit{eff}}(t, x)$ by Eq. (2.56) which describes how the universe expands at the spatial point. We can follow the evolution of $a_{\mathit{eff}}(t, x)$ by the evolution of $a(t, \Omega)$, $F(t, \Omega)$, and $\widetilde{G}(t, \Omega)$. The behavior of $a_{\mathit{eff}}(t, x)$ is characterized by four parameters $\widetilde{\phi}_0, \Omega, \nabla_l\nabla^l\Omega/\Omega$, and $\nabla_l\Omega\nabla^l\Omega/\Omega^2$. In addition to the value of $\widetilde{\phi}_0$ and Ω, the spatial derivatives of Ω affect the evolution of the local scale factor.

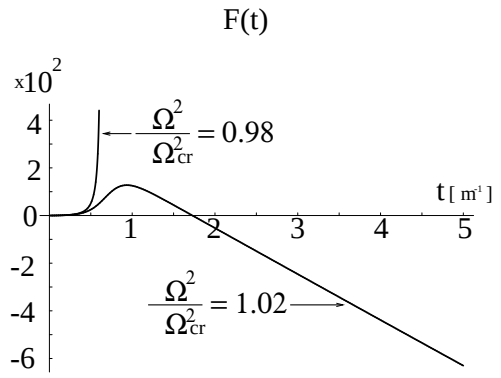

Fig. 2.9 Typical examples of the time evolution of $F(t, \Omega)$.

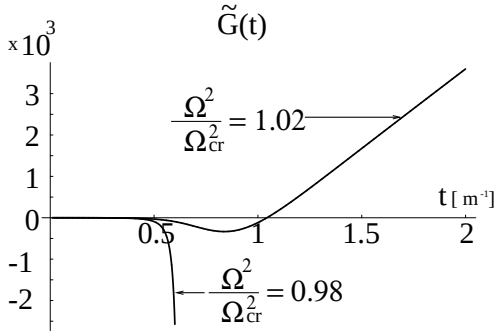

Fig. 2.10 Typical examples of the time evolution of $\widetilde{G}(t, \Omega)$.

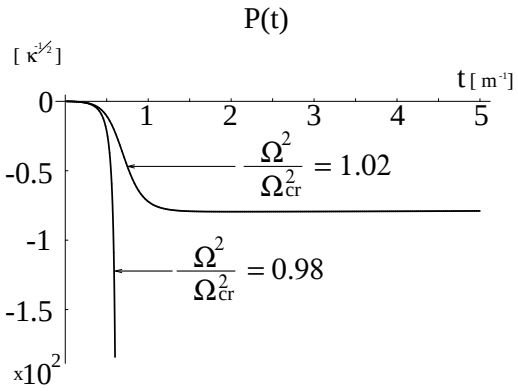

Fig. 2.11 Typical examples of the time evolution of $P(t, \Omega)$.

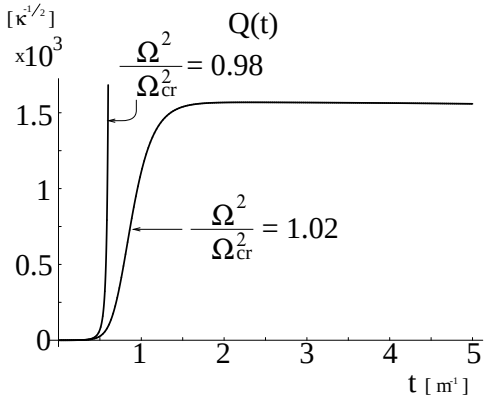

Fig. 2.12 Typical examples of the time evolution of $Q(t, \Omega)$.

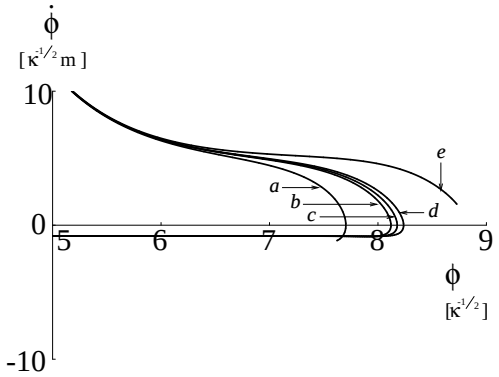

Fig. 2.13 The trajectories in $(\phi, \dot{\phi})$ space. $\nabla_l \Omega \nabla^l \Omega / \Omega^2 = 0$ and $\nabla_l \nabla^l \Omega / \Omega = 0.01$(a), 0.001(b), 0(c), -0.001(d) and -0.01(e). At the endpoint of the trajectory the approximation breaks down.

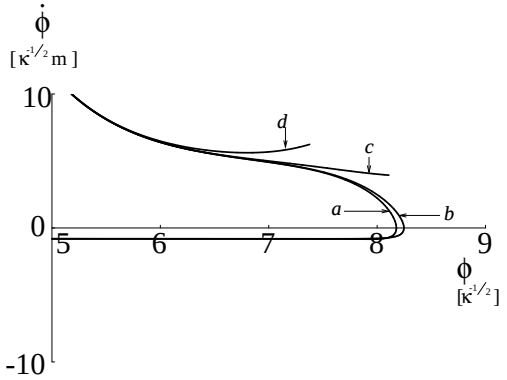

Fig. 2.14 The trajectories in $(\phi, \dot{\phi})$ space. $\nabla_l \nabla^l \Omega / \Omega = 0$ and $\nabla_l \Omega \nabla^l \Omega / \Omega^2 = 0$(a), 0.0001(b), 0.001(c) and 0.01(d). At the endpoint of the trajectory the approximation breaks down.

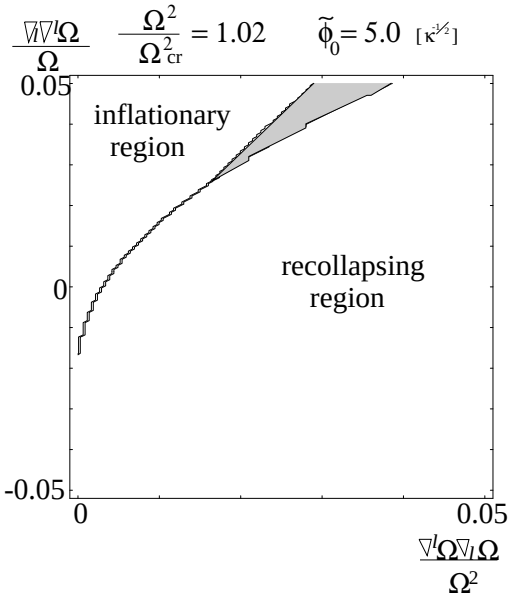

Fig. 2.15 An inflationary region and a recollapsing region for fixed $\widetilde{\phi}_0 = 5.0\kappa^{-1/2}$ ($\Omega^2_{cr} \approx 0.70m^{-2}$) are shown in the parameter space ($\nabla_l\nabla^l\Omega/\Omega$, $\nabla_l\Omega\nabla^l\Omega/\Omega^2$). A meshed region is a region where the approximation breaks down. At lowest order, universe will recollapse.

The effective local expansion rate and acceleration rate are given by Eqs. (2.57) and (2.58). We can divide the four-dimensional parameter space ($\widetilde{\phi}_0, \Omega, \nabla_l\nabla^l\Omega/\Omega, \nabla_l\Omega\nabla^l\Omega/\Omega^2$) into two regions: inflationary region and recollapsing region by a three-dimensional hyper surface. The effective local scale factor with the parameters in the inflationary region enters the accelerating expansion phase: $\dot{a}_{\mathit{eff}}/a_{\mathit{eff}} > 0$ and $\ddot{a}_{\mathit{eff}}/a_{\mathit{eff}} > 0$. On the other hand, the effective local scale factor with the parameters in the recollapsing region enters the recollapsing phase: $\dot{a}_{\mathit{eff}}/a_{\mathit{eff}} < 0$ and $\ddot{a}_{\mathit{eff}}/a_{\mathit{eff}} < 0$. We assume the approximation is valid while these conditions described by Eqs. (2.59) and (2.60) hold. We evolve the universe numerically while both of these conditions, Eqs. (2.59) and (2.60), hold.

Numerically evolving of the effective local expansion rate and acceleration rate, we see how the two spatial gradients, $\nabla_l\nabla^l\Omega/\Omega$ and $\nabla_l\Omega\nabla^l\Omega/\Omega^2$, affect the occurrence of inflation. For fixed $\widetilde{\phi}_0$, the inflationary region and recollapsing region are shown in Figs. 2.15–2.17. Between these two regions, there is a fuzzy region where error becomes large and one of inequalities in Eqs. (2.59) and (2.60) does not hold before the effective local scale factor enters the accelerating expansion phase or the recollapsing phase. We see that the positive (negative) $\nabla_l\nabla^l\Omega/\Omega$ helps the universe to enter the inflationary (recollapsing) phase. On the other hand, $\nabla_l\Omega\nabla^l\Omega/\Omega^2$ tends to prevent the onset of inflation.

From the numerical results, we obtain the time independent condition for the onset of inflation in the vicinity of $\Omega/\Omega_{cr} - 1 = 0$ and $\nabla_l\nabla^l\Omega/\Omega = \nabla_l\Omega\nabla^l\Omega/\Omega^2 = 0$ in the parameter space, within the first order of GECF,

$$\frac{1}{\Omega^2}\left[1 + \alpha\left(-\frac{\nabla_l\nabla^l\Omega}{\Omega} + \beta\frac{\nabla_l\Omega\nabla^l\Omega}{\Omega^2}\right)\right] < \frac{1}{\Omega^2_{cr}(\widetilde{\phi}_0)}, \tag{2.96}$$

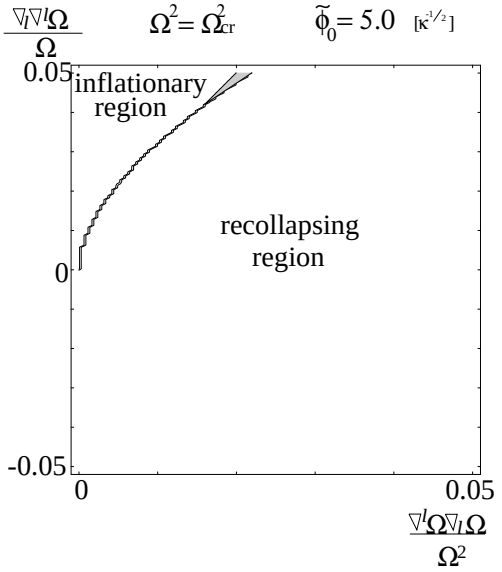

Fig. 2.16 An inflationary region and a recollapsing region for fixed $\widetilde{\phi}_0 = 5.0\kappa^{-1/2}$ ($\Omega^2_{cr} \approx 0.70m^{-2}$) are shown in the parameter space ($\nabla_l\nabla^l\Omega/\Omega$, $\nabla_l\Omega\nabla^l\Omega/\Omega^2$). A meshed region is a region where the approximation breaks down. At lowest order, universe will approach a static solution.

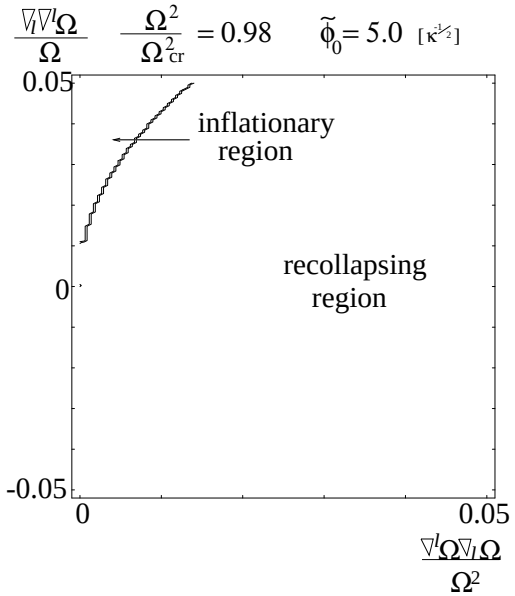

Fig. 2.17 An inflationary region and a recollapsing region for fixed $\widetilde{\phi}_0 = 5.0\kappa^{-1/2}$ ($\Omega^2_{cr} \approx 0.70m^{-2}$) are shown in the parameter space ($\nabla_l\nabla^l\Omega/\Omega$, $\nabla_l\Omega\nabla^l\Omega/\Omega^2$). A meshed region is a region where the approximation breaks down. At lowest order, universe will inflate.

where α and β are constants. The parameter α shows the strength of the effect of inhomogeneities on the occurrence of inflation. In the massive scalar inflaton model, the value of α is about 2.0. The value of β depends on the initial value of the scalar field $\widetilde{\phi}_0$: $\beta = 4.3$ for $\widetilde{\phi}_0 = 5.0\kappa^{-1/2}$ and $\beta = 3.3$ for $\widetilde{\phi}_0 = 10.0\kappa^{-1/2}$. In the early stage where $a^2(t,\Omega) = \Omega^2 t^{2/3}$, the spatial curvature ${}^3R_{init}$ in the first order approximation is

$$ {}^3R_{init}(t,\Omega) = \frac{2}{t^{2/3}\Omega^2}\left[3 - 2\frac{\nabla_l\nabla^l\Omega}{\Omega} + \frac{\nabla_l\Omega\nabla^l\Omega}{\Omega^2}\right]. \tag{2.97} $$

By use of Eq. (2.97), the criterion (2.96) is rewritten as

$$ {}^3R_{init}(t,\Omega) + \widetilde{\alpha}\left[\frac{({}^3R_{init})_{;l}^{\ ;l}}{{}^3R_{init}} + \widetilde{\beta}\frac{({}^3R_{init})_{;l}({}^3R_{init})^{;l}}{{}^3R_{init}^2}\right] < {}^3R_{cr}(t,\widetilde{\phi}_0), \tag{2.98} $$

where ${}^3R_{cr}(t,\widetilde{\phi}_0)$ is the marginal value of the spatial curvature for inflation in the closed Friedmann model that appears in Eq. (2.95) and the parameters $\widetilde{\alpha}$ and $\widetilde{\beta}$ are

$$ \widetilde{\alpha} = (3\alpha - 2), \quad \widetilde{\beta} = \frac{12\alpha - 3\alpha\beta - 7}{2(3\alpha - 2)}. \tag{2.99} $$

The criterion (2.98) is a condition on the initial value of the spatial curvature and its spatial derivatives. Because $\widetilde{\alpha}$ and $\widetilde{\beta}$ are several numbers when $\widetilde{\phi}_0 = (5.0 \sim 10.0)\kappa^{-1/2}$, the onset of inflation occurs if the initial value of spatial curvature ${}^3R_{init}$ is less than the critical value ${}^3R_{cr}(t,\widetilde{\phi}_0)$ over a region which has several times the size of the local curvature radius $({}^3R_{init})^{-1/2}$.

Comparison with numerical simulation

Goldwirth and Piran studied how inhomogeneities influence the inflationary epoch numerically in the case of spherical symmetry [23]. They conclude that the crucial feature necessary for inflation is a sufficiently high average value of the scalar field (suitable value for inflation in homogeneous universe) over a region of several Hubble radius. In order to compare their results with ours, we impose $\Omega^2(x)$ to spherically symmetric form, $\Omega^2(\chi,\theta,\varphi) = \Omega^2(\chi)$, in the spherical coordinate where $h_{ij} = \mathrm{diag}[1, \sin^2\chi, \sin^2\chi\sin^2\theta]$. We consider $\Omega^2(\chi)$ in the form

$$ \Omega^2(\chi) = \Omega_\pi^2 + (\Omega_0^2 - \Omega_\pi^2)\left[\frac{1 - \exp\left[-\Delta^{-2}\cos^2\frac{\chi}{2}\right]}{1 - \exp\left[-\Delta^{-2}\right]}\right], \tag{2.100} $$

where Ω_0^2 and Ω_π^2 are the value of Ω at $\chi = 0$ and $\chi = \pi$, respectively, and Δ is a parameter. We fix $\widetilde{\phi}_0 = 5.0\kappa^{-1/2}$, for example, then $\Omega_{cr}^2 \approx 0.70m^{-2}$ (see Fig. 2.8). The form of Ω^2 for $(\Omega_0^2 + \Omega_\pi^2)/2 = \Omega_{cr}^2$ and $\Omega_0^2 - \Omega_\pi^2 = 4 \times 10^{-7}m^{-2}$ is shown in Fig. 2.18. Varying Δ, we show inflationary and recollapsing regions in the three-dimensional space (see Fig. 2.19).

At the origin $\chi = 0$, universe can enter the inflationary phase whenever Δ is smaller than about 0.95. From Fig. 2.18, we see that the region of a suitable value of Ω^2 is

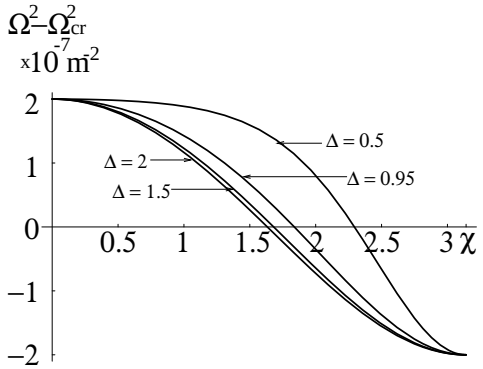

Fig. 2.18 The shape of $\Omega^2(\chi)$ for varying Δ.

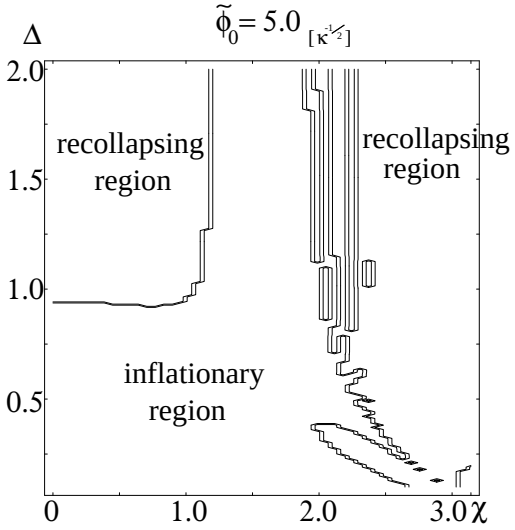

Fig. 2.19 An inflationary region and a recollapsing region in the three-dimensional space for fixed $\widetilde{\phi}_0 = 5.0\kappa^{-1/2}$ are shown in the case that Ω^2 is given in Fig. 2.18.

$0 \leq \chi \leq 1.85$. Comparing the physical length $L \sim a(t,\Omega)\chi$ for this region and the initial curvature radius $({}^3R_{init})^{-1/2} \sim a(t,\Omega)/\sqrt{6}$, we get $L \sim 4.5({}^3R_{init})^{-1/2}$. In this case, inflation occurs at the origin when the initial value of spatial curvature is less than the critical value over the region, which has 4.5 times size of the initial curvature radius.

2.4 Discussion of this chapter

In order to take the inhomogeneities of short wavelength into account perturbatively by the series expansion, we assume that the lowest order metric is written in the quasi-isotropic form. This assumption restricts the freedom of gravity. In this section, we discuss the general solution in the lowest order.

For simplicity, we investigate the universe filled with a perfect fluid. In this case, the Einstein equations are Eqs. (2.6)–(2.8) without the cosmological constant.

At lowest order, the traceless part and the trace part of Eq. (2.6) become respectively

$$\frac{1}{2\sqrt{\gamma}}\partial_t\left[\sqrt{\gamma}(K_i^j - \frac{1}{3}K\delta_i^j)\right] = 0, \tag{2.101}$$

$$\frac{1}{2\sqrt{\gamma}}\partial_t(\sqrt{\gamma}K) = \frac{3(2-\Gamma)}{4(2-3\Gamma)}(2\dot{K} + k_l^m K_m^l). \tag{2.102}$$

Equation (2.101) is integrated into

$$K_i^j = \frac{1}{3}K\delta_i^j + a^{-3}S_i^j(x), \tag{2.103}$$

where " shear matrix " $S_i^j(x)$ is traceless, which represents an anisotropy of the universe and a local scale factor $a \equiv (\det \gamma_{ij})^{1/6}$.

From Eq. (2.103), Eq. (2.102) becomes

$$\partial_t\left(\frac{\dot{a}}{a}\right) + \frac{3\Gamma}{2}\left(\frac{\dot{a}}{a}\right)^2 + \frac{2-\Gamma}{16}S_l^m S_m^l a^{-6} = 0. \tag{2.104}$$

Integrating Eq. (2.104), we have

$$\partial_t(a^3) = \sqrt{\xi^4(x) + 4\alpha^3(x)a^{3(2-\Gamma)}}, \tag{2.105}$$

where

$$\xi^2(x) \equiv \left(\frac{3S_{lm}S^{lm}}{8}\right)^{1/2}, \tag{2.106}$$

and $\alpha(x)$ is an arbitrary function of space.

In general, we can not integrate Eq. (2.105) analytically. For simplicity, we concentrate on the dust case ($\Gamma = 1$). Integrating Eq. (2.105), we obtain

$$a^3 = \alpha^3(x)\tilde{t}^2 + \xi^2\tilde{t}, \tag{2.107}$$

where $\tilde{t} \equiv t - t_0(x)$ and $t_0(x)$ is an arbitrary function of space.

From Eq. (2.103), the matrix S_i^j is self-adjoint with respect to the metric γ_{ij} where $S_i^k\gamma_{jk} = S_j^k\gamma_{ik}$. Therefore S_i^j is diagonalizable in the orthogonal basis with respect to γ_{ij}. Let us denote by $\lambda_a(x)$ its eigenvalue and by e_a^i associated independent eigenvector that we shall normalize to unity. We define its dual vectors $e_i^a(x)$ as $e_a^i e_i^b = \delta_a^b$. Since $S_i^j(x)$ is a traceless matrix, we have

$$\sum_{a=1}^{3} \lambda_a = 0. \tag{2.108}$$

In particular, we define $\eta_{ab} \equiv \gamma_{ij}e_a^i e_b^j$. From Eq. (2.103), we get

$$\dot{\gamma}_{ab} = \lambda_a a^{-3}\gamma_{ab}, \tag{2.109}$$

where

$$\gamma_{ab} = \frac{\eta_{ab}}{a^2}, \tag{2.110}$$

$$\eta_{ab} = \delta_{ab}a^2 \exp\left[\lambda_a \int dt a^{-3}\right]. \tag{2.111}$$

From Eqs. (2.107) and (2.111), we have

$$\eta_{ab} = \delta_{ab}\beta_a(x)\widetilde{t}^{2/3+\lambda_a\xi^{-2}}(\alpha^3\widetilde{t} + \xi^2)^{2/3-\lambda_a\xi^{-2}}, \tag{2.112}$$

where $\beta_a(x)$ is an integration constant.

Since $\det\gamma_{ij} = a^6$, we have

$$\det(e_i^a)^2\beta_1\beta_2\beta_3 = 1. \tag{2.113}$$

From Eqs. (2.7) and (2.8) without the cosmological constant and with $\Gamma = 1$, the energy density $\overset{(0)}{\rho}$ and the three velocity $\overset{(0)}{u}_i$ are

$$\overset{(0)}{\rho} = \frac{4}{3\kappa(\widetilde{t}^2 + \xi^2\alpha^{-3}\widetilde{t})}, \tag{2.114}$$

and

$$\overset{(0)}{u}_i = \frac{1}{\kappa\rho}\left[2\left(\frac{\dot{a}}{a}\right)_{,i} - \frac{1}{2}\left(\frac{S_i^j}{a^3}\right)_{;j}\right], \tag{2.115}$$

respectively.

Here we can see a gross feature of the lowest order solution (2.112). From Eq. (2.112), η_{ab} becomes

$$\eta_{ab} \sim \begin{cases} \widetilde{t}^{2p_a}\delta_{ab} & (t \sim t_0), \\ \widetilde{t}^{4/3}\delta_{ab} & (t \gg t_0), \end{cases} \tag{2.116}$$

where

$$p_a \equiv \frac{1}{3} + \frac{\lambda_a}{2\xi^2}. \tag{2.117}$$

At the early time ($t \sim t_0$), the metric is Kasner-like [5] . Note that Kasner solution is an exact solution in the vacuum case where the line element is of the form

$$ds^2 = -dt^2 + t^{2P_a}\delta_{ab}dx^a dx^b, \tag{2.118}$$

where P_a is called the Kasner parameter which satisfies

$$\sum_{a=1}^{3} P_a = 1, \tag{2.119}$$

$$\sum_{a=1}^{3} P_a^2 = 1. \tag{2.120}$$

The parameter p_a in Eq. (2.116) corresponds to the Kasner parameter and satisfies Eqs. (2.119) and (2.120).

At the late time ($t \gg t_0$), the metric becomes the flat FRW metric.

In short, at the early time, the effect of the anisotropy of the universe is dominant and the effect of the matter is dominant in the course of time. The quasi-isotropic form of the lowest order metric is a good approximation in the expanding universe.

[5] In the case of $0 < \Gamma < 2$, the behavior of metric is same as one for $\Gamma = 1$ [42].

Chapter 3

Renormalization group approach

The essence of the RG is to extract the structurally stable features of a system which is insensitive to details. Applying the RG method, we understand the asymptotic behaviors of the system in which we are interested. Recently the RG idea is applied to the study of the long-time asymptotics of the nonlinear partial differential equations [41, 49, 50].

In the perturbation theory, the RG method has been applied to improve the expansion scheme and remove divergences from a perturbation series and analyse the long-time behavior of the system [49, 50, 51]. The RG equation may be interpreted as representing the fact that the physical quantities $\mathcal{O}(a, \mu)$, where a collectively represents independent variables, should not depend on the renormalization point μ,

$$\frac{d\mathcal{O}(a;\mu)}{d\mu} = 0.$$

The renormalization point μ plays a role of the initial point and the renormalization condition for the physical qualities such as the coupling constants at the energy scale μ may be viewed as setting initial values of these qualities. Chen, Goldenfeld, and Oono [49] have demonstrated that various singular perturbation methods and reductive perturbations may be understood in a unified fashion from the RG point of view. Kunihiro [50] has shown that the RG method can be interpreted geometrically in terms of the classical theory of envelopes.

Bricmont, Kupiainen, and Lin [41] applied the RG method, so called constructive RG method, to study the long-time asymptotics of the nonlinear parabolic differential equations. The RG transformation there is the integration of the equation up to a finite time followed by a rescaling of the dependent and independent variables. The RG transformation together with the original differential equation gives a RG equation. Using the RG transformation, the problem at infinite time is reduced to the problem at finite time. A fixed point of the RG transformation corresponds to a scale-invariant solution of the differential equation. We can obtain the long-time behavior of the equation by studying the flow around fixed points. Moreover the RG method teaches us how universal the long-time behavior of the system we considered is.

As an application of this RG method to the system of gravity, Koike, Hara, and Adachi [52] analyzed the Einstein equations to understand the problem of the critical behavior of the black hole mass in gravitational collapse found by numerical study [53]. A pedagogical

exposition of the RG method in the deterministic system is given by Tasaki [54] in a simple but very illustrative example of the motion of a point particle in the Newtonian gravity.

Here we apply the RG to the Einstein equations in the cosmological situation. For simplicity, we shall consider only two cases. One is a homogeneous and isotropic universe filled with a perfect fluid and the other is a spherically symmetric universe filled with dust. We shall study the flow near the fixed points of the RG equations, which have self-similarity.

The astronomical observations indicate that the present universe has a hierarchical structure such as galaxies, clusters of galaxies, and superclusters, and that the two-point correlation function of the galaxies and of the clusters of galaxies can be expressed roughly by a single power law [3, 30]. The scale-invariant Harrison-Zel'dovichi spectrum for the primordial density perturbation has been successful in the study of the structure formation of the universe [55]. These suggest that the present universe has some self-similarity and that the scale invariant solution plays an important role in cosmology. If so, it is important to study the role of the scale invariant solution in the expansing universe.

In this chapter, we apply the RG method to the Einstein equations in the cosmological context. In section 3.1, we illustrate the application of the RG method to the heat equation with a nonlinear term. In section 3.2, we apply the RG method to the Einstein equations.

3.1 Brief review

In this section, we review the RG method for studying the long-time asymptotics of nonlinear partial differential equations [41].

We apply the RG method to a simple example and carry out analysis of RG flow in the vicinity of the scale-invariant fixed point by using the linear perturbation. Finally we mention the universality class.

3.1.1 RG method: heat equation with nonlinear term

We consider the heat equation with a nonlinear term as a simple example:

$$\frac{\partial u(x,t)}{\partial t} = \frac{1}{2}\left[u''(x,t) + \lambda u^2(x,t)\right], \tag{3.1}$$

where the prime denotes the spatial derivative and λ is a coupling constant.

RG transformation

Equation (3.1) has scale invariance under the following scale transformation:

$$x \longrightarrow Lx, \tag{3.2}$$
$$t \longrightarrow L^2 t, \tag{3.3}$$
$$u(x,t) \longrightarrow L^2 u(Lx, L^2 t), \tag{3.4}$$

where L is a parameter of the scale transformation and is taken to be larger than 1. Namely, if $u(x,t)$ is a solution of Eq. (3.1), the scaled function

$$\overset{(L)}{u}(x,t) = L^2 u(Lx, L^2 t) \tag{3.5}$$

is also a solution of Eq. (3.1). We can thus obtain a one-parameter family of solutions, provided that $u(x,t)$ is a solution.

Here we define the RG transformation $\mathcal{R}_L$ of a function of x by

$$\mathcal{R}_L u(x,1) = \overset{(L)}{u}(x,1). \tag{3.6}$$

In short, the $\mathcal{R}_L$ is a map from one set of initial data to another. It is convenient to take the initial time to be $t = 1$. The RG transformation $\mathcal{R}_L$ has a semigroup property:

$$\mathcal{R}_{L^n} = \mathcal{R}_{L^{n-1}} \circ \mathcal{R}_L. \tag{3.7}$$

Letting $t = 1$ and then $L^2 = t$ in Eqs. (3.5) and (3.6), we can express an arbitrary solution $u(x,t)$ as an initial data $u(\cdot, 1)$ transformed by RG transformations:

$$u(x,t) = t^{-1} \overset{(t^{1/2})}{u}(xt^{-1/2}, 1). \tag{3.8}$$

The large L means late time. Repeating the RG transformation (3.6), we can see the long-time behavior of the solution $u(x,t)$ in Eq. (3.1).

RG equation

Denoting $L = e^\tau$, we have from Eq. (3.5) that

$$\frac{d\overset{(L)}{u}}{d\tau} = L\frac{d\overset{(L)}{u}}{dL} = 2\overset{(L)}{u} + x\overset{(L)}{u'} + 2\frac{\partial\overset{(L)}{u}}{\partial t}. \tag{3.9}$$

Using the original partial differential equation (3.1) we have

$$\frac{d\overset{(L)}{u}}{d\tau} = 2\overset{(L)}{u} + \lambda\overset{(L)}{u^2} + x\overset{(L)}{u'} + \overset{(L)}{u''}. \tag{3.10}$$

This is the equation satisfied by the scaled function $\overset{(L)}{u}$, which we call the RG equation. We note that Eq. (3.10) has no explicit scale L dependence because of the scale invariance of the original equation (3.1).

Fixed point

We investigate the fixed point of the RG equation (3.10). The fixed point u^* is defined by

$$\mathcal{R}_L u^* = u^* \tag{3.11}$$

for any $L > 1$. This condition means that the field profile is unchanged after time evolution followed by a suitable rescaling. In general this condition is equivalent to

$$\frac{d\overset{(L)}{u^*}}{d\tau} = 0. \tag{3.12}$$

From Eq. (3.10), u^* satisfies the following equation,

$$2u^* + \lambda u^{*2} + xu^{*\prime} + u^{*\prime\prime} = 0. \tag{3.13}$$

In the homogeneous case, we can easily obtain the fixed points

$$u^* = 0 \quad \text{and} \quad -2/\lambda. \tag{3.14}$$

RG flow around a fixed point

To investigate the character of the fixed point, Eq. (3.14), we consider a linear perturbation around the fixed point, Eq. (3.14). The perturbed quantity $\overset{(L)}{\delta u}$ is defined by

$$\overset{(L)}{u} = u^* + \overset{(L)}{\delta u}, \tag{3.15}$$

where $\overset{(L)}{\delta u}$ is assumed small. Substituting Eq. (3.15) into Eq. (3.10) and neglecting the second order term $\overset{(L)}{\delta u^2}$, we obtain the linearized equation for $\overset{(L)}{\delta u}$:

$$\frac{d\overset{(L)}{\delta u}}{d\tau} = \begin{cases} 2\overset{(L)}{\delta u} + x\overset{(L)}{\delta u'} + \overset{(L)}{\delta u''} & (u^* = 0), \\ -2\overset{(L)}{\delta u} + x\overset{(L)}{\delta u'} + \overset{(L)}{\delta u''} & (u^* = -2/\lambda). \end{cases} \tag{3.16}$$

We require the boundary condition

$$\overset{(L)}{\delta u} \longrightarrow 0 \quad (|x| \longrightarrow \infty). \tag{3.17}$$

We are going to find the normal modes with the ansatz:

$$\overset{(L)}{\delta u} = f(x)e^{-x^2/2+\omega\tau}, \tag{3.18}$$

where $f(x)$ is a function to be determined below and ω is a constant. From Eqs. (3.16) and (3.18), we have

$$\begin{aligned} &f'' - xf' - (\omega - 1)f = 0 \quad (u^* = 0), \\ &f'' - xf' - (\omega + 3)f = 0 \quad (u^* = -2/\lambda)\,. \end{aligned} \tag{3.19}$$

The regularity at $x = 0$ and the boundary condition at $|x| = \infty$ imply

$$f(x) = H_n(x), \tag{3.20}$$

$$\omega = \begin{cases} 1 - n & (u^* = 0), \\ -3 - n & (u^* = -2/\lambda), \end{cases} \tag{3.21}$$

where $H_n(x)$ is the Hermite polynomial and $n = 0, 1, 2, \ldots$.

From Eq. (3.21), $u^* = -2/\lambda$ is an attractor because all ω's are negative. On the other hand, $u^* = 0$ has only one relevant mode ($n = 0$).

We can discuss the long-time behavior of a solution of the nonlinear diffusion equation (3.1), if $u(x, 1)$ is sufficiently close to the self-similar profile u^*. From Eq. (3.14), we obtain the two self-similar profiles. Suppose the initial spatial profile of $\overset{(L)}{\delta u}$ is expressed as a superposition of the normal modes $H_n e^{-x^2/2}$. As we have seen from Eq. (3.21), if $u(x, 1)$ is sufficiently close to the fixed point $u^* = -2/\lambda$, the solution approaches $-2t^{-1}/\lambda$ in the course of time because all modes of perturbation are irrelevant. On the other hand, there is only one growing mode ($n = 0$) of perturbation around the fixed point $u^* = 0$. As time goes on, the behavior of the solution near this fixed point is dominated by the relevant mode $n = 0$. This relevant mode corresponds a Gaussian distribution $t^{-1/2}e^{-x^2/(2t)}$.

From this instructive example, we see that if the perturbation around the fixed point has a finite number of relevant modes or no relevant modes, we have some prediction power for the long-time behavior of the nonlinear partial differential equation.

3.1.2 Universality class

We consider the universality of the long-time behavior of a solution of above differential equation (3.1). In order to do so, we investigate the following equation:

$$\frac{\partial u(x,t)}{\partial t} = \frac{1}{2}\left[u''(x,t) + \lambda u^2(x,t) + F(u(x,t))\right], \tag{3.22}$$

where $F(u(x,t))$ is a function of $u(x,t)$. This equation (3.22) can be seen the original equation (3.1) including some phenomenological term such as viscosity. Using the scale transformation (3.2)–(3.4), we easily understand the universality class of the long-time behavior of a solution in Eq. (3.1). Under the scale transformation (3.2)–(3.4), we assume $F(u)$ scales as

$$F(u(x,t)) \longrightarrow L^n F(u(Lx, L^2 t)), \tag{3.23}$$

where n is a constant. If $F(u) = 0$, the equation (3.22) is scaled up by L^2 under the scale transformation (3.2)–(3.4). Since $L > 1$ means the late time, if $n < 2$ the additional term $F(u)$ is negligible in course of time. In this case, a solution in Eq. (3.22) has the same long-time behavior as one in Eq. (3.1). In short, the long-time behavior of the system described by Eq. (3.1) and Eq. (3.22) belong to the same universality class. On the other hand, if $n \geq 2$, the additional term is proportioned to the other term or dominates in course of time. The long-time behavior of a solution in Eq. (3.22) is different from one in Eq. (3.1). Thus we can easily see how universal the long-time behavior of a solution in Eq. (3.1) is by use of the scale transformation.

3.2 Application of Einstein equations in cosmology

In this section, we apply the RG method, which is explained in the previous section, to the Einstein equations.

Take a synchronous reference frame where the line element is

$$\begin{aligned} ds^2 &= g_{\mu\nu}dx^\mu dx^\nu \\ &= -dt^2 + \gamma_{ij}(x^k, t)dx^i dx^j. \end{aligned} \tag{3.24}$$

The matter is taken to be a perfect fluid characterized by the energy-momentum tensor (2.5). We assume that the equation of state of the fluid is

$$p = (\Gamma - 1)\rho, \tag{3.25}$$

where Γ is a constant. The Einstein equations are

$$\dot{\gamma}_{ij} = 2K_{ij}, \tag{3.26}$$

$$\dot{K}_{ij} = -{}^3R_{ij} - KK_{ij} + 2K_i^l K_{lj} + \frac{\kappa\rho}{2}[2\Gamma u_i u_j + (2-\Gamma)\gamma_{ij}], \tag{3.27}$$

$$\kappa\rho = \frac{{}^3R + K^2 - K_l^m K_m^l}{2(1 + \Gamma u_l u^l)}, \tag{3.28}$$

$$\kappa\Gamma\rho u_i = -\frac{1}{\sqrt{1+u_l u^l}}(K^j_{i;j} - K_{,i}), \tag{3.29}$$

where K_{ij} is the extrinsic curvature, ${}^3R_{ij}$ is the Ricci tensor associated with γ_{ij}, and $\kappa \equiv 8\pi G$. An overdot denotes the derivative with respect to t and a semicolon denotes the covariant derivative with respect to γ_{ij}.

Hereafter we consider the RG transformation for the dynamical variables γ_{ij} and K_{ij}. In the following subsections, we investigate the two cases; the one is a homogeneous and isotropic universe, and the other is a spherically symmetric inhomogeneous dust universe.

3.2.1 Homogeneous and isotropic case

We consider the homogeneous and isotropic universe as a simple case. This case is rather trivial because the field equation becomes an ordinary differential equation. Nonetheless, this gives a nice warming up model to familiarize us with the RG approach to the universe. In this case, the spatial metric is written by

$$\gamma_{ij}(x^k, t) = a^2(t)\left[1 + \frac{k(t)r^2}{4}\right]^{-2}\delta_{ij}, \tag{3.30}$$

where $r^2 \equiv \delta_{ij}x^i x^j$, and $a(t)$ and $k(t)$ are the functions of time t to be studied. Substituting Eq. (3.30) into Eqs. (3.26)–(3.29), we get

$$\dot{a} = aH, \tag{3.31}$$

$$\dot{H} = -3H^2 - \frac{2k}{a^2} + \frac{2-\Gamma}{2}\kappa\rho, \tag{3.32}$$

$$\dot{k} = 0, \tag{3.33}$$

$$\kappa\rho = 3\left[H^2 + \frac{k}{a^2}\right], \tag{3.34}$$

where H is the Hubble parameter. From the conservation law of the energy density, we have

$$\kappa\rho = Ma^{-3\Gamma}, \tag{3.35}$$

where M is an arbitrary constant.

RG transformation

First, we consider the following scale transformation.

$$t \longrightarrow Lt, \tag{3.36}$$

$$a(t) \longrightarrow \overset{(L)}{a}(t) \equiv L^{-2/(3\Gamma)}a(Lt), \tag{3.37}$$

$$k(t) \longrightarrow \overset{(L)}{k}(t) \equiv L^{2(3\Gamma-2)/(3\Gamma)}k(Lt), \tag{3.38}$$

where L is a parameter of the scale transformation and larger than 1. From Eqs. (3.32) and (3.35), under this scale transformation the variables H and ρ are scaled in the following way,

$$H(t) \longrightarrow \overset{(L)}{H}(t) = LH(Lt), \tag{3.39}$$

$$\rho(t) \longrightarrow \overset{(L)}{\rho}(t) = L^2\rho(Lt). \tag{3.40}$$

The equations of motion (3.31)–(3.34) are invariant under the scale transformation, Eqs. (3.36)–(3.40), and equivalently the scaled variables satisfy the original equation.

Second, we define the RG transformation $\mathcal{R}_L$:

$$\mathcal{R}_L a(1) = \overset{(L)}{a}(1), \qquad \mathcal{R}_L H(1) = \overset{(L)}{H}(1), \qquad \mathcal{R}_L k(1) = \overset{(L)}{k}(1). \tag{3.41}$$

Letting $t = L$, we have the formulas

$$a(t) = t^{2/(3\Gamma)}\ \overset{(t)}{a}\ (1), \tag{3.42}$$

$$H(t) = t^{-1}\ \overset{(t)}{H}\ (1), \tag{3.43}$$

$$k(t) = t^{-2(3\Gamma-2)/(3\Gamma)}\ \overset{(t)}{k}\ (1), \tag{3.44}$$

which we shall use later to see the long-time behavior of a, H, and k.

RG equation

Third, we derive the RG equation. Letting $L = e^\tau$, the infinitesimal transformation of $\overset{(L)}{a}$, $\overset{(L)}{H}$, and $\overset{(L)}{k}$ with respect to τ is

$$\frac{d\overset{(L)}{a}}{d\tau} = -\frac{2}{3\Gamma}\overset{(L)}{a} + \frac{\partial\overset{(L)}{a}}{\partial t}, \tag{3.45}$$

$$\frac{d\overset{(L)}{H}}{d\tau} = \overset{(L)}{H} + \frac{\partial\overset{(L)}{H}}{\partial t}, \tag{3.46}$$

$$\frac{d\overset{(L)}{k}}{d\tau} = \frac{2(3\Gamma-2)}{3\Gamma}\overset{(L)}{k} + \frac{\partial\overset{(L)}{k}}{\partial t}. \tag{3.47}$$

Using the equations of motion (3.31), (3.32), and (3.33), Eqs. (3.45)–(3.47) can be rewritten as

$$\frac{d\overset{(L)}{a}}{d\tau} = -\frac{2}{3\Gamma}\overset{(L)}{a} + \overset{(L)}{a}\overset{(L)}{H}, \tag{3.48}$$

$$\frac{d\overset{(L)}{H}}{d\tau} = \overset{(L)}{H} + \left[-\overset{(L)}{H^2} + \frac{2-3\Gamma}{6}\kappa\overset{(L)}{\rho}\right], \tag{3.49}$$

$$\frac{d\overset{(L)}{k}}{d\tau} = \frac{2(3\Gamma-2)}{3\Gamma}\overset{(L)}{k}. \tag{3.50}$$

These equations (3.48)–(3.50) are the RG equations.

Fixed point

Here we investigate the fixed point of the RG equations. The fixed point (a^*, H^*, k^*) is defined by

$$\mathcal{R}_L a^* = a^*, \qquad \mathcal{R}_L H^* = H^*, \qquad \mathcal{R}_L k^* = k^*. \tag{3.51}$$

The above conditions can be rewritten as

$$\frac{d\overset{(L)}{a^*}}{d\tau} = 0, \qquad \frac{d\overset{(L)}{H^*}}{d\tau} = 0, \qquad \frac{d\overset{(L)}{k^*}}{d\tau} = 0. \tag{3.52}$$

From Eqs. (3.35) and (3.48)–(3.50), the fixed point is

$$a^* = \left(\frac{3M\Gamma^2}{4}\right)^{1/(3\Gamma)}, \quad H^* = \frac{2}{3\Gamma}, \quad k^* = 0, \quad \kappa\rho^* = 3H^{*2}. \tag{3.53}$$

This fixed point corresponds to a flat Friedmann universe.

Note that if Γ is taken to be $2/3$, there is another fixed point where k^* is nonzero. For the nonzero k^* case, the term of the spatial curvature can be absorbed into the term of the energy density of matter because the dependence of the scale factor on each term is the same. Thus the $k^* = 0$ case includes the nonzero k^* case. Hereafter we concentrate on only the $k^* = 0$ case.

RG flow around a fixed point

In order to study the flow in the RG around the fixed point, we consider the perturbation around the fixed point. The perturbed quantities $\overset{(L)}{\delta a}$, $\overset{(L)}{\delta H}$, and $\overset{(L)}{\delta k}$ are defined by

$$\overset{(L)}{a} = a^* + \overset{(L)}{\delta a}, \qquad \overset{(L)}{H} = H^* + \overset{(L)}{\delta H}, \qquad \overset{(L)}{k} = k^* + \overset{(L)}{\delta k}, \tag{3.54}$$

where $\overset{(L)}{\delta a}$, $\overset{(L)}{\delta H}$, and $\overset{(L)}{\delta k}$ are assumed to be small qualities. From Eqs. (3.48)–(3.50), the perturbed quantities satisfy the linearized equations

$$\frac{d\overset{(L)}{\delta a}}{d\tau} = a^*\overset{(L)}{\delta H}, \tag{3.55}$$

$$\frac{d\overset{(L)}{\delta H}}{d\tau} = -\overset{(L)}{\delta H} - \frac{3\Gamma}{2a^*}\overset{(L)}{\delta k}, \tag{3.56}$$

$$\frac{d\overset{(L)}{\delta k}}{d\tau} = \frac{2(3\Gamma-2)}{3\Gamma}\overset{(L)}{\delta k}, \tag{3.57}$$

where we neglect the second order term δa^2 and δH^2 and use the linearized equation of Eq. (3.34):

$$\kappa\overset{(L)}{\delta\rho} = \frac{4}{\Gamma}\overset{(L)}{\delta H} + \frac{3}{a^{*2}}\overset{(L)}{\delta k}. \tag{3.58}$$

Substituting Eq. (3.55) into Eq. (3.56), $\overset{(L)}{\delta a}$ satisfies

$$\frac{d^2\overset{(L)}{\delta a}}{d\tau^2} + \frac{d\overset{(L)}{\delta a}}{d\tau} + \frac{3\Gamma}{2a^*}\overset{(L)}{\delta k} = 0. \tag{3.59}$$

We solve Eq. (3.59):

$$\overset{(L)}{\delta a} = f_1 e^{-\tau} + f_2 e^{[2(3\Gamma-2)/(3\Gamma)]\tau}, \tag{3.60}$$

where f_1 and f_2 are arbitrary constants. From the solution (3.60), we can see the flow in the RG around the fixed point. If $3\Gamma - 2 < 0$, the fixed point (3.53) is an attractor. On the other hand, if $3\Gamma - 2 > 0$, the second term in Eq. (3.60) is a single relevant mode. Note that in the case $3\Gamma - 2 > 0$, the matter we consider satisfies the strong energy condition.

From the flow in the RG around the fixed point, we can see the long-time behavior of the homogeneous and isotropic universe. If $3\Gamma - 2 < 0$ and setting the initial profile in the vicinity of the fixed point (a^*, H^*, k^*), the spacetime will approach the flat Friedmann universe $a(t) = a^* t^{2/(3\Gamma)}$. On the other hand, if $3\Gamma - 2 > 0$, the spacetime will deviate from the flat Friedmann universe because there is a relevant mode $\delta a(t) = f_2 t^{2(3\Gamma-2)/(3\Gamma)}$.

In the context of the usual cosmological perturbation around a flat Friedmann universe, the f_1 mode corresponds to the decaying mode and the f_2 mode corresponds to the growing mode, which implies the gravitational instability, when the matter should satisfy the strong energy condition.

3.2.2 Spherically symmetric case

We consider the spherically symmetric *inhomogeneous* case. In this case, the spatial metric is written by

$$\gamma_{ij}(x^k, t)dx^i dx^j = A^2(r,t)dr^2 + B^2(r,t)(d\theta^2 + \sin^2\theta d\phi^2). \tag{3.61}$$

Namely, $\gamma_{rr} = A^2(r,t), \gamma_{\theta\theta} = B^2(r,t)$, and $\gamma_{\phi\phi} = B^2\sin^2\theta$ while the other components of the spatial metric vanish. As a simple case, we investigate the universe filled with dust, i.e., $\Gamma = 1$ and we can set $u^i = 0$ in Eqs. (3.26)–(3.29). The Einstein equations are

$$\dot{\gamma_{ij}} = 2K_{ij}, \tag{3.62}$$

$$\dot{K_{ij}} = -{}^3R_{ij} + 2K_{il}K^l_j - KK_{ij} + \frac{1}{2}\kappa\rho\gamma_{ij}, \tag{3.63}$$

$$\kappa\rho = \frac{1}{2}\left[{}^3R + K^2 - K^m_l K^l_m\right], \tag{3.64}$$

$$K^j_{i;j} - K_{,i} = 0. \tag{3.65}$$

RG transformation

Here we consider the following scale transformation.

$$r \longrightarrow Lr, \tag{3.66}$$

$$t \longrightarrow L^\alpha t, \tag{3.67}$$

$$\gamma_{rr}(r,t) \longrightarrow \overset{(L)}{\gamma}_{rr}(r,t) \equiv L^{2-2\alpha}\gamma_{rr}(Lr, L^\alpha t), \tag{3.68}$$

$$\gamma_{\theta\theta}(r,t) \longrightarrow \overset{(L)}{\gamma}_{\theta\theta}(r,t) \equiv L^{-2\alpha}\gamma_{\theta\theta}(Lr, L^\alpha t), \tag{3.69}$$

$$K_{rr}(r,t) \longrightarrow \overset{(L)}{K}_{rr}(r,t) \equiv L^{2-\alpha}K_{rr}(Lr, L^\alpha t), \tag{3.70}$$

$$K_{\theta\theta}(r,t) \longrightarrow \overset{(L)}{K}_{\theta\theta}(r,t) \equiv L^{-\alpha}K_{\theta\theta}(Lr, L^\alpha t), \tag{3.71}$$

$$\rho(r,t) \longrightarrow \overset{(L)}{\rho}(r,t) \equiv L^{2\alpha}\rho(Lr, L^\alpha t), \tag{3.72}$$

where α is an arbitrary constant because the coordinate transformation $r \to r^\beta$ yields a substitution of α/β for α in Eqs. (3.66)–(3.72). Without loss of generality, we take α to be positive. Because of the scale invariance of the Einstein equations (3.62)–(3.65), the scaled variables $\overset{(L)}{\gamma}_{rr}$, $\overset{(L)}{\gamma}_{\theta\theta}$, $\overset{(L)}{K}_{rr}$, $\overset{(L)}{K}_{\theta\theta}$, and $\overset{(L)}{\rho}$ also satisfy Eqs. (3.62)–(3.65).

RG equation

We derive the RG equation. Letting $L = e^\tau$, the infinitesimal transformation of $\overset{(L)}{\gamma}_{ij}$ and $\overset{(L)}{K}_{ij}$ with respect to τ is

$$\frac{d\overset{(L)}{\gamma}_{rr}}{d\tau} = 2(1-\alpha)\overset{(L)}{\gamma}_{rr} + r\partial_r\overset{(L)}{\gamma}_{rr} + 2\alpha\overset{(L)}{K}_{rr}, \tag{3.73}$$

$$\frac{d\overset{(L)}{\gamma}_{\theta\theta}}{d\tau} = -2\alpha\overset{(L)}{\gamma}_{\theta\theta} + r\partial_r\overset{(L)}{\gamma}_{\theta\theta} + 2\alpha\overset{(L)}{K}_{\theta\theta}, \tag{3.74}$$

$$\begin{aligned}\frac{d\overset{(L)}{K}_{rr}}{d\tau} &= (2-\alpha)\overset{(L)}{K}_{rr} + r\partial_r\overset{(L)}{K}_{rr} \\ &\quad +\alpha\left[\frac{1}{4}\overset{(L)}{{}^3R}\overset{(L)}{\gamma}_{rr} - \overset{(L)}{{}^3R}_{rr} + 2\overset{(L)}{K}_{rl}\overset{(L)}{K}{}^l_r - \overset{(L)}{K}\overset{(L)}{K}_{rr} + \frac{1}{4}\left(\overset{(L)}{K}{}^2\overset{(L)}{\gamma}_{rr} - \overset{(L)}{K}{}^m_l\overset{(L)}{K}{}^l_m\overset{(L)}{\gamma}_{rr}\right)\right],\end{aligned} \tag{3.75}$$

$$\begin{aligned}\frac{d\overset{(L)}{K}_{\theta\theta}}{d\tau} &= -\alpha\overset{(L)}{K}_{\theta\theta} + r\partial_r\overset{(L)}{K}_{\theta\theta} \\ &\quad +\alpha\left[\frac{1}{4}\overset{(L)}{{}^3R}\overset{(L)}{\gamma}_{\theta\theta} - \overset{(L)}{{}^3R}_{\theta\theta} + 2\overset{(L)}{K}_{\theta l}\overset{(L)}{K}{}^l_\theta - \overset{(L)}{K}\overset{(L)}{K}_{\theta\theta} + \frac{1}{4}\left(\overset{(L)}{K}{}^2\overset{(L)}{\gamma}_{\theta\theta} - \overset{(L)}{K}{}^m_l\overset{(L)}{K}{}^l_m\overset{(L)}{\gamma}_{\theta\theta}\right)\right],\end{aligned}$$

(3.76)

where $\overset{(L)}{{}^3R_{ij}}$ is the Ricci tensor associated with $\overset{(L)}{\gamma_{ij}}$. In the derivation of Eqs. (3.73)–(3.76), the equations of motion (3.62) and (3.63) are used. These equations (3.73)–(3.76) are the RG equations.

In terms of $\overset{(L)}{A}$ and $\overset{(L)}{B}$ ($\overset{(L)}{A^2} = \overset{(L)}{\gamma_{rr}}$ and $\overset{(L)}{B^2} = \overset{(L)}{\gamma_{\theta\theta}}$), the RG equations (3.73)–(3.76) read

$$\frac{d^2\overset{(L)}{A}}{d\tau^2} + \left[2(\alpha-1) + \frac{1}{\overset{(L)}{B}}\frac{d\overset{(L)}{B}}{d\tau} - \frac{r\overset{(L)}{B'}}{\overset{(L)}{B}}\right]\frac{d\overset{(L)}{A}}{d\tau} - 2r\frac{d\overset{(L)}{A'}}{d\tau} =$$

$$-r^2\overset{(L)}{A''} + (2\alpha-3)r\overset{(L)}{A'} - \frac{r\overset{(L)}{B'}}{\overset{(L)}{B}}\overset{(L)}{A} + \frac{1}{2}\left(\frac{r\overset{(L)}{B'}}{\overset{(L)}{B}}\right)^2\overset{(L)}{A} - \frac{r^2\overset{(L)}{A'}\overset{(L)}{B'}}{\overset{(L)}{B}} - \frac{\alpha^2-4\alpha+2}{2}\overset{(L)}{A} \tag{3.77}$$

$$+\frac{\alpha^2(\overset{(L)}{A^3} - 2\overset{(L)}{A'}\overset{(L)}{B}\overset{(L)}{B'} - \overset{(L)}{A}\overset{(L)}{B'^2} + 2\overset{(L)}{A}\overset{(L)}{B}\overset{(L)}{B''})}{2\overset{(L)}{A^2}\overset{(L)}{B^2}} + \frac{1}{\overset{(L)}{B^2}}\left[\frac{\overset{(L)}{A}}{2}\frac{d\overset{(L)}{B}}{d\tau} + \overset{(L)}{A}\overset{(L)}{B} - r\overset{(L)}{A}\overset{(L)}{B'} + r\overset{(L)}{A'}\overset{(L)}{B}\right]\frac{d\overset{(L)}{B}}{d\tau},$$

$$\frac{d^2\overset{(L)}{B}}{d\tau^2} + \left[2\alpha + \frac{1}{2\overset{(L)}{B}}\frac{d\overset{(L)}{B}}{d\tau} - \frac{r\overset{(L)}{B'}}{\overset{(L)}{B}}\right]\frac{d\overset{(L)}{B}}{d\tau} - 2r\frac{d\overset{(L)}{B'}}{d\tau} =$$

$$-r^2\overset{(L)}{B''} + (2\alpha-1)r\overset{(L)}{B'} - \frac{r^2\overset{(L)}{B'^2}}{2\overset{(L)}{B}} + \frac{\alpha^2(\overset{(L)}{B'^2} - \overset{(L)}{A^2})}{2\overset{(L)}{A^2}\overset{(L)}{B}} - \frac{\alpha^2}{2}\overset{(L)}{B}, \tag{3.78}$$

where the prime denotes the derivative with respect to r. From Eqs. (3.64) and (3.65), we obtain

$$\overset{(L)}{\kappa\rho} = \frac{2}{\alpha^2\overset{(L)}{A}}\left[\alpha + \frac{1}{\overset{(L)}{B}}\frac{d\overset{(L)}{B}}{d\tau} - \frac{r\overset{(L)}{B'}}{\overset{(L)}{B}}\right]\frac{d\overset{(L)}{A}}{d\tau} + \frac{1}{\alpha^2\overset{(L)}{B}}\left[2(2\alpha-1) - 2\frac{r\overset{(L)}{A'}}{\overset{(L)}{A}} - 2\frac{r\overset{(L)}{B'}}{\overset{(L)}{B}} + \frac{1}{\overset{(L)}{B}}\frac{d\overset{(L)}{B}}{d\tau}\right]\frac{d\overset{(L)}{B}}{d\tau}$$
$$+\frac{3\alpha-2}{\alpha} - \frac{2}{\alpha}\frac{r\overset{(L)}{A'}}{\overset{(L)}{A}} - \frac{2(2\alpha-1)}{\alpha^2}\frac{r\overset{(L)}{B'}}{\overset{(L)}{B}} + \frac{2}{\alpha^2}\frac{r^2\overset{(L)}{A'}\overset{(L)}{B'}}{\overset{(L)}{A}\overset{(L)}{B}} + \frac{1}{\alpha^2}\frac{r^2\overset{(L)}{B'^2}}{\overset{(L)}{B^2}}$$
$$+\frac{1}{\overset{(L)}{A^3}\overset{(L)}{B^2}}\left[\overset{(L)}{A^3} + 2\overset{(L)}{A'}\overset{(L)}{B}\overset{(L)}{B'} - \overset{(L)}{A}\overset{(L)}{B'^2} - 2\overset{(L)}{A}\overset{(L)}{B}\overset{(L)}{B''}\right], \tag{3.79}$$

$$\overset{(L)}{B'}\frac{d\overset{(L)}{A}}{d\tau} - \overset{(L)}{A}\frac{d\overset{(L)}{B'}}{d\tau} - r\overset{(L)}{A'}\overset{(L)}{B'} + r\overset{(L)}{A}\overset{(L)}{B''} = 0. \tag{3.80}$$

Letting $t = L^\alpha$, the original variables $A(r,t)$ and $B(r,t)$ are expressed by the scaled variables $\overset{(L)}{A}$ and $\overset{(L)}{B}$:

$$A(r,t) = t^{(\alpha-1)/\alpha}\,\overset{(t^{1/\alpha})}{A}\,(rt^{-1/\alpha}, 1), \tag{3.81}$$

$$B(r,t) = t\,\overset{(t^{1/\alpha})}{B}\,(rt^{-1/\alpha}, 1). \tag{3.82}$$

Fixed point

Here we investigate the fixed point of the RG equations (3.77) and (3.78) defined by

$$\frac{dA^*}{d\tau} = 0, \qquad \frac{dB^*}{d\tau} = 0. \tag{3.83}$$

At the fixed point,

$$A(r,t) = t^{(\alpha-1)/\alpha} \overset{(t^{1/\alpha})}{A^*}(rt^{-1/\alpha}, 1) = t^{(\alpha-1)/\alpha} \times (\text{ function of } rt^{-1/\alpha} \text{ only }) \tag{3.84}$$

and

$$B(r,t) = t \overset{(t^{1/\alpha})}{B^*}(rt^{-1/\alpha}, 1) = t \times (\text{ function of } rt^{-1/\alpha} \text{ only }) \tag{3.85}$$

is a self-similar solution[1] . The precise form of these are as follows.

For $c = 0$,

$$A^*(r,1) = \frac{\alpha r^{\alpha/3-1}(1-3pr^\alpha)}{3(1-pr^\alpha)^{1/3}}, \tag{3.86}$$

$$B^*(r,1) = r^{\alpha/3}(1-pr^\alpha)^{2/3}, \tag{3.87}$$

$$\kappa\rho^*(r,1) = \frac{4}{3(1-pr^\alpha)(1-3pr^\alpha)}, \tag{3.88}$$

For $c > 0$,

$$A^*(r,1) = \frac{\alpha}{(1+c)^{1/2}r}\left[\frac{2}{9c}(\cosh\eta - 1)r^\alpha - c^{1/2}\frac{\sinh\eta}{\cosh\eta - 1}\right], \tag{3.89}$$

$$B^*(r,1) = \frac{2}{9c}r^\alpha(\cosh\eta - 1), \tag{3.90}$$

$$\sinh\eta - \eta = \frac{9c^{3/2}}{2}(r^{-\alpha} - p), \tag{3.91}$$

$$\kappa\rho^*(r,1) = \frac{9c^2}{r^\alpha(\cosh\eta-1)^2\left[\frac{2r^\alpha}{9c}(\cosh\eta-1) - c^{1/2}\frac{\sinh\eta}{\cosh\eta-1}\right]}, \tag{3.92}$$

For $c < 0$,

$$A^*(r,1) = \frac{\alpha}{(1-|c|)^{1/2}r}\left[\frac{2}{9|c|}(1-\cos\eta)r^\alpha - |c|^{1/2}\frac{\sin\eta}{1-\cos\eta}\right], \tag{3.93}$$

$$B^*(r,1) = \frac{2}{9|c|}r^\alpha(1-\cos\eta), \tag{3.94}$$

$$\eta - \sin\eta = \frac{9|c|^{3/2}}{2}(r^{-\alpha} - p), \tag{3.95}$$

$$\kappa\rho^*(r,1) = \frac{9c^2}{r^\alpha(1-\cos\eta)^2\left[\frac{2r^\alpha}{9|c|}(1-\cos\eta) - |c|^{1/2}\frac{\sin\eta}{1-\cos\eta}\right]}, \tag{3.96}$$

[1] In the spherically symmetric spacetime filled with dust, the general solution of the Einstein equations is the Tolman-Bondi solution (G.1) and (G.2) in the Appendix G. Therefore we can obtain the fixed point from the Tolman-Bondi solution with self-similarity rather than solving Eqs. (3.83) directly.

where c and p are constants.

The constant c can be interpreted as the total energy of the universe in the analogy of the Newtonian mechanics. By the signature of the constant c, these fixed points are classified into the following three. The universe with $c = 0$ is similar to the flat Friedmann universe. The universes with a positive c or a negative c are similar to the open and closed Friedmann universes, respectively. Especially when $c = p = 0$, the above fixed point coincides with the flat Friedmann universe and the spacetime becomes homogeneous.

In the context of the RG, we can treat the time evolution of the field variables as the map from one set of initial data to another. If the initial data is taken to be the above fixed point A^*, B^*, and ρ^*, the spacetime will evolve into the Tolman-Bondi solution with self-similarity. In the cases of $c = 0$ and $c > 0$, the fixed point is not regular if $p > 0$. For $c < 0$, the fixed point has singularities irrespective of the signature of p because the spacetime is similar to the closed Friedmann universe and will recollapse. Since we should set a regular initial data in the physical situation, we investigate only the case of $c = 0$ ($p < 0$) and $c > 0$ ($p \leq 0$) where the fixed point is everywhere regular (see Fig. 3.1). Note we exclude the case of $c = p = 0$ because we have already studied it in the previous subsection.

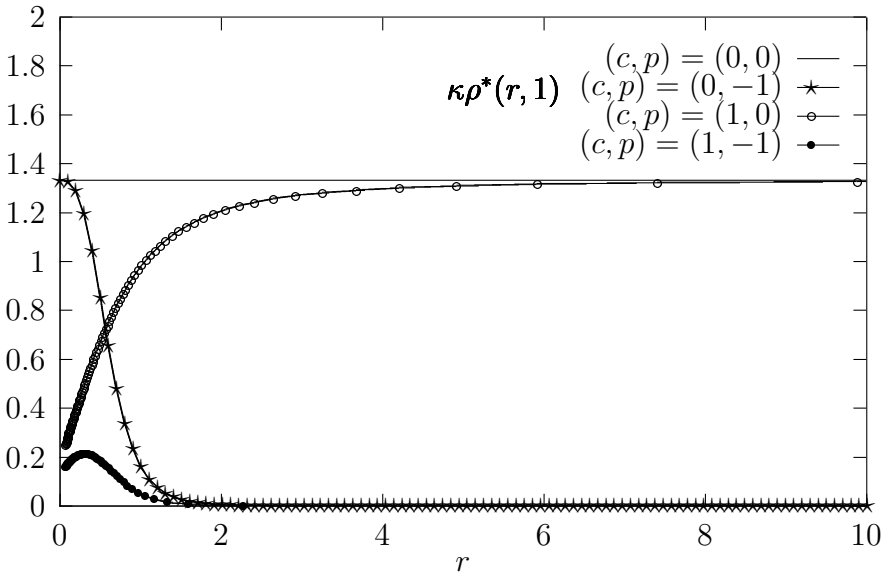

Fig. 3.1 A typical example of the density profile at fixed point $\kappa\rho^*(r, 1)$ for $\alpha = 3$.

RG flow around a fixed point

To study the behavior of the flow in the RG around the fixed point, we consider the linear perturbation around the fixed point. The linear perturbation around the self-similar Tolman-Bondi solution has also been discussed by Tomita [56] in a different context from

ours [2] . For simplicity, we concentrate on the spherical modes of linear perturbation. The perturbed quantities $\overset{(L)}{\delta A}$ and $\overset{(L)}{\delta B}$ are defined by

$$\overset{(L)}{\gamma}_{rr} = A^{*2} + 2A^* \overset{(L)}{\delta A}, \tag{3.97}$$

$$\overset{(L)}{\gamma}_{\theta\theta} = B^{*2} + 2B^* \overset{(L)}{\delta B}. \tag{3.98}$$

We assume the spatial metric variables for $\overset{(L)}{\delta A}$ and $\overset{(L)}{\delta B}$ in the following form,

$$\overset{(L)}{\delta A} = a(r)e^{\omega\tau}, \tag{3.99}$$

$$\overset{(L)}{\delta B} = b(r)e^{\omega\tau}. \tag{3.100}$$

The perturbed quantities $a(r)$ and $\overset{(L)}{\delta\rho}$ are expressed by $b(r)$;

$$\frac{a}{A^*} = \frac{b'}{B^{*\prime}} - \frac{c_1}{2(1+c)} r^{\omega}, \tag{3.101}$$

$$\frac{\overset{(L)}{\delta\rho}}{\rho^*} = e^{\omega\tau}\left[\frac{9(\omega+\alpha)}{4\alpha} c_2 r^{\omega} - 2\frac{b}{B^*} - \frac{b'}{B^{*\prime}}\right], \tag{3.102}$$

where c_1 and c_2 are arbitrary constants (see the Appendix G).

As for the spherical modes of the perturbation, we can easily obtain the solutions. For $c = 0$,

$$b(r) = r^{\omega}\left[\frac{9}{20} c_1 r^{-\alpha/3}(1-pr^{\alpha})^{4/3} + \frac{3}{4} c_2 r^{\alpha/3}(1-pr^{\alpha})^{2/3} - \frac{2}{3} c_3 r^{4\alpha/3}(1-pr^{\alpha})^{-1/3}\right], \tag{3.103}$$

where c_3 is another arbitrary constant. The density contrast is

$$\begin{aligned}\frac{\overset{(L)}{\delta\rho}}{\rho^*} = e^{\omega\tau} r^{\omega}\Bigg\{ & -\frac{9}{20\alpha} c_1 r^{-2\alpha/3}(1-pr^{\alpha})^{2/3}(1-3pr^{\alpha})^{-1}\left[3\omega+\alpha-3(\omega+3\alpha)pr^{\alpha}\right] \\ & -\frac{9\omega}{2\alpha} c_2 p r^{\alpha}(1-3pr^{\alpha})^{-1} + \frac{2}{\alpha} c_3 r^{\alpha}(1-pr^{\alpha})^{-1}(1-3pr^{\alpha})^{-1}\left[\omega+2\alpha-(\omega+3\alpha)pr^{\alpha}\right]\Bigg\}.\end{aligned} \tag{3.104}$$

In the expression for the linear perturbation, Eq. (3.104), there are three terms corresponding to c_1, c_2, and c_3 so that there should be a gauge mode hidden in Eq. (3.104)

[2] The RG equations also is seen as the Einstein equations in the new coordinate system $(\tau, \xi, \theta, \phi)$, where $\tau = (\ln t)/\alpha$, $\xi = r/t^{1/\alpha}$, $\overset{(L)}{A}(\xi,\tau) = t^{(1-\alpha)/\alpha} A(r,t)$, and $\overset{(L)}{B}(\xi,\tau) = t^{-1}B(r,t)$. One might be puzzled by observing that in this new coordinate system, the lapse function can be zero at $\xi^2 \overset{(L)}{A} = \alpha^2$. However, there is no physical meaning of this point because the Einstein equations are found to be regular at this point.

because the number of physical modes has to be 2. Actually there remains a gauge freedom corresponding to the coordinate transformation of r, Eq. (G.8). The gauge mode is given by

$$\begin{aligned}\frac{\delta\overset{(L)}{\rho}_g}{\rho^*} &= fr^{\omega+1}e^{\omega\tau}\frac{\rho^{*\prime}}{\rho^*} \\ &= e^{\omega\tau}r^{\omega}f\left[2\alpha pr^{\alpha}(2-3pr^{\alpha})(1-pr^{\alpha})^{-1}(1-3pr^{\alpha})^{-1}\right],\end{aligned} \tag{3.105}$$

with f being an arbitrary constant. Because we should fix the freedom of gauge, we choose f so that $(\delta\overset{(L)}{\rho}+\delta\overset{(L)}{\rho}_g)/\rho^*$ behave as nicely as possible at $r=\infty$ because we are interested in the perturbation modes which are finite at $r=\infty$.

We use the following condition as a convenient gauge condition.

$$f = -\frac{9(\omega+3\alpha)}{40\alpha^2}p^{2/3}c_1 + \frac{3\omega}{4\alpha^2}c_2 - \frac{\omega+3\alpha}{3\alpha^2 p}c_3. \tag{3.106}$$

We fix the gauge mode by the above condition and obtain the physical perturbation $\delta\overset{(L)}{\widetilde{\rho}} = \delta\overset{(L)}{\rho} + \delta\overset{(L)}{\rho}_g$ as follows.

$$\begin{aligned}\frac{\delta\overset{(L)}{\widetilde{\rho}}}{\rho^*} = e^{\omega\tau}r^{\omega}\Big\{&\Delta_1(1-3pr^{\alpha})^{-1}\left[p^{-2/3}r^{-2\alpha/3}(1-pr^{\alpha})^{2/3}\left[3\omega+\alpha-3(\omega+3\alpha)pr^{\alpha}\right]\right. \\ &\left.+(\omega+3\alpha)pr^{\alpha}(2-3pr^{\alpha})(1-pr^{\alpha})^{-1}\right] + \Delta_2 pr^{\alpha}(1-pr^{\alpha})^{-1}(1-3pr^{\alpha})^{-1}\Big\},\end{aligned} \tag{3.107}$$

where

$$\Delta_1 = -\frac{9p^{2/3}}{20\alpha}c_1, \tag{3.108}$$

$$\Delta_2 = -\frac{3\omega}{2\alpha}\left(c_2 - \frac{4}{9p}c_3\right). \tag{3.109}$$

Since we consider only the case of $p<0$, the coordinate r can be taken from 0 to ∞. We demand the regularity condition that $\delta\overset{(L)}{\widetilde{\rho}}/\rho^*$ should be finite at the boundary, $r=0$ and $r=\infty$. This condition implies that Δ_1 modes with $2\alpha/3 \le \omega \le \alpha$ and Δ_2 modes with $-\alpha \le \omega \le \alpha$ are allowed. The mode with $\omega=0$ corresponds to a change of p in the self-similar solution, Eqs. (3.88), and ρ^* remains constant independent of τ in the direction. Although this fixed point is not a repeller, it has many relevant modes, Δ_1 with $0<\omega\le\alpha$ and Δ_2 with $0<\omega\le\alpha$. Note that a suitable linear combination of the Δ_1 and Δ_2 modes will have an asymptotic behavior $\approx r^{\omega-2\alpha}$ at $r=\infty$. For such modes, $2\alpha/3 \le \omega \le 2\alpha$ is allowed. These modes which satisfy the regularity condition are not discrete but continuous. We suppose that this special feature arises because our matter is assumed to be dust. To summarize, the possible value of ω ranges from $-\alpha$ to 2α. The flow of the RG in the vicinity of the fixed point is shown in Fig. 3.2.

In the case of $c=p=0$ where the fixed point corresponds to the flat Friedmann universe, the c_2 modes in the density contrast (3.104) are gauge modes. The regularity

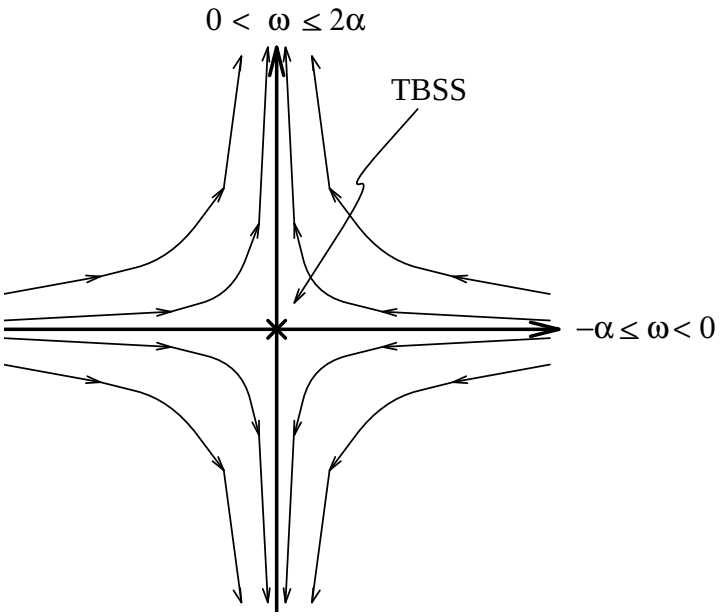

Fig. 3.2 TBSS represents the Tolman-Bondi solution with self-similarity in the case of $c = 0$ and $p < 0$. The axes correspond to the modes of linear perturbation Eq. (3.107).

condition implies that the c_1 mode with $\omega = 2\alpha/3$ and the c_3 mode with $\omega = -\alpha$ are allowed. This result corresponds to the homogeneous and isotropic case in the previous section. Compared with the usual cosmological perturbation in the synchronous comoving reference frame, this result appears to be strange because the only spherical modes of the linear perturbation allowed are constant in space. However, the time coordinate used in this RG method is different from the usual cosmic time coordinate, and the solution allowed by the regularity condition in each case does not coincide in general. Moreover, in the homogeneous universe, there is no nontrivial characteristic profile of field variables. If the fixed point is a homogeneous universe, the RG method may have no advantage since the RG approach respects the self-similar profile. But if the fixed point is an inhomogeneous universe, we believe that the RG method may be useful.

Compared with the $c = 0 (p < 0)$ case, the value of ω allowed in the case $(p = 0)$ is the lower limit in the case $(p < 0)$. The effect of the nonlinearity of gravity makes the growth rate of the density contrast large.

For $c > 0$,

$$b(r) = r^{\omega}\Bigg\{-\frac{1}{9c^2}c_1\left[2(\cosh\eta - 1) - \frac{3\sinh\eta(\sinh\eta - \eta)}{\cosh\eta - 1}\right] + \frac{1}{2c}c_2\left[\cosh\eta - 1 - \frac{\sinh\eta(\sinh\eta - \eta)}{\cosh\eta - 1}\right] - \frac{c^{1/2}\sinh\eta}{\cosh\eta - 1}c_3\Bigg\}. \tag{3.110}$$

The density contrast is

$$\frac{\delta\overset{(L)}{\rho}}{\rho^*} = \frac{e^{\omega\tau}r^{\omega}}{\alpha\left[\frac{2r^{\alpha}}{9c}(\cosh\eta-1)-\frac{c^{1/2}\sinh\eta}{\cosh\eta-1}\right]}\Bigg\{ \\ \frac{1}{9c^2}c_1\left[(\omega+3\alpha)r^{\alpha}\left(2(\cosh\eta-1)-\frac{3\sinh\eta(\sinh\eta-\eta)}{\cosh\eta-1}\right)\right. \\ \left.+\frac{27c^{3/2}\alpha}{2}\left(-\frac{\sinh\eta}{\cosh\eta-1}+\frac{(2\cosh\eta+1)(\sinh\eta-\eta)}{(\cosh\eta-1)^2}\right)\right] \\ -\frac{1}{2c}c_2\left[r^{\alpha}\left(2\alpha(\cosh\eta-1)-(\omega+3\alpha)\frac{\sinh\eta(\sinh\eta-\eta)}{\cosh\eta-1}\right)\right. \\ \left.+\frac{9c^{2/3}}{2}\left(\frac{(\omega-\alpha)\sinh\eta}{\cosh\eta-1}+\frac{\alpha(2\cosh\eta+1)(\sinh\eta-\eta)}{(\cosh\eta-1)^2}\right)\right] \\ +c^{1/2}c_3\left[(\omega+3\alpha)r^{\alpha}\frac{\sinh\eta}{\cosh\eta-1}-\frac{9\alpha c^{2/3}(2\cosh\eta+1)}{2(\cosh\eta-1)^2}\right]\Bigg\}. \tag{3.111}$$

The gauge mode is given by

$$\frac{\delta\overset{(L)}{\rho}_g}{\rho^*} = fr^{\omega+1}e^{\omega\tau}\frac{\rho^{*\prime}}{\rho^*} \\ = -\frac{\alpha f e^{\omega\tau}r^{\omega}}{\left[\frac{2r^{\alpha}}{9c}(\cosh\eta-1)-\frac{c^{1/2}\sinh\eta}{\cosh\eta-1}\right]} \\ \times\left[\frac{4}{9c}r^{\alpha}(\cosh\eta-1)-\frac{4c^{1/2}\sinh\eta}{\cosh\eta-1}+\frac{9c^2r^{-\alpha}(2\cosh\eta+1)}{2(\cosh\eta-1)^2}\right]. \tag{3.112}$$

Similarly to the case of $c=0$, we demand the regularity condition at $r=0$ and $r=\infty$.

(i) Case 1 ($p<0$).

We use the following convenient gauge condition:

$$f = \frac{1}{4\alpha^2}\left\{\frac{\omega+3\alpha}{c}c_1\left[2-3\frac{\sinh\eta_0(\sinh\eta_0-\eta_0)}{(\cosh\eta_0-1)^2}\right]\right. \\ \left.-\frac{9}{2}c_2\left[2\alpha-(\omega+3\alpha)\frac{\sinh\eta_0(\sinh\eta_0-\eta_0)}{(\cosh\eta_0-1)^2}\right]+\frac{9c^{2/3}(\omega+3\alpha)(\sinh\eta_0)}{(\cosh\eta_0-1)^2}c_3\right\}, \tag{3.113}$$

where $\eta=\eta_0$ corresponds to $r\to\infty$ and η_0 is thus given by $\sinh\eta_0-\eta_0=-9pc^{3/2}/2$.

By using the above condition, Eq. (3.113), we obtain the physical perturbation $\delta\overset{(L)}{\widetilde{\rho}} = \delta\overset{(L)}{\rho}+\delta\overset{(L)}{\rho}_g$ as follows:

$$\frac{\delta\overset{(L)}{\widetilde{\rho}}}{\rho^*} = \frac{e^{\omega\tau}r^{\omega}}{\alpha\left[\frac{2r^{\alpha}}{9c}(\cosh\eta-1)-\frac{c^{1/2}\sinh\eta}{\cosh\eta-1}\right]}\Bigg\{$$

$$\Delta_1^+ \left[3(\omega+3\alpha) r^\alpha (\cosh\eta - 1) \left(\frac{\sinh\eta_0(\sinh\eta_0 - \eta_0)}{(\cosh\eta_0 - 1)^2} - \frac{\sinh\eta(\sinh\eta - \eta)}{(\cosh\eta - 1)^2} \right) \right.$$
$$+ \frac{9c^{3/2}}{2} \left\{ \left(4\omega + 9\alpha - 6(\omega+3\alpha) \frac{\sinh\eta_0(\sinh\eta_0 - \eta_0)}{(\cosh\eta_0 - 1)^2} \right) \frac{\sinh\eta}{\cosh\eta - 1} \right.$$
$$\left. \left. + 3\alpha \frac{(2\cosh\eta + 1)(\sinh\eta - \eta)}{(\cosh\eta - 1)^2} \right\} \right]$$
$$+ \Delta_2^+ \left[(\omega+3\alpha) r^\alpha (\cosh\eta - 1) \left(\frac{\sinh\eta}{(\cosh\eta - 1)^2} - \frac{\sinh\eta_0}{(\cosh\eta_0 - 1)^2} \right) \right.$$
$$\left. \left. - \frac{9c^{3/2}\alpha(2\cosh\eta + 1)}{2(\cosh\eta - 1)^2} + \frac{9(\omega+3\alpha)c^{2/3}\sinh\eta_0}{4(\cosh\eta_0 - 1)^2} \left(\frac{4\sinh\eta}{\cosh\eta - 1} \frac{9c^{3/2}(2\cosh\eta + 1)}{2(\cosh\eta - 1)^2 r^\alpha} \right) \right] \right\}, \tag{3.114}$$

where

$$\Delta_1^+ = \frac{1}{9c^2} c_1, \tag{3.115}$$

$$\Delta_2^+ = -\frac{9pc^{1/2}}{4} \left(c_2 - \frac{4}{9p} c_3 \right), \tag{3.116}$$

and $\sinh\eta - \eta = 9c^{3/2}(r^{-\alpha} - p)/2$.

The regularity condition at $r = 0$ and $r = \infty$ implies that Δ_1^+ modes with $\omega = \alpha$ and Δ_2^+ modes with $0 \leq \omega \leq \alpha$ are allowed. In this case, this fixed point is a repeller up to the zero mode because all other modes which satisfy the regularity condition have a positive ω. Note that a suitable linear combination of the Δ_1^+ and Δ_2^+ modes will have an asymptotic behavior $\approx r^{\omega - 2\alpha}$. Therefore the possible value of ω ranges from 0 to 2α. The flow of the RG in the vicinity of the fixed point is shown in Fig. 3.3.

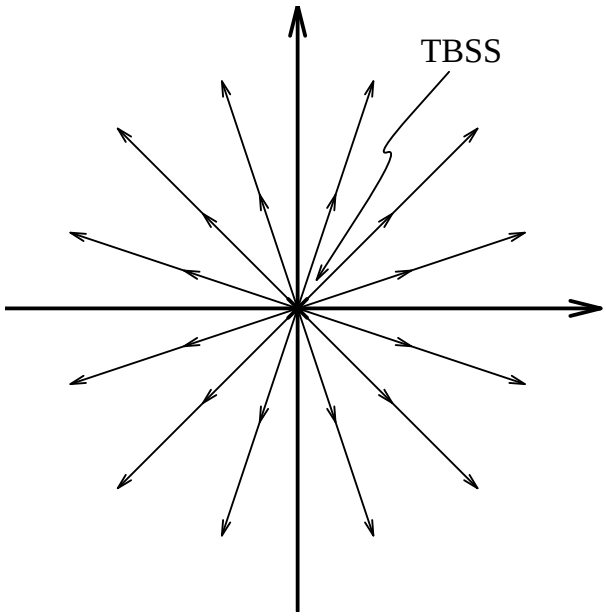

Fig. 3.3 TBSS represents the Tolman-Bondi solution with self-similarity in the case of $c > 0$ and $p < 0$. The axes correspond to the modes of linear perturbation Eq. (3.114).

(ii) Case 2 ($p = 0$).

The gauge condition which we use is

$$f = -\frac{9}{4\alpha}c_2. \tag{3.117}$$

By using the above condition, Eq. (3.117), we obtain the physical perturbation

$$\begin{aligned}\frac{\delta\overset{(L)}{\widetilde{\rho}}}{\rho^*} = &\frac{e^{\omega\tau}r^{\omega}}{\alpha\left[\frac{2r^{\alpha}}{9c}(\cosh\eta-1)-\frac{c^{1/2}\sinh\eta}{\cosh\eta-1}\right]}\Bigg\{\\ &\Delta_1^+\left[(\omega+3\alpha)r^{\alpha}\left(2(\cosh\eta-1)-\frac{3\sinh\eta(\sinh\eta-\eta)}{\cosh\eta-1}\right)\right.\\ &\left.+\frac{27c^{3/2}\alpha}{2}\left(-\frac{\sinh\eta}{\cosh\eta-1}+\frac{(2\cosh\eta+1)(\sinh\eta-\eta)}{(\cosh\eta-1)^2}\right)\right]\\ &+\Delta_2^+\left[\frac{(\omega+3\alpha)r^{\alpha}\sinh\eta}{\cosh\eta-1}-\frac{9\alpha c^{2/3}(2\cosh\eta+1)}{2(\cosh\eta-1)^2}\right]\Bigg\},\end{aligned} \tag{3.118}$$

where

$$\Delta_1^+ = \frac{1}{9c^2}c_1, \tag{3.119}$$

$$\Delta_2^+ = c^{1/2}c_3. \tag{3.120}$$

The regularity condition at $r = 0$ and $r = \infty$ implies that no modes are allowed.

From the linear perturbation analysis around the fixed point, we see that the long-time behavior of the spherically symmetric dust universe is separated into two types. One is the case that the fixed point is a repeller. In this case, the Tolman-Bondi solution with self-similarity does not play an important role in an expanding universe because this fixed point is unstable and the spacetime will diverge from this fixed point. In the other case, the fixed point has both relevant and irrelevant modes. Although this fixed point is not a repeller, it has continuously many relevant modes. Thus it is not as straightforward as in the case of gravitational collapse [52] to extract the long-time behavior of the universe, because it is sensitive to the initial condition and therefore we cannot uniquely predict the outcome.

3.3 Discussion of this chapter

In the cosmological problem, only the statistical quantities are meaningful if we think of a comparison with observations. There are some works in the RG approach [33, 34, 57] on the universe which has a hierarchical structure. We may contemplate further development of the RG approach to the cosmology formulated in the present work by introducing some kind of volume or statistical average for observables such as the energy density and the Hubble constant of the universe. As for the volume average, in the context of the averaging problem as to how to construct an effective cosmological model, some works have been done [57, 58, 59, 60, 61, 62, 63]. Although this problem is important to understand the structure formation in the present universe, by the nonlinearity of gravity it is difficult to average an inhomogeneous spacetime. A statistical concept is needed not only for comparison with observations but also for us to proceed further in the analysis of the RG equation because we have continuously many relevant (growing) modes around the fixed points. That is, the long-time behavior of the universe is sensitive to the initial configuration over which we have no *a priori* control and we have to consider the statistical likelihood of the initial values. We remark that the introduction of a volume average in a finite region of the universe potentially introduces the scale invariance violation by hand because the exact scale invariance holds only for an infinite space. Note that in quantum field theories and statistical physics of the second order phase transition the scale invariance violations are hidden in the form of a cutoff of the spectrum of physical modes. We shall elaborate our present observation in our future work.

The self-similar solution given by Eqs. (3.81) and (3.82) through the fixed point of the RG equation is essentially a function of $t^{-1/\alpha}r = t^{1-1/\alpha}r/t$, which is roughly the fraction of the physical distance to the horizon scale of the Friedmann universe. Also note that in the case of a nonlinear diffusion equation, Eq. (3.8) implies that the self-similar solution is a function of the ratio of the distance x to the diffusion length $\sqrt{t}$. In the both cases, the self-similar solution is a function of the distance in units of a physically relevant time-dependent scale. We believe this is a general phenomenon and the physical background of the RG equation which governs how dynamical variables deviate from the self-similar solution.

Chapter 4

Summary and discussion

The presently standard analytical method for the investigation of the dynamics in the inhomogeneous universe is the amplitude expansion (AE) method. In this method, the metric is expanded in powers of the amplitude of fluctuations. The obvious drawback of this perturbation scheme is the technical difficulty to treat the nonlinearity of fluctuations to higher orders. In this thesis, we studied the dynamics in inhomogeneous universe by use of the gradient expansion (GE) method and the renormalization group (RG) approach.

As for the GE method, quantities can be expanded according to the order of its spatial derivatives (the spatial curvature terms). It is assumed that the spatial derivatives are much smaller than the time derivatives. In the usual GE method, the disadvantage over the AE method is that we can not treat the short wavelength components of fluctuations and the universe with a nonsmall spatial curvature. The advantage over the AE method is that the nonlinearity of fluctuations is easily tractable. Moreover, we improved the usual GE method in order to treat the universe with the nonsmall spatial curvature.

As for the RG method, we can see the dynamics as a map from one set of initial data to another by use of the scale transformation and the equation of motion. Repeating the RG transformation, we can see the long-time behavior of the system we considered. The fixed point of the RG transformation corresponds to the self-similar solution and the character of the fixed point is determined by the RG equation. The advantage over the AE method is that we can treat the nonlinearity of gravity since the fixed point has information of the nonlinearity and we can see easily the universality class of the long-time behavior without solving the equation of motion explicitly. The disadvantage is that we can not obtain meaningful information from the RG equation if the fixed point is trivial (*e.g.* a homogeneous and isotropic universe).

The GE method is similar to the RG method in some sense. By use of the GE method, we obtain the dynamics of the universe on a large scale. On the other hand, we get the long-time behavior of the universe by the RG approach. In the both methods, we hope that we can extract the "average dynamics" from the inhomogeneous universe.

In Chapter 2, we applied the improved GE to study how the inhomogeneities of spatial curvature affect the occurrence of inflation in the inhomogeneous universe which is constructed by the gradient expansion from a locally closed Friedmann (GECF), in which the inhomogeneities are described by a function $\Omega(x)$ and its spatial gradients. The two inflation models have been considered. One is a simple model universe with a cosmolog-

ical constant and radiation fluid. The other is a chaotic inflation model which is driven by a massive scalar field. We expanded the spatial metric up to the second order spatial derivatives $\nabla_i\nabla_j\Omega/\Omega$ and $\nabla_i\Omega\nabla_j\Omega/\Omega^2$. We solved the ordinary differential equations for the coefficient functions of these derivative terms numerically and evolved the inhomogeneous spatial metric [47]. We assumed that the inhomogeneities were generated by a single function $\Omega(x)$ whereas the universe needed not to have any symmetries.

How the inhomogeneities described by $\nabla_l\nabla^l\Omega/\Omega$ and $\nabla_l\Omega\nabla^l\Omega/\Omega^2$ affect the onset of inflation is shown in Figs. 2.5–2.7 for the cosmological constant model and Figs. 2.15–2.17 for the scalar field model. The term $\nabla_l\Omega\nabla^l\Omega/\Omega^2$, which contains only nonlinear terms in the context of AE, tends to prevent inflation and positive (negative) $\nabla_l\nabla^l\Omega/\Omega$ helps the universe to inflate (collapse). This is related to the fact that the spatial curvature grows rapidly when $\nabla_l\Omega\nabla^l\Omega/\Omega^2$ is large.

From the numerical results, we get the criterion for the onset of inflation in a simple time independent form Eq. (2.61). This means that the spatial curvature in the early stage should be less than the critical curvature value ${}^3R_{cr}$ over a region which has several times size of the local curvature radius $({}^3R_{init}(t))^{-1/2}$ for the onset of inflation in the future. We can compare the effect of inhomogeneities in the inflation model which is driven by a cosmological constant with the one in the model driven by a massive scalar field. The value of α in the scalar field model is larger than the one in the cosmological constant model. It means that the inflationary model driven by a massive scalar field is more sensitive to the inhomogeneities than the one by a cosmological constant.

If the homogeneous universe enters the inflationary phase, it never recollapses. However, for the inhomogeneous universe even if the local scale factor enters the inflationary phase, it would be possible to recollapse. It may be also possible that the recollapsing local scale factor re-expands again in the inhomogeneous universe. In order to observe the fate of the inhomogeneous universe, we should sum up all order terms of the series expansion. It is actually very difficult. In this thesis we investigated the behavior of solutions up to the first order of the expansion while the criteria of the validity of the approximation Eqs. (2.59) and (2.60) hold. For the purpose to know how the inhomogeneities affect the onset of inflation, it is worth clarifying the behavior of the approximate solutions of the order.

In Chapter 3, applying the RG method to the Einstein equations in a cosmological situation, we investigated the role of the scale invariance which the Einstein equations have. We considered the spherically symmetric but inhomogeneous universe filled with dust, where the Einstein equations have scale invariance, Eqs. (3.68)–(3.71), and applied the RG method to study its long-time asymptotics. The fixed point of the RG transformation is a self-similar solution with scale invariance of the Einstein equations. In order to study the flow of the RG around the fixed point, the linear perturbation analysis is used. We impose the regularity on the perturbation at the boundary where the radial coordinate r equals zero or infinity. This boundary means that the area radius equals zero or infinity in the case of $c = 0$; on the other hand, in the case of $c > 0$, it equals a finite or infinity. The fixed point is the Tolman-Bondi solution with self-similarity, which includes the flat Friedmann universe. The behavior of the fixed point is separated into the two types. The both types have many relevant modes of the perturbation. The fixed points of the RG flow are self-similar solutions of the Einstein equations, which are worth studying in their own right and have been studied by many people [39, 40]. Our approach

has an obvious advantage that the fixed point is in general not always spherical symmetric like the Tolman-Bondi solution of the dust filled universe. More importantly, we can systematically treat the *dynamics* of the universe near the self-similar solution, adopting the scale as a "time" of the evolution. The RG flow near the fixed points is a new aspect in the study of the self-similarity in the universe [38]. The Tolman-Bondi solution with self-similarity is unstable against almost all spherical modes of linear perturbation. The spacetime will deviate from this fixed point. It is necessary to study the nonspherical mode of perturbation to say something more definite.

Here we reconsider the stability of the Tolman-Bondi solution with self-similarity in the viewpoint of observations. Actually we observe astronomical objects along the past light cone of us and cosmological observation normally describes the distance in the Universe in terms of the redshift. It is important to study the Tolman-Bondi solution with self-similarity in terms of the redshift since it is used as cosmological model which described a hierarchical structure in observational cosmology [38, 39, 40]. On the redshift space, the density distribution in the fixed point seen by an observer at the origin look identical at all time except the overall scale and is described in terms of the redshift z and the observer time t_{obs}, see the Appendix H. As for the perturbation around the fixed point, the stability of the fixed point in the redshift description will be different from the results in the previous chapter because of the Sachs-Wolfe effects which is a gravitational effect due to the presence of matter between the light source and the observer. We are planning to compute the anomalous exponent for the density fluctuations in terms of the redshift.

Acknowledgments

This work is collaborated with Professor A. Hosoya, Professor H. Ishihara, T. Koike (Keio Univ.), and Professor J. Soda (Kyoto Univ.). I would like to thank K. Nakamura for discussions. This research is supported in part by the Japan Society for the Promotion of Science.

Appendix A

The relation between the exponent of the two-point correlation function of galaxies and the fractal dimension

we show the relation between the fractal dimension (D) and the exponent of the two-point correlation function of galaxies [3, 30].

(i) Two-point correlation function

Assuming the galaxy can be treated as a point with a same mass, statistical analysis of the large scale distribution of the matter in the universe are performed only on the number density,

$$n(\vec{r}) = \sum_{i=1}^{N} \delta(\vec{r} - \vec{r}_i). \tag{A.1}$$

Using Eq. (A.1), the two-point correlation function $\xi(r)$ [64] is defined as

$$\xi(r) = \frac{< n(\vec{r}_0) n(\vec{r}_0 + \vec{r}) >}{< n >^2} - 1, \tag{A.2}$$

where the average is defined by

$$< \cdots > = \frac{1}{V} \int_V (\cdots) d\vec{r}_0, \tag{A.3}$$

and

$$< n > = \frac{N}{V} \tag{A.4}$$

is the average density of galaxies in the sample (V is the sample volume and N is the number contained in V). Note that in Eq. (A.2) the angular average over all the possible directions of $\vec{r}$ is performed and only the radial dependence is considered. It is easily shown that the two-point correlation function $\xi(r)$ can be related to the

joint probability of finding an object in a volume δV_1 centered at $\vec{r}_1$ and another in δV_2 centered at $\vec{r}_2$,

$$P_{12} = < n >^2 \left[1 + \xi(r_{12})\right] \delta V_1 \delta V_2, \tag{A.5}$$

where r_{12} denotes the scaler distance between $\vec{r}_1$ and $\vec{r}_2$. Integrating Eq. (A.5) over V for both δV_1 and δV_2, we obtain that

$$\int_V \xi(r) dr = 0. \tag{A.6}$$

This means that if $\xi(r)$ is positive for some range of values of r, there must be other ranges in which it is negative.

The two-point correlation function computed for the catalog of galaxies (ξ_{GG}) and clusters of galaxies (ξ_{CC}) is written by a single power law:

$$\xi(r)_{GG} \simeq \left(\frac{r}{5h^{-1}\mathrm{Mpc}}\right)^{-\gamma} \quad (\gamma \simeq 1.7), \tag{A.7}$$

$$\xi(r)_{CC} \simeq \left(\frac{r}{25h^{-1}\mathrm{Mpc}}\right)^{-\gamma} \quad (\gamma \simeq 1.7 \sim 1.8). \tag{A.8}$$

(ii) Fractal dimension

A fractal is a system where more and more structures appear at smaller and smaller scales and the structures at small scales are similar to the one at large scales. Such structures are characterized by the fractal dimension.

For a simple example, we consider the self-similar distribution of point particles in three-dimensional space. In this case, we can find N_0 particles within a volume of size r_0. If we consider a larger volume of size $r_1 = L \cdot r_0$, we find $N_1 = \widetilde{L} \cdot N_0$ particles. In general, in a volume of size $r_n = L^n \cdot r_0$, we have $N_n = \widetilde{L^n} \cdot N_0$ particles. Then we can write a relation between N and r in the form;

$$N(r) = B \cdot r^D, \tag{A.9}$$

where the fractal dimension

$$D = \frac{\log \widetilde{L}}{\log L} \tag{A.10}$$

and the prefactor

$$B = \frac{N_0}{r_0^D} \tag{A.11}$$

is related to the lower cut-offs N_0 and r_0 of structure.

From Eq. (A.9), we can compute the average density $< n >$ for a sample of radius R_s. Assuming the sample volume is a sphere,

$$< n >= \frac{N(R_s)}{V(R_s)} = \frac{3B}{4\pi} R_s^{-(3-D)}. \tag{A.12}$$

Moreover we define the conditional density from an occupied point as

$$\Gamma(r) = \frac{1}{S(r)}\frac{dN(r)}{dr} = \frac{DB}{4\pi}r^{-(3-D)}, \tag{A.13}$$

where $S(r)$ is the area of a spherical shell of radius r.

Now, we consider the relation between the two pint correlation function and the fractal dimension.

From Eqs. (A.1) and (A.3),

$$\frac{< n(\vec{r}_0)n(\vec{r}_0+\vec{r}) >}{< n >} = \frac{1}{N}\sum_{i=1}^{N} n(\vec{r}_i+\vec{r}), \tag{A.14}$$

where $\vec{r}_i$ refers to the coordinates of all the objects of system. By performing an angular average over the directions of $\vec{r}$,

$$\begin{aligned}\frac{1}{N}\sum_{i=1}^{N}\frac{1}{4\pi r^2}\int d\Omega\int_r^{r+dr} r^2 dr n(\vec{r}_i+\vec{r}) &= \frac{1}{N}\sum_{i=1}^{N}\frac{1}{4\pi r^2}\frac{dN_i(r)}{dr} \\ &= \frac{1}{S(r)}\frac{dN(r)}{dr},\end{aligned} \tag{A.15}$$

where $dN_i(r)$ is the total number of objects labelled by the index j whose position $\vec{r}_i$ is such that

$$r \le |\vec{r}_i - \vec{r}_j| \le r + dr. \tag{A.16}$$

From the definition of the conditional density Eq. (A.13), we have

$$\xi(r) = \frac{\Gamma(r)}{< n >} - 1. \tag{A.17}$$

Using Eqs. (A.12) and (A.13), we obtain

$$\xi(r) = \frac{D}{3}\left(\frac{r}{R_s}\right)^{-(3-D)} - 1. \tag{A.18}$$

For $r \ll R_s$, the two-point correlation function can be approximated by a power law,

$$\xi(r) \sim r^{-(3-D)}. \tag{A.19}$$

From Eq. (A.19), the exponent of the two-point correlation function of galaxies and clusters of galaxies Eqs. (A.7) and (A.8) is related to the fractal dimension:

$$\gamma = 3 - D. \tag{A.20}$$

Note that from the definition of the two-point correlation function Eq. (A.2), $\xi(r)$ is an appropriate function to characterize correlation of the system where the average density is a well defined quantity, which becomes a constant value at large scale. Actually in the fractal distribution the average density is not a well defined quantity. Pietronero *et al.* [30, 3] pointed out that the conditional density rather than the two-point correlation function should be used for analysis of the galaxies distribution. Using the statistical analysis by the conditional density, a log-log plot of $\Gamma(r)$ of galaxies and clusters of galaxies can be fitted by the same line whose slope corresponds to the fractal dimension 2.

Appendix B

The linear approximate solutions in the AE

We review the linear approximation in the AE [25]. Assuming that the spacetime deviates only by a small amount from a homogeneous and isotropic spacetime, the spacetime can be split into two parts, the first being the background spacetime, the other describing the perturbation.

The background line element is

$$\begin{aligned} ds^2 &= g_{\mu\nu}dx^\mu dx^\nu, \\ &= -dt^2 + a^2(t)h_{ij}dx^i dx^j, \\ &= a^2(\eta)\left[-d\eta^2 + h_{ij}dx^i dx^j\right], \end{aligned} \tag{B.1}$$

where η is the conformal time $d\eta = a^{-1}dt$.

We choose the background metric to be the FRW metric, in which case

$$h_{ij} = \delta_{ij}\left[1 + \frac{k}{4}(x^2 + y^2 + z^2)\right]^{-2}, \tag{B.2}$$

where $k = 0$, 1, and -1 depending on whether the three-dimensional hypersurface η =const. is flat, closed, open respectively.

Considering the perturbation, the full line element may be represented by

$$ds^2 = \overset{(0)}{g}_{\mu\nu}\, dx^\mu dx^\nu + \delta g_{\mu\nu}dx^\mu dx^\nu, \tag{B.3}$$

where $\delta g_{\mu\nu}$ describes the perturbation.

For simplicity, we consider that the background model is a flat Friedmann universe filled with a perfect fluid Eq.(2.5).

In this case, the background solution is

$$a(\eta) = \eta^{2/(3\Gamma-2)}, \quad \overset{(0)}{h}_{ij} = \delta_{ij} \tag{B.4}$$

$$\overset{(0)}{\rho}(\eta) = a^{-3\Gamma}(\eta), \quad \overset{(0)}{u}_i = 0 \tag{B.5}$$

The perturbed quantities of the energy density of matter ρ and the three velocity u_i are defined as follows.

$$\rho = \overset{(0)}{\rho} + \delta\rho, \tag{B.6}$$

$$u_i = \overset{(0)}{u}_i + \delta u_i. \tag{B.7}$$

For convenience sake, we choose the synchronous gauge, which is defined by $\delta g_{00} = 0$ and $\delta g_{0i} = 0$, using the freedom of the coordinate transformations.

Substituting Eqs. (B.3), (B.6), and (B.7) into Eqs. (2.6)–(2.8) with $\Lambda = 0$ and taking the linear part of the perturbed quantities, the perturbed Einstein equations can be obtained.

$$\delta g^l_{i,jl} + \delta g^l_{j,il} - \delta g_{,ij} - \delta g^{,l}_{ij,l} + \delta g^{''}_{ij} + 2\frac{a^{'}}{a}\delta g^{'}_{ij} = 0 \quad (i \neq j), \tag{B.8}$$

$$\delta g^{''} + \frac{3\Gamma - 4}{2}\left(\delta g^{,l}_{,l} - \delta g^{,lm}_{lm}\right) + (3\Gamma - 1)\frac{a^{'}}{a}\delta g^{'} = 0, \tag{B.9}$$

$$\frac{\delta\rho}{\overset{(0)}{\rho}} = \frac{1}{6}\left(\frac{a}{a^{'}}\right)^2\left[\delta g^{,lm}_{lm} - \delta g^{,l}_{,l} + 2\frac{a^{'}}{a}\delta g^{'}\right], \tag{B.10}$$

$$\delta u_i = \frac{a}{4(2a'^2 - aa'')}\left(\delta g_{,i} - \delta g^{,l}_{il}\right), \tag{B.11}$$

where

$$\delta g = \delta g_{ll}, \quad \delta g' = \frac{\partial\delta g}{\partial\eta}, \quad \delta g_{,ij} = \frac{\partial^2\delta g}{\partial x^i \partial x^j}. \tag{B.12}$$

Here, we consider the infinitesimal coordinate transformations

$$x^\mu \longrightarrow x^\mu + \xi^\mu \quad (\xi^\mu \ll 1), \tag{B.13}$$

described by four functions ξ^μ of space and time. The above coordinate transformations induces a change in the perturbed metric $\delta g_{\mu\nu}$,

$$g_{\mu\nu} \longrightarrow g_{\mu\nu} + \nabla_\nu\xi_\mu + \nabla_\mu\xi_\nu, \tag{B.14}$$

where ∇_μ is a covariant derivative respect to the background metric $\overset{(0)}{g}_{\mu\nu}$. The quantity which is changed under the coordinate transformations Eq. (B.13) is unphysical and is called gauge mode. In order to get rid of the gauge mode, it is necessary to pick a special gauge where there is no residual coordinate freedom or use a gauge invariant quantity which is made up of the linear combination of the perturbed quantities.

Under the synchronous gauge, there is the residual gauge freedom which leads to the unphysical gauge modes,

$$\delta g_{ij} = \chi_{,ij}(x)\int\frac{d\eta}{a} + \frac{a^{'}}{a^2}\chi(x)\delta_{ij} + \varphi_{i,j}(x) + \varphi_{j,i}(x), \tag{B.15}$$

$$\xi^i = a^2\chi^{,i}(x)\int\frac{d\eta}{a^2} + \varphi^i(x), \tag{B.16}$$

where $\chi(x)$ and $\varphi^i(x)$ are arbitrary function of space.

In general, the metric perturbations may be categorized into three distinct types: scalar, vector, tensor perturbations, and can be expanded as a proper form in the Fourier space. For each type, we investigate the perturbations.

B.1 Tensor mode

In this section, we investigate the tensor mode of the perturbations.

Tensor perturbations are constructed using a symmetric three tensor $G_{ij} = G_{ij}\exp(ikx)$ which satisfies the constraints

$$G^l_l = 0, \quad G_{ij}k^i = 0. \tag{B.17}$$

This mode corresponds to the freedom of the gravitational wave.

The tensor mode of the metric perturbations can be described by

$$\delta g_{ij} = \nu(\eta) G_{ij}, \tag{B.18}$$

where $\nu(\eta)$ is an arbitrary function of η.

From Eq. (B.8), we have

$$\nu^{''} + 2\frac{a^{'}}{a}\nu^{'} + k^2\nu = 0. \tag{B.19}$$

Integrating Eq. (B.19), we obtain

$$\nu = \begin{cases} \eta^{-1}\sin k\eta, & \eta^{-1}\cos k\eta & \left(\Gamma = \frac{4}{3}\right), \\ \eta^{-3}(\sin k\eta - k\eta\cos k\eta), & \eta^{-3}(\cos k\eta + k\eta\sin k\eta) & (\Gamma = 1). \end{cases} \tag{B.20}$$

Since tensor modes can not be constructed by the residual gauge mode Eq. (B.15), these are physical quantities.

B.2 Vector mode

In this section, we consider the vector mode of the perturbations.

Vector perturbations are constructed using the three vector $S_i = S_i\exp(ikx)$ which satisfies the constraints

$$S_i k^i = 0. \tag{B.21}$$

The vector mode of the metric perturbations can be described by

$$\delta g_{ij} = \sigma(\eta) S_{ij}, \tag{B.22}$$

where $\sigma(\eta)$ is an arbitrary function of η and $S_{ij} = S_i k_j + S_j k_i$.

From Eqs. (B.8) and (B.11), we have

$$\sigma^{''} + 2\frac{a^{'}}{a}\sigma^{'} = 0, \tag{B.23}$$

$$\delta u^i = \frac{a\sigma^{'}}{4(2a'^2 - aa'')} S_i. \tag{B.24}$$

Integrating Eq. (B.23), we obtain

$$(\sigma, \delta u^i) = \begin{cases} (-\eta^{-1}, \eta^{-1}) & \left(\Gamma = \frac{4}{3}\right), \\ \left(-\frac{1}{3}\eta^{-3}, \frac{1}{24}\eta^{-4}\right) & (\Gamma = 1). \end{cases} \tag{B.25}$$

From Eq. (B.15), the gauge modes are

$$\varphi_i = \sigma_0(x) S_i, \tag{B.26}$$

$$\delta g_{ij} = \sigma_0(x) S_{ij}, \tag{B.27}$$

where $\sigma_0(x)$ is an arbitrary function of space. However, from Eq. (B.24), since this gauge mode dose not affect on δu^i, the perturbation δu^i is a physical quantity.

B.3 Scalar mode

In this section, we investigate the scalar mode of the perturbations.

Scalar perturbations are constructed by two ways; either by multiplying the background spatial metric $\overset{(0)}{g}_{ij}$ with a scalar $Q = \exp(ikx)$, or by taking covariant derivatives, which is respect to $\overset{(0)}{g}_{ij}$, of a scalar function $P_i = ik_i k^{-2} Q$.

The scalar mode of the metric perturbations can be described by

$$\delta g_{ij} = \lambda(\eta) P_{ij} + \mu(\eta) Q_{ij}, \tag{B.28}$$

where

$$Q_{ij} = \frac{1}{3}\delta_{ij} Q, \quad P_{ij} = \left(\frac{1}{3}\delta_{ij} - \frac{k_i k_j}{k^2}\right) Q, \tag{B.29}$$

and $\lambda(\eta)$ and $\mu(\eta)$ are arbitrary functions of η.

From Eqs. (B.8)–(B.11), we have

$$\frac{\delta\rho}{\overset{(0)}{\rho}} = \frac{1}{9}\left(\frac{a}{a'}\right)^2 \left[k^2(\lambda+\mu) + 3\frac{a'}{a}\mu'\right] Q, \tag{B.30}$$

$$\delta u^i = \frac{ak^2}{6(2a'^2 - aa'')}(\lambda+\mu) P_i, \tag{B.31}$$

$$\lambda'' + 2\frac{a'}{a}\lambda' - \frac{k^2}{3}(\lambda+\mu) = 0, \tag{B.32}$$

$$(\lambda+\mu)'' + 2\frac{a'}{a}(\lambda+\mu)' + (\Gamma - 1)\left[3\frac{a'}{a}\mu' + k^2(\lambda+\mu)\right] = 0. \tag{B.33}$$

Since in the structure formation in the universe, we interest in the density perturbations $\delta\rho$, which depend on only the scalar modes, we concentrate on the density contrast $\delta\rho/\overset{(0)}{\rho}$.

From Eq. (B.15), there are two gauge modes,

$$\lambda = -\mu = \text{const.}, \quad (\chi = 0, \varphi_i = P_i), \tag{B.34}$$

$$\lambda = -k^2 \int \frac{d\eta}{a}, \quad \lambda + \mu = -3\frac{a^{'}}{a^2}, \quad (\chi = Q, \varphi_i = 0). \tag{B.35}$$

Since the density contrast Eq. (B.30) is changed by the above gauge modes, the density contrast computed under the synchronous gauge is unphysical.

Thus we choose a new gauge which is defined by

$$\delta g_{0i} = 0, \quad \delta u_i = 0. \tag{B.36}$$

The density contrast computed under Eq. (B.36) is

$$\frac{\delta\rho}{\overset{(0)}{\rho}} = \frac{1}{9}\left(\frac{a}{a^{'}}\right)^2 \left[k^2(\lambda+\mu) - 3\frac{a^{'}}{a}\lambda^{'}\right] Q. \tag{B.37}$$

Since this density contrast dose not contain residual gauge modes, it is a physical quantity.

Eliminating $\lambda(\eta)$ and $\mu(\eta)$ by use of Eqs. (B.32), (B.33), and (B.37), we have

$$K^{''} + (4 - 3\Gamma)\frac{a^{'}}{a}K^{'} + \left[(\Gamma - 1)k^2 + \frac{3(3\Gamma^2 - 8\Gamma + 2)}{2}\left(\frac{a^{'}}{a}\right)\right] K = 0, \tag{B.38}$$

where $K = \delta\rho/\overset{(0)}{\rho}$.

Integrating Eq. (B.38), we obtain

$$K = \begin{cases} \left(1 + \frac{i\sqrt{3}}{k\eta} - \frac{2}{\eta^2}\right)\exp\left(\frac{ik\eta}{\sqrt{3}}\right) & \left(\Gamma = \frac{4}{3}\right), \\ \eta^2 Q, \quad \eta^{-3}Q & (\Gamma = 1). \end{cases} \tag{B.39}$$

Appendix C

The approximate solutions constructed by the GE method up to second order

We show the concrete form of the approximate solution up to second order obtained by use of the usual gradient expansion method (GEFF) [21]. For simplicity, the universe is assumed to filled with a perfect fluid. In this case, the Einstein equations are represented by Eqs. (2.6)–(2.8) where a cosmological constant Λ is taken to be zero.

At lowest order, we consider the quasi-isotropic universe in the form (2.2). The lowest order solutions are

$$\overset{(0)}{\gamma}_{ij} = a(t)^2 h_{ij}(x) = t^{2/(3\Gamma)} h_{ij}(x), \tag{C.1}$$

$$\overset{(0)}{\rho} = \frac{4}{3\kappa\Gamma^2} t^{-2}, \tag{C.2}$$

$$\overset{(0)}{u}_i = 0. \tag{C.3}$$

At next order, the spatial metric $\overset{(1)}{\gamma}_{ij}$ is constructed by the symmetric tensors of the second order in the spatial gradients of h_{ij} in the form

$$\overset{(1)}{\gamma}_{ij}(t,x) = a^2(t)\left[f_1(t) R_{ij} + g_1(t) R h_{ij}\right], \tag{C.4}$$

where R_{ij} is the Ricci tensor associated with $h_{kl}(x)$, $R \equiv h^{ij} R_{ij}$, and $f_1(t)$ and $g_1(t)$ are functions of time.

From Eq. (2.6) with $\Lambda = 0$, we obtain

$$f_1(t) = -\frac{9\Gamma^2}{(9\Gamma^2-4)(9\Gamma-4)}\left[\frac{3}{4}\Gamma^2 - 3\Gamma + 1\right] t^{2-4/(3\Gamma)} + \alpha_1 t^{-1} - \frac{\beta_1}{3} t^{1-2/\Gamma} + \alpha_2, \tag{C.5}$$

$$g_1(t) = -\frac{9\Gamma^2}{(9\Gamma^2-4)} t^{2-4/(3\Gamma)} + \beta_1 t^{1-2/\Gamma} + \beta_2, \tag{C.6}$$

where α_1, α_2, β_1, and β_2 are constant. Hereafter we concentrate on the growing modes of the above solutions which become important in the expanding universe.

Thus the first order solutions are

$$\overset{(1)}{\gamma}_{ij} = a(t)^2 \left[-\frac{9\Gamma^2}{(9\Gamma^2-4)(9\Gamma-4)} \left(\frac{3}{4}\Gamma^2 - 3\Gamma + 1 \right) t^{2-4/(3\Gamma)} R h_{ij} - \frac{9\Gamma^2}{(9\Gamma^2-4)} t^{2-4/(3\Gamma)} R_{ij} \right], \tag{C.7}$$

$$\overset{(1)}{\rho} = \frac{3\Gamma}{2(9\Gamma-4)\kappa} t^{-4/(3\Gamma)} R, \tag{C.8}$$

$$\overset{(1)}{u}_i = \frac{27\Gamma^3(1-\Gamma)}{8(3\Gamma+2)(9\Gamma-4)} t^{3-4/(3\Gamma)} \partial_i R. \tag{C.9}$$

At second order, we solve the Einstein equations generated by ${}^3\overset{(2)}{R}(\gamma)$ associated with $\gamma_{ij} = \overset{(0)}{\gamma}_{ij} + \overset{(1)}{\gamma}_{ij}$. The term ${}^3\overset{(2)}{R}(\gamma)$ is

$${}^3\overset{(2)}{R}{}^j_i(\gamma) = \frac{1}{3} {}^3\overset{(2)}{R}(\gamma)\delta^j_i + \overline{{}^3\overset{(2)}{R}{}^j_i(\gamma)}, \tag{C.10}$$

$${}^3\overset{(2)}{R}(\gamma) = -\frac{1}{2a^2}[2f_1 R^2 + 2g_1 R^m_l R^l_m + (4f_1+g_1)\nabla_l\nabla^l R], \tag{C.11}$$

$$\begin{aligned} \overline{{}^3\overset{(2)}{R}{}^j_i(\gamma)} = -\frac{1}{2a^2} \Big[& (2f_1+3g_1)(RR^j_i - \frac{1}{3}R^2) - 4g_1(R_{il}R^{jl} - \frac{1}{3}R^m_l R^l_m \delta^j_i) \\ & + f_1(\nabla_i\nabla^j R - \frac{1}{3}\nabla_l\nabla^l R\delta^j_i) + g_1(\nabla_l\nabla^l R^j_i - \frac{1}{3}\nabla_l\nabla^l R\delta^j_i) \Big], \end{aligned} \tag{C.12}$$

where ∇_i denotes a covariant derivative with respect to h_{ij}.

The second order terms can be written in the form

$$\begin{aligned} \overset{(2)}{\gamma}_{ij} = a(t)^2 \Big[& a_2(t)R^2 h_{ij} + b_2(t) R R_{ij} + c_2(t) R_{lm}R^{lm} h_{ij} + d_2(t) R_{il}R^l_j \\ & + e_2(t)\nabla_l\nabla^l R h_{ij} + f_2(t)\nabla_i\nabla_j R + g_2(t)\nabla_l\nabla^l R_{ij} \Big], \end{aligned} \tag{C.13}$$

$$\overset{(2)}{\rho} = \rho_2(t)R^2 + \mu_2(t)R_{lm}R^{lm} + \varepsilon_2(t)\nabla_l\nabla^l R_{ij}, \tag{C.14}$$

$$\begin{aligned} \overset{(2)}{u}_i = & u_2(t) R\nabla_i R + v_2(t) R^l_i \nabla_l R + w_2(t) R^{lm}\nabla_i R_{lm} \\ & + x_2(t) R^l_m \nabla_l R^m_i + y_2(t)\nabla_i\nabla_l\nabla^l R. \end{aligned} \tag{C.15}$$

From Eq. (2.6) with $\Lambda = 0$, the functions a_2–g_2 are

$$a_2 = \frac{81\Gamma^4 \left(-\frac{729}{64}\Gamma^7 + \frac{405}{16}\Gamma^6 - \frac{1701}{16}\Gamma^5 + 1638\Gamma^4 - \frac{7737}{4}\Gamma^3 + 639\Gamma^2 + 21\Gamma - 28 \right)}{(3\Gamma+2)^2(3\Gamma-2)^2(9\Gamma-4)^2(15\Gamma-8)(9\Gamma-2)} t^{4-8/(3\Gamma)}, \tag{C.16}$$

$$b_2 = \frac{81\Gamma^4(9\Gamma^3 - 171\Gamma^2 + 54\Gamma + 8)}{4(3\Gamma+2)^2(3\Gamma-2)^2(9\Gamma-4)(9\Gamma-2)} t^{4-8/(3\Gamma)}, \tag{C.17}$$

$$c_2 = \frac{162\Gamma^4(-12\Gamma^2 + 3\Gamma + 2)}{(3\Gamma+2)^2(3\Gamma-2)^2(15\Gamma-8)(9\Gamma-2)} t^{4-8/(3\Gamma)}, \tag{C.18}$$

$$d_2 = \frac{81\Gamma^4(15\Gamma+2)}{2(3\Gamma+2)^2(3\Gamma-2)^2(9\Gamma-2)} t^{4-8/(3\Gamma)}, \tag{C.19}$$

$$e_2 = \frac{81\Gamma^4(-3\Gamma^3+6\Gamma^2+12\Gamma-8)}{16(3\Gamma+2)(3\Gamma-2)^2(15\Gamma-8)(9\Gamma-2)}t^{4-8/(3\Gamma)}, \tag{C.20}$$

$$f_2 = -\frac{81\Gamma^4(3\Gamma^2-12\Gamma+4)}{16(3\Gamma+2)(3\Gamma-2)^2(9\Gamma-4)(9\Gamma-2)}t^{4-8/(3\Gamma)}, \tag{C.21}$$

$$g_2 = -\frac{81\Gamma^4}{4(3\Gamma+2)(3\Gamma-2)^2(9\Gamma-2)}t^{4-8/(3\Gamma)}. \tag{C.22}$$

From Eq. (2.7) with $\Lambda = 0$, the functions ρ_2–ε_2 are

$$\rho_2(t) = \frac{27\Gamma^3(245\Gamma^5+108\Gamma^4-180\Gamma^3-936\Gamma^2+800\Gamma-160)}{16\kappa(3\Gamma+2)^2(3\Gamma-2)(9\Gamma-4)^2(15\Gamma-8)}t^{2-8/(3\Gamma)}, \tag{C.23}$$

$$\mu_2(t) = \frac{54\Gamma^3}{\kappa(3\Gamma+2)^2(3\Gamma-2)(15\Gamma-8)}t^{2-8/(3\Gamma)}, \tag{C.24}$$

$$\varepsilon_2(t) = \frac{27\Gamma^3(\Gamma-1)}{4\kappa(3\Gamma+2)(3\Gamma-2)(15\Gamma-8)}t^{2-8/(3\Gamma)}. \tag{C.25}$$

From Eq. (2.8), the functions u_2–y_2 are

$$u_2(t) = \frac{243\Gamma^5(\Gamma-1)(729\Gamma^5-1944\Gamma^4+936\Gamma^3+2352\Gamma^2-2096\Gamma+448)}{64(3\Gamma+2)^2(3\Gamma-2)(9\Gamma-4)^2(15\Gamma-8)(9\Gamma-2)}t^{5-8/(3\Gamma)}, \tag{C.26}$$

$$v_2(t) = 0, \tag{C.27}$$

$$w_2(t) = -\frac{243\Gamma^5(\Gamma-1)}{(3\Gamma+2)^2(3\Gamma-2)(15\Gamma-8)(9\Gamma-2)}t^{5-8/(3\Gamma)}, \tag{C.28}$$

$$x_2(t) = 0, \tag{C.29}$$

$$y_2(t) = -\frac{243\Gamma^5(\Gamma-1)^2}{16(3\Gamma+2)(3\Gamma-2)(15\Gamma-8)(9\Gamma-2)}t^{5-8/(3\Gamma)}. \tag{C.30}$$

Appendix D

Rule of the order of the spatial tensor

When we calculate the first order approximation, we determine the order of spatial tensor which contains the sixth order terms in the spatial gradient at least because they appear in the spatial curvature ${}^3\overset{(1)}{R}_i{}^j$. Here we explain the rule we adopted when we calculate the first order approximation.

For scalar: $(\nabla^{(2)}\Omega)$ and $(\nabla^{(4)}\Omega)$ are the scalar of the second order terms in the spatial gradient and the fourth order terms, respectively. $(\nabla^{(2)}\Omega)$ consists of two terms,

$$\frac{\nabla_l\nabla^l\Omega}{\Omega}, \quad \frac{\nabla_l\Omega\nabla^l\Omega}{\Omega^2}.$$

$(\nabla^{(4)}\Omega)$ is classified into the following three types,

$$\nabla_l\nabla^l(\nabla^{(2)}\Omega), \quad \nabla_l(\nabla^{(2)}\Omega)\nabla^l\Omega, \quad (\nabla^{(2)}\Omega)(\nabla^{(2)}\Omega).$$

For spatial tensor: We adopt the tensors $(\nabla^{(4)}\Omega)_{ij}$ consist of the following terms,

$$\frac{\nabla_i\nabla_j\nabla_l\nabla^l\Omega}{\Omega},$$
$$\frac{\nabla_i\nabla_j\Omega\nabla_l\nabla^l\Omega}{\Omega^2}, \frac{\nabla_i\Omega\nabla_j\nabla_l\nabla^l\Omega}{\Omega^2}, \frac{\nabla_l\nabla_i\nabla_j\Omega\nabla^l\Omega}{\Omega^2}, \frac{\nabla_i\nabla_j(\nabla_l\Omega\nabla^l\Omega)}{\Omega^2},$$
$$\frac{\nabla_i\Omega\nabla_j\Omega\nabla_l\nabla^l\Omega}{\Omega^3}, \frac{\nabla_i\nabla_j\Omega\nabla_l\Omega\nabla^l\Omega}{\Omega^3}, \frac{\nabla_i\Omega\nabla_j(\nabla_l\Omega\nabla^l\Omega)}{\Omega^3},$$
$$\frac{\nabla_i\Omega\nabla_j\Omega\nabla_l\Omega\nabla^l\Omega}{\Omega^4},$$

because the trace of these terms belong to the above scalar category.

The sixth order terms in the spatial gradient appear in the spatial curvature ${}^3\overset{(1)}{R}_i{}^j$ are transformed into the following terms by use of the commutation relation,

$$\frac{\nabla_l\nabla_m\nabla_i\nabla_j\Omega\nabla^l\nabla^m\Omega}{\Omega^2}, \frac{\nabla_l\nabla_i\nabla_j\Omega\nabla^l\nabla_m\nabla^m\Omega}{\Omega^2},$$
$$\frac{\nabla_i\nabla_j(\nabla_l\nabla_m\nabla^m\Omega\nabla^l\Omega)}{\Omega^2}, \frac{\nabla_i\nabla_j(\nabla_l\nabla^l(\nabla_m\Omega\nabla^m\Omega))}{\Omega^2}.$$

We treat them as higher order terms. They don't affect the calculation in the first order approximation because their trace contain the spatial derivative of $(\nabla^{(2)}\Omega)$.

Appendix E

Expression for the spatial curvature in the first order approximation

In the GECF or GEOF, we expand the spatial metric up to the second order of the spatial gradients in the form

$$\gamma_{ij} = \overset{(0)}{\gamma}{}^{\pm}_{ij} + \overset{(1)}{\gamma}{}^{\pm}_{ij}, \tag{E.1}$$

where

$$\begin{aligned}
\overset{(0)}{\gamma}{}^{\pm}_{ij} &= a_{\pm}^2(t,\Omega(x))h^{\pm}_{ij}, \\
\overset{(1)}{\gamma}{}^{\pm}_{ij} &= a_{\pm}^2(t,\Omega(x))\left[\frac{1}{3}F(t,\Omega)\frac{\nabla_l\nabla^l\Omega}{\Omega}h^{\pm}_{ij} + \overline{F}(t,\Omega)\frac{\overline{\nabla_i\nabla_j\Omega}}{\Omega}\right. \\
&\quad \left. + \frac{1}{3}G(t,\Omega)\frac{\nabla_l\Omega\nabla^l\Omega}{\Omega^2}h^{\pm}_{ij} + \overline{G}(t,\Omega)\frac{\overline{\nabla_i\Omega\nabla_j\Omega}}{\Omega^2}\right].
\end{aligned}$$

From the inverse of γ_{ij}, we get

$$\begin{aligned}
\overset{(1)}{\gamma}{}^{ij}_{\pm} &= -\frac{1}{a_{\pm}^2}\left[\frac{1}{3}F\frac{\nabla_l\nabla^l\Omega}{\Omega}h^{ij}_{\pm} + \overline{F}\frac{\overline{\nabla^i\nabla^j\Omega}}{\Omega}\right. \\
&\quad \left. + \frac{1}{3}(G+2\overline{F}^2)\frac{\nabla_l\Omega\nabla^l\Omega}{\Omega^2}h^{ij}_{\pm} + (\overline{G}-\overline{F}^2)\frac{\overline{\nabla^i\Omega\nabla^j\Omega}}{\Omega^2}\right].
\end{aligned} \tag{E.2}$$

The spatial Ricci and scalar curvatures are

$$\begin{aligned}
{}^3\overset{(1)}{R}{}_{ij}(\gamma_{ij}) &= -\left[\frac{4}{3}\frac{a'_{\pm}\Omega}{a_{\pm}} - \frac{2}{3}\overline{F}\right]\frac{\nabla_l\nabla^l\Omega}{\Omega}h^{\pm}_{ij} \\
&\quad + \frac{2}{3}\left[-2\frac{a''_{\pm}\Omega^2}{a_{\pm}} + \left(\frac{a'_{\pm}\Omega}{a_{\pm}}\right)^2 + \overline{F}'\Omega - \overline{F} + \frac{a'_{\pm}\Omega}{a_{\pm}}\overline{F} - \overline{F}^2\right]\frac{\nabla_l\Omega\nabla^l\Omega}{\Omega^2}h^{\pm}_{ij} \\
&\quad - \left[\frac{a'_{\pm}\Omega}{a_{\pm}} - 2\overline{F}\right]\frac{\overline{\nabla_i\nabla_j\Omega}}{\Omega} \\
&\quad + \left[-\frac{a''_{\pm}\Omega^2}{a_{\pm}} + 2\left(\frac{a'_{\pm}\Omega}{a_{\pm}}\right)^2 + 2\overline{F}'\Omega - 2\overline{F} - \frac{a'_{\pm}\Omega}{a_{\pm}}\overline{F} + \frac{5\overline{F}^2}{2}\right]\frac{\overline{\nabla_i\Omega\nabla_j\Omega}}{\Omega^2},
\end{aligned}$$

$$
\begin{aligned}
{}^{3}\overset{(1)}{R}_{i}{}^{j}(\gamma_{ij}) = &-\frac{1}{a_\pm^2}\left\{\frac{2}{3}\left[\pm F-\overline{F}+2\frac{a'_\pm\Omega}{a_\pm}\right]\frac{\nabla_l\nabla^l\Omega}{\Omega}\delta_i^j\right.\\
&+\frac{2}{3}\left[\pm G+\overline{F}-\overline{F}'\Omega\pm 2\overline{F}^2-\overline{F}^2+\Omega^2\left(2\frac{a''_\pm}{a_\pm}-\frac{a'^2_\pm}{a_\pm^2}\right)\right]\frac{\nabla_l\Omega\nabla^l\Omega}{\Omega^2}\delta_i^j\\
&+\left[\frac{a'_\pm\Omega}{a_\pm}\pm 2\overline{F}-2\overline{F}\right]\frac{\overline{\nabla_i\nabla^j\Omega}}{\Omega}\\
&\left.+\left[\pm 2\overline{G}+2\overline{F}-2\overline{F}'\Omega-(\pm 2+\frac{1}{2})\overline{F}^2-2\left(\frac{a'_\pm\Omega}{a_\pm}\right)^2+\frac{a''_\pm\Omega^2}{a_\pm}\right]\frac{\overline{\nabla_i\Omega\nabla^j\Omega}}{\Omega^2}\right\},\\
{}^{3}\overset{(1)}{R}\,(\gamma_{ij}) = &-\frac{1}{a_\pm^2}\left\{2\left[\pm F-\overline{F}+2\frac{a'_\pm\Omega}{a_\pm}\right]\frac{\nabla_l\nabla^l\Omega}{\Omega}\right.\\
&\left.+2\left[\pm G+\overline{F}-\overline{F}'\Omega\pm 2\overline{F}^2-\overline{F}^2+\Omega^2\left(2\frac{a''_\pm}{a_\pm}-\frac{a'^2_\pm}{a_\pm^2}\right)\right]\frac{\nabla_l\Omega\nabla^l\Omega}{\Omega^2}\right\},
\end{aligned}
\tag{E.3}
$$

where $a'_\pm \equiv \partial a_\pm/\partial\Omega$.

Appendix F

Equations for a', a'', ϕ_0', ϕ_0'', and $\overline{F}'$

We derive the equation for a', a'', ϕ_0', ϕ_0'', and $\overline{F}'$.
From Eqs. (2.71) and (2.73) we obtain

$$\ddot{a}(t,\Omega) = \frac{\dot{a}^2(t,\Omega)}{a(t,\Omega)} + \frac{1}{a(t,\Omega)} - \frac{\kappa}{2} a(t,\Omega)\dot{\phi}_0^2(t,\Omega). \tag{F.1}$$

Differentiating Eqs. (2.74) and (F.1) with respect to Ω, we find the equations which $a'(t,\Omega)$ and $\phi'(t,\Omega)$ must satisfy

$$\ddot{a}' = 2\frac{\dot{a}}{a}\dot{a}' - \left[\frac{\dot{a}^2+1}{a^2} + \frac{\kappa}{2}\dot{\phi}_0^2\right] a' - \kappa\dot{\phi}_0\dot{\phi}_0' a, \tag{F.2}$$

$$\ddot{\phi}_0' = -3\frac{\dot{a}}{a}\dot{\phi}_0' - \left(\frac{dV}{d\phi}\right)'\Big|_0 - 3\frac{a\dot{a}' - \dot{a}a'}{a^2}\dot{\phi}_0. \tag{F.3}$$

Differentiating Eqs. (F.2) and (F.3) again, we find

$$\begin{aligned}\ddot{a}'' = {} & 2\frac{\dot{a}}{a}\dot{a}'' - \left[\frac{\dot{a}^2+1}{a^2} + \frac{\kappa}{2}\dot{\phi}_0^2\right] a'' + 2\frac{\dot{a}'^2}{a} - 4\frac{a'\dot{a}\dot{a}'}{a^2} + 2\frac{a'^2(\dot{a}^2+1)}{a^3} \\ & -2\kappa a'\dot{\phi}_0\dot{\phi}_0' - \kappa a\left(\dot{\phi}_0\dot{\phi}_0'' + \dot{\phi}_0'^2\right),\end{aligned} \tag{F.4}$$

$$\ddot{\phi}'' = -3\frac{\dot{a}}{a}\dot{\phi}_0'' - \left(\frac{dV}{d\phi}\right)''\Big|_0 - 6\dot{\phi}_0'\frac{a\dot{a}' - \dot{a}a'}{a^2} - 3\dot{\phi}_0\left[\frac{\dot{a}''}{a} - 2\frac{a'\dot{a}'}{a^2} - \frac{a''\dot{a}}{a^2} + 2\frac{\dot{a}a'^2}{a^3}\right]. \tag{F.5}$$

Similarly from Eq. (2.83), we find that $\overline{F}'$ must satisfy

$$\begin{aligned}\dot{\overline{F}}' = {} & 2\frac{a\dot{a}' - a'\dot{a}}{a^2} + 2\Omega\left[\frac{\dot{a}''}{a} - 2\frac{a'\dot{a}'}{a^2} - \frac{a''\dot{a}}{a^2} + 2\frac{\dot{a}a'^2}{a^3}\right] \\ & +\kappa\left(\dot{\phi}_0\phi_0' + \dot{\phi}_0'\phi_0'\Omega + \dot{\phi}_0\phi_0''\Omega\right).\end{aligned} \tag{F.6}$$

Appendix G

Tolman-Bondi solution with self-similarity

In the spherically symmetric universe filled with dust, the most general solution of the Einstein equations is the Tolman-Bondi solution [65]:

$$A(r,t) = \frac{B'(r,t)}{\sqrt{1+C_1(r)}}, \tag{G.1}$$

$$B(r,t) = \begin{cases} \left(\frac{9C_2(r)}{4}\right)^{1/3}[t-C_3(r)]^{2/3} & \text{for } C_1(r)=0, \\ \frac{C_2(r)}{2C_1(r)}(\cosh\eta-1) \quad \left(t-C_3(r)=\frac{C_2(r)}{2C_1^{3/2}(r)}(\sinh\eta-\eta)\right) & \text{for } C_1(r)>0, \\ \frac{C_2(r)}{2\lvert C_1(r)\rvert}(1-\cos\eta) \quad \left(t-C_3(r)=\frac{C_2(r)}{2\lvert C_1^{3/2}(r)\rvert}(\eta-\sin\eta)\right) & \text{for } C_1(r)<0, \end{cases} \tag{G.2}$$

$$\kappa\rho(r,t) = \frac{C_2'(r)}{B^2B'}, \tag{G.3}$$

where $C_1(r)$, $C_2(r)$, and $C_3(r)$ are arbitrary functions of r and a prime denotes the derivative with respect to r. By taking $C_1(r)=c$, $C_2(r)=4r^\alpha/9$, and $C_3(r)=pr^\alpha$, we obtain the Tolman-Bondi solution with self-similarity, Eqs. (3.88)–(3.96).

As for the calculation of linear perturbation, since we concentrate on the spherical modes of perturbation around a self-similar solutions, it is enough to consider the linear perturbation of the arbitrary functions $C_1(r)$, $C_2(r)$, and $C_3(r)$. The perturbed quantities $\delta C_1(r)$, $\delta C_2(r)$, and $\delta C_3(r)$ can be expressed by a superposition of modes with different ω and taken in the following form:

$$\delta C_1(r) = c_1 r^\omega, \tag{G.4}$$
$$\delta C_2(r) = c_2 r^{\omega+\alpha}, \tag{G.5}$$
$$\delta C_3(r) = c_3 r^{\omega+\alpha}. \tag{G.6}$$

By a coordinate transformation of r,

$$r \longrightarrow r + F(r), \tag{G.7}$$

where $F(r)$ is an arbitrary function of r, we obtain the gauge mode of linear perturbation. This function $F(r)$ also can be expressed by the superposition of modes with different ω in the form

$$F(r) = fr^{\omega+1}. \tag{G.8}$$

Appendix H

Tolman-Bondi solution with self-similarity and redshift space

We see Tolman-Bondi solution with self-similarity in term of redshift z.

Consider the null geodesic along the radial coordinate r. The null geodesic equation is given by the Euler-Lagrange equation derived from the Lagrangian,

$$\mathcal{L} = \frac{1}{2}\left[-\dot{t}^2 + A^2(t,r)\dot{r}^2\right] \tag{H.1}$$

with the null constraint

$$-\dot{t}^2 + A^2(t,r)\dot{r}^2 = 0, \tag{H.2}$$

where the dot implies the derivative with respect to the affine parameter. The geodesic equation is

$$\ddot{t} + A\frac{\partial A}{\partial t}\dot{r}^2 = 0, \tag{H.3}$$

$$-\frac{\partial(A^2\dot{r})}{\partial t} + A\frac{\partial A}{\partial r}\dot{r}^2 = 0. \tag{H.4}$$

The last equation is not independent but derivable from the constraint and the first one.

Since we are interested in the past light cone, we have to solve

$$\dot{t} = -A(t,r)\dot{r}, \tag{H.5}$$

$$\frac{\ddot{t}}{\dot{t}} + F(t)\dot{t} = 0, \tag{H.6}$$

$$F(t) = \frac{1}{A}\frac{\partial A(t,r)}{\partial t}. \tag{H.7}$$

The solution to this equation is formally

$$\dot{t} = \exp\left[-\int^t F(t')dt'\right], \tag{H.8}$$

Suppose a light signal is emitted from $r = r_1$ at t_1 and reaches the observer at the origin at t_{obs}. The red-shift z is then given by

$$1 + z = \frac{\dot{t}|_{t_1}}{\dot{t}|_{t_{obs}}} = \exp\left[\int_{t_1}^{t_{obs}} F(t')dt'\right], \tag{H.9}$$

where $F(t)$ is $\frac{1}{A}\frac{\partial A(t,r)}{\partial t}|_{r=r(t)}$ with $r(t)$ being the solution to

$$\dot{t} = -A(t,r)\dot{r} \tag{H.10}$$

with the condition

$$r(t_1) = r_1, \qquad r(t_{obs}) = 0. \tag{H.11}$$

Because Einstein equations have scale invariance, the spatial metric can be expressed by a one parameter family of initial conditions in Eqs. (3.81) and (3.82). The energy density also can be expressed in the form:

$$\kappa\rho(r,t) = \frac{4\alpha}{9\sqrt{1+c}}\frac{x^{\alpha-1}t^{-2}}{\overset{(t^{1/\alpha})}{A}(x,1)\overset{(t^{1/\alpha})}{B}{}^2(x,1)}, \tag{H.12}$$

with x being the scaling variables $r/t^{1/\alpha}$.

Obviously the null-geodesic equations (H.5)–(H.7) are invariant under the scale transformation (3.66)–(3.72). However, the scale transformation does change the initial conditions $r(t_1) = r_1$ to $r(L^{-\alpha}t_1) = L^{-1}r_1$ so that we have a one parameter family of past light-cones which sweep the whole causal past of the present observer. We shall fix $t_{obs} = 1$ later on and treat L^α as the time of observer at the origin who looks back the past along the past light cone.

At the fixed point,

$$A^*(r,t) = t^{(\alpha-1)/\alpha} \times A(x,1), \tag{H.13}$$

$$B^*(r,t) = t \times B(x,1), \tag{H.14}$$

$$\kappa\rho^*(r,t) = \frac{4\alpha}{9\sqrt{1+c}}\frac{x^{\alpha-1}t^{-2}}{A(x,1)B^2(x,1)}. \tag{H.15}$$

The null-geodesic can be expressed by

$$r(t) = t_{obs}^{1/\alpha} r\left(\frac{t}{t_{obs}}\right). \tag{H.16}$$

From Eq. (H.16),

$$\frac{t}{t_{obs}} = \text{function of } x. \tag{H.17}$$

Thus the null geodesic equation can be rewritten as

$$\frac{dx}{d\log(t)} = -\left[\frac{1}{A(x,1)} + \frac{x}{\alpha}\right], \tag{H.18}$$

with the initial condition $x = 0$ at $t = t_0$.

The redshift becomes

$$\begin{aligned} 1 + z &= \exp\left[\int_{t_1}^{t_0} \frac{dt'}{t'}\left(\frac{\alpha - 1}{\alpha} - \frac{dA(x,1)}{dx} - \frac{x}{\alpha}\frac{d\log A(x,1)}{dx}\right)\right] \\ &= \exp\left[\int_0^{x_1} dx \left(\frac{\alpha - 1}{\alpha} - \frac{dA(x,1)}{dx} - \frac{x}{\alpha}\frac{d\log A(x,1)}{dx}\right)\left(\frac{1}{A(x,1)} + \frac{x}{\alpha}\right)^{-1}\right]. \end{aligned} \tag{H.19}$$

This gives x and then $\kappa\rho^*$ in terms of the redshift z except for the overall scale of t_{obs}.

Bibliography

[1] P. J. E. Peebles, *Principles of Physical Cosmology* (Princeton Univ. Press, Princeton) (1993).

[2] E. W. Kolb and M. S. Turner, *The Early Universe* (Redwood City, Calif, Addison-Wesley) (1990).

[3] F. S. Labini, M. Montuori, and L. Pietronero, *Phys. Rep.* **293**, 61 (1998).

[4] E. M. Gouveia Dal Pino, A. Hetem, J. E. Horvath, C. A. W. Souza, T. Villela, and J. C. N. Araujo, *Astrophys. J.* **442**, L45 (1995).

[5] W. Israel, *Nuovo Cimento* **44B**, 1 (1966); **48B**, 463 (1967).

[6] Y. Suto, *Prog. Theor. Phys.* **90**, 1173 (1993) and references therein.

[7] A. Einstein and E. G. Straus, *Rev. Mod. Phys.* **17**, 120 (1945); **18**, 148 (1946).

[8] R. W. Lindquist and J. A. Wheeler, *Rev. Mod. Phys.* **29**, 432 (1957).

[9] R. Kantowski, *Astrophys. J.* **155**, 1023 (1969).

[10] K. Lake, *Astrophys. J.* **240**, 744 (1980).

[11] W. B. Bonnor, *Astrophys. J.* **316**, 49 (1987) and references therein.

[12] E. M. Lifshitz, *Zh. Eksp. Teor. Fiz.* **16**, 587 (1946);
E. M. Lifshitz and I. M. Khalatnikov, *Adv. Phys.* **12**, 185 (1963).

[13] J. M. Bardeen, *Phys. Rev.* D **23**, 1882 (1980).

[14] H. Kodama and M. Sasaki *Prog. Theor. Phys. Suppl.* **78**, 1 (1984).

[15] D. Langlois, *Class. Quantum Grav.* **11**, 389 (1994).

[16] K. Tomita, *Prog. Theor. Phys.* **37**, 831 (1967); **45**, 1747 (1971); **47**, 1971 (1972).

[17] L. R. Abramo, R. H. Brandenberger, and V. M. Mukhanov, *Phys. Rev.* D **56**, 3248 (1997).

[18] M. Bruni, S. Matarrese, S. Mollerach, and S. Sonego, *Class. Quantum Grav.* **14**, 2585 (1997).

[19] Belinski, Khalatnikov, and Lifshitz, *Adv. Phys.* **19**, 525 (1970).

[20] K. Tomita, *Prog. Theor. Phys.* **48**, 1503 (1972); **50**, 1285 (1973); **54**, 730 (1975); K. Tomita, *Phys. Rev.* D **48**, 5634 (1993).

[21] G. L. Comer, D. Deruelle, D. Langlois, and J. Parry, *Phys. Rev.* D **49**, 2759 (1994).

[22] D. S. Salopek and J. M. Stewart, *Class. Quantum Grav.* **9**, 1943 (1992); *Phys. Rev.* D **47**, 3235 (1993); J. Parry, D. S. Salopek, and J. M. Stewart, *Phys. Rev.* D **49**, 2872 (1994).

[23] D. S. Goldwirth, and T. Piran, *Phys. Rev.* D **40**, 3263 (1989); D. S. Goldwirth, *Phys. Rev.* D **43**, 3204 (1991).

[24] K. Nakao, T. Nakamura, K. Oohara, and K. Maeda, *Phys. Rev.* D **43**, 1788 (1991); H. Sinkai and K. Maeda, *Phys. Rev.* D **49**, 6367 (1994).

[25] V. F. Mukhanov, H. A. Feldman, and R. H. Brandenberger, *Phys. Rep.* **215**, 203 (1992).

[26] N. Deruelle and D. S. Goldwirth, *Phys. Rev.* D **51**, 1563 (1995).

[27] Y. Nambu and A. Taruya, *Class. Quantum Grav.* **13**, 705 (1996).

[28] R. M. Wald, *Phys. Rev.* D **28**, 2118 (1983).

[29] S. Borgani, *Phys. Rep.* **251**, 1 (1995).

[30] P. H. Coleman and L. Pietronero, *Phys. Rep.* **213**, 311 (1992).

[31] T. Vicsek and A. S. Szalay, *Phys. Rev. Lett.* **58**, 2818 (1987).

[32] L. Pietronero, A. Erzan, and C. Evertsz, PRL **61**, 861 (1988).

[33] T. Goldman, D. Hochberg, R. Laflamme, and J. Pérez-Mercader, *Phys. Lett.* A **222**, 177 (1996); D. Hochberg and J. Perez-Mercader, *Gen. Relativ. Gravit.* **28**, 1427 (1996).

[34] J. F. Barbero G., A. Dominguez, T. Goldman, and J. Pérez–Mercader, *Europhys. Lett.* **38**, 637 (1997).

[35] G. de Vaucouleurs, Sience **167**, 1203 (1970).

[36] J. R. Wertz, ApJ **164**, 227 (1971).

[37] L. L. Feng, H. J. Mo, and R. Ruffini, AA **243**, 283 (1991); R. Fabbri and R. Ruffni, AA **254**, 7 (1992).

[38] M. B. Ribeiro *Astrophys. J.* **388**, 1 (1992); **395**, 29 (1992).

[39] P. S. Wesson *Astrophys. J.* **228**, 647 (1979).

[40] K. Tomita, *Gen. Relativ. Gravit.* **29**, 815 (1997).

[41] J. Bricmont, A. Kupiainen, and G. Lin, *Commun. Pure and Appl. Math.* **XLVII**, 893 (1994).

[42] D. Deruelle and D. Langlois, *Phys. Rev.* D **52**, 2007 (1995).

[43] O. Iguchi, H. Ishihara, and J. Soda, *Phys. Rev.* D **55**, 3337 (1997).

[44] A. H. Guth, *Phys. Rev.* D **23**, 347 (1981);
K. Sato, *Mon. Not. R. Astron. Soc.* **195**, 467 (1981);
Linde, *Prog. Phys.* **47**, 925 (1984).

[45] See,e.g., D. S. Goldwirth and T. Piran, *Phys. Rep.* **214**, 223 (1992) and references there in.

[46] V. A. Belinskii, L. P. Grishchuk, Ya. B. Zel'dovich, and I. M. Khalatnikov, *Sov. Phys. JETP* **62**, 195 (1985);
V. A. Belinskii, H. Ishihara, I. M. Khalatnikov, and H. Sato, *Prog. Theor. Phys.* **79**, 676 (1988).

[47] K. Tomita and D. Deruelle, *Phys. Rev.* D **50**, 7216 (1994).
The behavior of F and $\widetilde{G}$ shown in Figs.2.2 and 2.3 is consistent with their analysis while $(\dot{a}_+/a_+)^2 > {}^3R$.

[48] O. Iguchi and H. Ishihara, *Phys. Rev.* D **56**, 3216 (1997).

[49] L. Y. Chen, N. Goldenfeld, and Y. Oono, *Phys. Rev.* E **54**, 376 (1996) and references therein.

[50] T. Kunihiro, *Prog. Theor. Phys.* **94**, 503 (1995); **95**, 835 (1996); **97**, 179 (1997).

[51] M. Gell-Mann and F. E. Low, *Phys. Rep.* **95**, 1300 (1953).

[52] T. Koike, T. Hara, and S. Adachi, *Phys. Rev. Lett.* **74**, 5170 (1995).

[53] M. W. Choptuik, *Phys. Rev. Lett.* **70**, 9 (1993).

[54] H. Tasaki, Parity **11**, 11 (1996) (Maruzen, Tokyo, *in Japanese*).

[55] E. R. Harrison, *Phys. Rev.* D **1**, 2726 (1970);
Ya. B. Zel'dovichi, *Mon. Not. R. Astron. Soc.* **160**, 1P (1972).

[56] K. Tomita, *Phys. Rev.* D **56**, 3341 (1997) and earlier references therein.

[57] M. Carfora and K. Piotrkowska, *Phys. Rev.* D **52**, 4393 (1995).

[58] R. A. Isaacson, *Phys. Rep.* **166**, 1263 (1968); **166**, 1272 (1968).

[59] T. Futamase, *Mon. Not. R. Astron. Soc.* **237**, 187 (1989);
Phys. Rev. D **53**, 681 (1996).

[60] S. Bildhauer and T. Futamase, *Gen. Relativ. Gravit.* **1251**, 187 (1991).

[61] X. Zalaletdinov, *Gen. Relativ. Gravit.* **24**, 1015 (1992);
Gen. Relativ. Gravit. **25**, 673 (1993).

[62] T. Buchert and J. Ehlers, *Astron. Astrophys.* **320**, 1 (1997).

[63] H. Russ, M. H. Soffel, M. Kasai, and G. Börner, *Phys. Rev.* D **56**, 2044 (1997).

[64] P. J. E. Peebles, *The Large Scale Structure of The Universe*
(Princeton Univ. Press, Princeton) (1980).

[65] R. C. Tolman, *Proc. Natl. Acad. Sci.* **20**, 169 (1934);
H. Bondi, *Mon. Not. R. Astron. Soc.* **410**, 107 (1947).